

What Do We Learn from Coupling a Next Generation Land Surface Model to a Mesoscale
Atmospheric Model?

By

LIYI XU

B.S. in Environmental and Resource Science, University of California, Davis, 2004

DISSERTATION

Submitted in partial satisfaction of the requirements for the degree of

DOCTOR OF PHILOSOPHY

in

Atmospheric Science

in the

OFFICE OF GRADUATE STUDIES

of the

UNIVERSITY OF CALIFORNIA

DAVIS

Approved:

(Dr. Kyaw Tha Paw U)

(Dr. Richard L. Snyder)

(Dr. Shu-Hua Chen)

Committee in Charge
2012

UMI Number: 3565412

All rights reserved

INFORMATION TO ALL USERS

The quality of this reproduction is dependent upon the quality of the copy submitted.

In the unlikely event that the author did not send a complete manuscript and there are missing pages, these will be noted. Also, if material had to be removed, a note will indicate the deletion.



UMI 3565412

Published by ProQuest LLC (2013). Copyright in the Dissertation held by the Author.

Microform Edition © ProQuest LLC.

All rights reserved. This work is protected against unauthorized copying under Title 17, United States Code



ProQuest LLC.
789 East Eisenhower Parkway
P.O. Box 1346
Ann Arbor, MI 48106 - 1346

© Liyi Xu, 2012. All rights reserved.

I would like to dedicate this Doctoral dissertation to my loving parents,
Yizhong Xu and Zhong Hui. There is no doubt in my mind that without
their continued caring support I could not have completed this process.

Contents

List of figures	x
List of tables	xi
Acknowledgments and Thanks	xii
Abstract	xiii
I Introduction	1
II Validation of the Coupling between the Mesoscale Atmospheric Model WRF and the Next Generation Land Surface Model ACASA	5
1. Introduction	5
2. Models, methodology and data	8
2.1. The Weather Research and Forecasting (WRF) model	8
2.2. The Advance Canopy-Atmosphere-Soil Algorithm (ACASA) model .	10
2.3. The WRF-ACASA coupling	13
2.4. Model setup	14
2.5. Data	17
3. Results and Discussion	21
4. Conclusion	40
III The Role of Surface Representations: Leaf Area Index, Land Use Covers, and Model Complexity in Calculating Evapotranspiration	45
1. Introduction	45

2.	Models, Methodology and Data	49
2.1.	Models	49
2.2.	Data	51
2.3.	Model setup	55
3.	Results and Discussion	57
4.	Summary and Conclusion	86

IV	Tracing the Carbon Dioxide Exchanges over Californias Complex Ecosystems and Terrains using the WRF-ACASA Coupled Model	91
1.	Introduction	91
2.	Models, methodology and data	94
2.1.	Model description	94
2.2.	Carbon dioxide tracer	97
2.3.	Data	98
2.4.	Model setup	100
3.	Results and discussion	101
4.	Summary and conclusion	117
V	Summary and Future Direction	121
References		126

List of Figures

II.1	The schematic diagram of the WRF-ACASA coupling.	14
II.2	The complex topography and land cover of the study domain is represented here by: (left) Dominant vegetation type and (right) Leaf Area Index (LAI) from USGS used by the WRF model. The horizontal grid spacing of 8 km is needed to resolve the major topographical and ecological features of the domain.	16
II.3	Map of the location of the California Air Resources Boards surface stations.	18
II.4	Time series of the surface air temperature at Mojave Desert Station during June 2006. The black line represents the entire set of surface temperature observation with gaps presented. The red line represent the daily mean temperature calculated using only days with all 24 hours of observation available.	20
II.5	Monthly mean surface air temperature simulated by WRF-ACASA and WRF-NOAH and for the surface observations for the months of February, May, August and November 2006.	22
II.6	Time series of surface air temperature simulated by WRF-ACASA and WRF-NOAH and for the surface observations for four different stations and for the months of February, May, August and November 2006.	25
II.7	Diurnal cycle of surface air temperature for each seasons for the Northeast Plateau, Mojave Desert, San Joaquin Valley, and Mountain County stations. The solid and the two dash black lines represent the surface observation and ± 1 standard deviation from the mean respectively. The WRF-ACASA results are showed in blue and the WRF-NOAH results are in red.	28

II.8 Time series of surface air temperature simulated by WRF-ACASA and WRF-NOAH and for the surface observations for four different stations and for the months of February, May, August and November	31
II.9 Statistical analysis of two model simulations versus observed for R-square, Root Mean Square Error (RMSE), and Degree of Agreement for the four different seasons.	34
II.10 Time series of Dew point model predictions and observations for four basins during February, May, August, and November.	36
II.11 Mean diurnal dew point temperature trends for the four seasons and the four air basins: Northeast Plateau, Mojave Desert, San Joaquin Valley, and Mountain County stations.	37
II.12 Same as Fig. II.8 but for surface dew point temperature.	38
II.13 Same as Fig. II.8 but for surface relative humidity.	39
II.14 Taylor diagram of monthly mean surface air temperature, dew point temperature, relative humidity, wind speed, and solar radiation for both WRF-ACASA and WRF-NOAH for all ARB stations. WRF-ACASA is represented by blue dots and WRF-NOAH by red dots.	41
III.1 Maps of MODIS LAI and USGS LAI for the months of February, May, August and November 2006.	53
III.2 Maps of the location of the (left) 120 CIMIS stations (part of the ARB network) and of the (right) 6 AmeriFlux stations used in this study.	54

III.3 Seasonal diurnal patterns of reference ETo for the four model simulations for the CIMIS sites. The black lines are CIMIS ETo measurements with two dash lines representing one standard deviation above and below the mean diurnal patterns. The red lines are WRF-NOAH simulations and the blue lines are WRF-ACASA simulations with MODIS LAI. The dashed lines are for simulations with USGS LAI. Winter is assumed to be December, January, and February (DJF) spring is March, April, and May (MAM) summer is June, July, and August (JJA), and autumn is September, October, and November (SON).	58
III.4 Same as Fig. III.3 for the AmeriFlux sites.	60
III.5 Time series of reference evapotranspiration for the CIMIS sites. The solid black line represents observation. The blue lines are for WRF-ACASA, and the red lines are for WRF-NOAH. The solid lines are simulations with MODIS LAI, and the dashed lines are simulations with USGS LAI.	61
III.6 Same as Fig. III.5 for the AmeriFlux sites.	62
III.7 Scatter plots of daily ETo simulated by WRF-ACASA with both MODIS and USGS LAI over the six AmeriFlux locations. The daily ETo are sorted by seasons.	63
III.8 Same as Fig. III.7 but for WRF-NOAH.	64
III.9 Maps of ETo.	66
III.10 Taylor Diagram for the four WRF simulations vs. CIMIS station measurements.	69
III.11 Diurnal patterns of the actual evapotranspiration for 2005.	70
III.12 Same as Fig. III.11	71

III.13The time series of cumulative daily ET _a for the six AmeriFlux sites during year 2005 and 2006. The black lines are surface measurement of daily ET _a , the blue lines are WRF-ACASA simulations, and the red lines are WRF-NOAH simulations. The model simulations with MODIS LAI are presented using solid lines and the dash lines are WRF models with USGS LAI.	73
III.14Scatter plots of daily ET _a simulated by WRF-ACASA with both MODIS and USGS LAI over the six AmeriFlux locations. The daily ET _o are sorted by seasons.	75
III.15Same as Fig. III.14 but for WRF-NOAH.	76
III.16The diurnal pattern of stomatal resistances. The blue line is WRF-ACASA with MODIS, the green line is WRF-ACASA with USGS.	78
III.17Maps of ET _a	79
III.18The energy budget of WRF-ACASA with USGS LAI. The solid lines are for AmeriFlux station measurements, and the dash lines are for WRF-ACASA with USGS LAI simulations. Black is net radiation (R _n), red is sensible heat (H), blue is latent heat (LE), and green is ground heat flux (G).	81
III.19Same as Fig. III.18 but for WRF-ACASA with MODIS LAI.	82
III.20Same as Fig. III.18 but for WRF-NOAH.	83
III.21Same as Fig. III.19 but for WRF-NOAH.	84

III.22 Taylor diagram for model simulations and surface measurements of: air temperature, dew point temperature, and relative humidity for all six AmeriFlux sites. The order of the variables represented on the graphs is: actual evapotranspiration (ETa), reference evapotranspiration (ETo), 2-meter air temperature (T_2m), 2-meter dew point temperature (Td_2m), 2-meter relative humidity (RH_2m), and 10-meter wind speed (windspeed).	85
IV.1 Locations of the six AmeriFlux sites used in this study. In Northern California, Blodgett Forest site is northeast of the Tonsi and Vaira sites (shown as one point). All three Southern California sites are at the same location.	99
IV.2 Diurnal patterns of carbon dioxide flux for the AmeriFlux sites for year 2005.	101
IV.3 Same as Fig. IV.2 but for year 2006.	103
IV.4 Scatter plots of CO ₂ flux (FCO ₂) by season.	104
IV.5 Time series of annual NEE for model simulations and surface observations for year 2005.	106
IV.6 Same as Fig. IV.5 for year 2006.	107
IV.7 WRF-ACASA simulations of seasonal NEE with and without CO ₂ Tracer for 2006. Results for 2005 is similar to 2006.	109
IV.8 Annual NEE of carbon dioxide for year 2006 for WRF-ACASA simulations with and without CO ₂ tracer.	110

IV.9 Diurnal patterns of atmosphere carbon dioxide concentration for the six Amer-iFlux sites for year 2005. Black solid lines represent observation from Amer-iFlux sites, and black dash lines represent one standard deviation below and above the diurnal means. Blue lines are WRF-ACASA simulations with CO ₂ tracer.	111
IV.10 Same as Fig. IV.9 for year 2006.	112
IV.11 Map of atmospheric CO ₂ concentrations and wind patterns using the CO ₂ tracer by seasons and sigma levels for year 2006.	114
IV.12 Atmospheric CO ₂ concentration of May 1 2006 for 10 AM, 12 PM, and 2 PM.	116
IV.13 Vertical Cross-section of atmospheric CO ₂ concentration	117
IV.14 Differences in precipitation between the two WRF-ACASA models, i.e., with and without CO ₂ tracer simulations for year 2005 and 2006.	118

List of Tables

II.1 Selected sites from the Air Resources Board meteorological stations network.	19
II.2 Statistical between the models and observations for the 13 ARB basins by sea- son: December, January and February (DJF); March, April and May (MAM); June, July and August (JJA); September, October and November (SON). . .	32
III.1 Selected sites from the Air Resources Board meteorological stations network.	55
III.2 ETa RMSE from LAI bias. Difference = RMSE (MODIS) - RMSE(USGS). .	87
III.3 The ETa RMSE for WRF-ACASA and WRF-NOAH models from land use cover bias. Bad PFT (plant functional types) do not match between the observed and the models (the three Sky Oak sites). Good PFT are matched between the observed and the models for the Blodgett forest and the Tonzi Ranch.	87
III.4 The combined effect of surface representations (LAI and PFT) on the RMSE for WRF-ACASA and WRF-NOAH simulations.	89
IV.1 AmeriFlux sites used and information.	100
IV.2 AmeriFlux sites used and information.	105
IV.3 Time series of annual NEE of the six AmeriFlux sites for year 2005 and 2006. No time series of NEE is displayed for Sky Oak sites, USSO2 and USSO3, due to large amount of missing data in 2005.	108

Acknowledgments and Thanks

I owe sincere and earnest thankfulness to my loving husband, Erwan Monier, for his endless support and tireless help throughout my research and dissertation. Words cannot express how much I love you. I would also like to thank my parents for their continuous encouragement during my study. I would like to express my deepest gratitude to my advisor, Professor Kyaw Tha Paw U, for his guidance and support during my years at UC Davis both as an undergraduate and a graduate student. I would like to thank Dr. Dave Pyles, whose sincerity, support, and encouragement I will never forget. I extend my appreciation to my committee members for their time and guidance. In particular, I would like to thank Professor Shu-Hua Chen and Professor Richard Snyder for their encouragement and advice. In addition, I would like to thank Richard Massa for his help with the computer. Special thanks to the MIT Joint Program on the Science and Policy of Global Change for their generosity and computer support. Lastly, I also want to thank all my family and friends for their support and encouragement. I also want to acknowledge all the faculty and staff members of the Land, Air and Water Resources Department who create a great environment for learning and research. This work is in part supported by the National Science Foundation under Awards No. ATM-0619139.

Abstract

In this study, the Weather Research and Forecasting Model (WRF) is coupled with the Advanced Canopy-Atmosphere-Soil Algorithm (ACASA), a high complexity land surface model (LSM). Although WRF is a state-of-the-art regional atmospheric model with high spatial and temporal resolutions, the land surface schemes available in WRF are simple and lack the capability to simulate carbon dioxide, for example, the popular NOAH LSM. ACASA is a complex multilayer land surface model with interactive canopy physiology and full surface hydrological processes. It allows microenvironmental variables such as air and surface temperatures, wind speed, humidity, and carbon dioxide concentration to vary vertically.

Simulations of surface conditions as well as reference and actual evapotranspiration from WRF-ACASA and WRF-NOAH are compared with surface observations for year 2005 and 2006. Results show that the increase in complexity in the WRF-ACASA model not only maintains model accuracy, it also properly accounts for the dominant biological and physical processes describing ecosystem-atmosphere interactions that are scientifically valuable. The different complexities of physical and physiological processes in the WRF-ACASA and WRF-NOAH models also highlight the impacts of different land surface and model components on atmospheric and surface conditions.

Lastly, unlike the simple big-leaf WRF-NOAH model with no carbon dioxide simulation, the high complexity WRF-ACASA model is used to quantify the carbon dioxide exchange between the biosphere and atmosphere and to examine the importance of atmospheric carbon dioxide concentration on surface processes on a regional scale. A new carbon dioxide (CO_2) tracer is introduced into the WRF-ACASA coupled model to allow atmospheric CO_2

concentration to vary spatially and temporally according to surface plant physiological processes. The comparison between the two model simulations with and without a CO₂ tracer shows that the impact of atmospheric CO₂ concentration and transportation are important, and therefore these should not be neglected when simulating CO₂ flux at regional scales. Overall, this study shows that the high complexity WRF-ACASA model is robust and able to simulate the surface conditions and CO₂ fluxes well across the region, particularly when given accurate surface representations.

Chapter I

Introduction

Although the earth is mostly covered by ocean, the presence of land surfaces introduces much complexity into the earth system that drives numerous atmospheric and oceanic dynamics. The effects of complexity range from the simple land-sea contrasts in radiation processes, to wind flow dynamics, and also to the more complex biogeophysical processes of terrestrial systems. Various types of terrestrial ecosystems make up the land surface layer, each possessing complex canopy structures and surface heterogeneities that both sustain and are sustained by physical and physiological interactions with the atmosphere. These ecosystems, which are both extensive and dynamic components of the surface layer, heavily modify surface exchanges of energy, gas, moisture, and momentum in ways that develop the microenvironment, distinguishing vegetated surfaces from landscapes without vegetation. Such influences are known to occur on different spatial and temporal scales (Chen and Avissar, 1994; Pielke et al., 2002; Zhao et al., 2001).

The interaction between the terrestrial biosphere and the atmosphere is therefore one of the most active and important aspects of the entire Earth system. In particular, exchanges of thermal energy, water vapor, carbon dioxide, and momentum between the surface layer and the atmosphere vary significantly due to variegated sourcing of each flux acting amid turbulent flows that set up within the biospheric structures. For example, the turbulent transport of moisture and energy fluxes from both plant transpiration and surface evaporation to the planetary boundary layer (PBL) have a strong influence on the diurnal and vertical structures of the planetary boundary layer. For instance, nocturnal thermal emissions occurring

over sparsely vegetated regions within the California Great Central Valley surface often results in a shallow planetary boundary layer; the cold air pooling to within a few tens of meters of the surface. In contrast, similar nocturnal conditions acting over coniferous canopies in the southern Sierra Nevada would instead yield deeper, convectively mixed boundary layers, rough and fury with plumes, reaching several or more kilometers above the surface. This process plays an important role in the evolution of clouds and precipitation, which remain major areas of uncertainty in our understanding of the climate system. A particular set of feedbacks between these processes is completed when precipitation, which overwhelmingly originates from the Earth's surface, in turn alters ecological responses, including fluxes, within the surface layer. Consequently, the aforementioned exchanges of energy, water, and momentum between the surface layer and the atmosphere have large impacts on meteorological, hydrological and ecological properties. Evidence of these complex interactions between the surface layer and the atmosphere are demonstrated in a number of recent investigations (Pielke and Niyogi, 2010; Pielke and Avissar, 1990; de Arellano et al., 2004; Adegoke et al., 2007; Fesquet et al., 2009).

Since the surface layer is the only physical boundary in an atmospheric model, there is a consensus in the geosciences community that accurate simulations of atmosphere processes in an atmospheric model require good representations of the surface layer and its terrestrial system. Models that account for the effects of surface layer on climate and atmosphere conditions are referred to as the Land Surface Models (LSMs). Unfortunately, the current land surface models often overly simplify the surface layer by using single layer "big leaf" parameterizations and other assumptions, usually based around some form of bulk Monin-Obukhov-type similarity theory. These models take physical and physiological properties

known to act at the leaf-scale and use these to represent the entire ecosystem as one "big leaf" lying flat on the ground. Oversimplification of surface processes and their impacts on the atmosphere in these land surface models are likely to misrepresent the system as such, undermining the prediction and/or diagnoses of surface-atmosphere interactions.

In addition, the majority of land surface models do not simulate carbon dioxide flux, even as it is largely recognized as a major contributor to current climate change phenomena and is known to be a controller of plant physiology. Those that do include carbon dioxide processes may be oversimplified and may overestimate CO₂ uptake by plants under higher future atmospheric carbon concentration as suggested by Paw U (1997). Although carbon dioxide is not the most efficient greenhouse gas on a molecule-to-molecule basis, its abundance and large increase since the pre-industrial period make it the most important anthropogenic greenhouse gas. In addition to the oceanic reservoir, the terrestrial ecosystem is often recognized by scientists as the "missing sink" of anthropogenic carbon emissions (Wigley and Schimel, 2005). Furthermore, the latest IPCC assessment report suggests that uncertainties in climate change may be a result of uncertainties in future carbon cycle (Collins et al., 2006). Hence, carbon dioxide quantification is an important piece of the future climate change puzzle.

This study introduces the novel coupling of the mesoscale WRF model with the complex multilayer Advance Canopy-Atmosphere-Soil Algorithm (ACASA) model, to simulate surface conditions, evapotranspiration, as well as carbon dioxide fluxes over California's diverse terrain and ecosystems. The complex land surface processes in the WRF-ACASA model that drive local and mesoscale circulations are evaluated using surface observations in the first part of the study. The later chapters focus on the influence of surface representation and model complexity on plant physiological and atmospheric processes on regional scale. Fi-

nally, a new CO₂ tracer is also introduced in the model to study the influence of atmospheric carbon dioxide concentration on plant physiological processes.

Chapter II

Validation of the Coupling between the Mesoscale Atmospheric Model WRF and the Next Generation Land Surface Model ACASA

1. Introduction

Although the earth is mostly covered by ocean, the presence of land surfaces introduces much complexity into the earth system that drives numerous atmospheric and oceanic dynamics. The effects of complexity ranges from the simple land-sea contrasts in radiation processes, to the wind flow dynamics, and to the more complex biogeophysical processes of terrestrial systems. Various types of plants, soils, microbes, and all living organisms including humans are situated on and within the landscape that make up the earths terrestrial system of the biosphere. Though the surface layer represents a very small fraction of the planet, only the lowest 10% of the planetary boundary layer, it has been widely regarded as a crucial component of the climate system (Stull, 1988; Mintz, 1981; Rountree, 1991). The interaction between the land surface (biosphere) and the atmosphere is therefore one of the most active and important aspects of the natural system.

Vegetation at the land surface introduces complex structures, properties, and interactions to the surface layer. Therefore, vegetation heavily modifies surface exchanges of energy, gas, moisture, and momentum in ways that develop the microenvironment, distinguishing vegetated surfaces from landscapes without vegetation. Such influences are known to occur on different spatial and temporal scales (Chen and Avissar, 1994; Pielke et al., 2002; Zhao et al., 2001). In particular, often near-geostrophically-balanced wind patterns are disrupted

in the lower atmosphere when wind encounters vegetated surfaces i.e., the winds slow down and change direction as a result of turbulent flows that develop within and near the vegetated canopies (Wieringa, 1986; Pyles et al., 2004).

Depending in part on the canopy height and structure, wind and turbulent flows often vary considerably across different ecosystems—even when each is presented with the same meteorological and astronomical conditions aloft. Gradients in heating, air pressure, and other forcings develop across heterogeneous landscapes, helping to sustain atmospheric motion. Hence, since the surface layer is the only physical boundary in an atmospheric model, there is a consensus that accurate simulations of atmosphere processes in an atmospheric model require good representations of the surface layer and its terrestrial system. Models that account for the effects of surface layer on climate and atmosphere conditions are referred to as the Land Surface Models (LSMs).

Unfortunately, the current land surface models, i.e., the widely used set of four schemes present in the Weather Research and Forecasting (WRF) model (5-layer thermal diffusion, Pleim-Xiu, Rapid Update Cycle, and the popular NOAH, often overly simplify the surface layer by using a single layer "big leaf" parameterizations and other assumptions, usually based around some form of bulk Monin-Obukhov-type similarity theory (Chen and Dudhia, 2001a,b; Pleim and Xiu, 1995; Smirnova et al., 1997, 2000; Xiu and Pleim, 2001). These models scale the leaf-level physical and physiological properties as one extensive "big leaf" to represent the entire canopy.

The majority of the land surface models do not simulate carbon dioxide flux, even as it is largely recognized as a major contributor to the current climate change phenomenon and a controller of plant physiology. Plant transpiration in these models is often based on the

Jarvis parameterization, in which the stomatal control of transpiration is a multiplicative function of meteorological variables such as temperature, humidity, and radiation (Jarvis, 1976). However, a large number of studies show that there is a strong linkage between the physiological process of photosynthetic uptake and respiratory release of CO₂ to plant transpiration through stomata (Zhan and Kustas, 2001; Houborg and Soegaard, 2004). Hence, physiological processes related to CO₂ exchange rates should be included in surface-layer representation of water and energy exchanges.

Oversimplification of surface processes and their impacts on the atmosphere in these land surface models are likely to misrepresent and poorly predict surface and atmosphere interactions. Such models in earth science fields that use simplified equations and statistical relationship to represent complex processes in physics, physiology, hydrology, and thermodynamics require intense fine-tuning and optimization algorithms to match the observations (Duan et al., 1992). These empirical models are capable of producing good results, but their assumptions limit their ability to investigate relationship and feedbacks between different components of the system. For example, the empirical models are unable to characterize the relationship between canopy height and their sub-canopy energy distribution, and the effects of increased carbon dioxide concentrations on vegetation-atmosphere interactions. This is especially true for regional scale studies where the influence of the terrestrial system increases with better spatial resolution and heterogeneous land cover.

Recent computer and model developments have greatly improved atmospheric modeling abilities. Progressively more complex planetary boundary layer and surface schemes are being implemented into these atmosphere models with higher spatial and temporal resolution. However, the challenges involved in advancing the robustness of land surface models continue

to limit the realistic simulation of planetary boundary layer forcing by vegetation, topography, and soil. Some have argued that the increase in model complexity does not translate into higher accuracy due to the increase in uncertainty introduced by the large number of input parameters needed by the more process-based models (Raupach and Finnigan, 1988; Jetten et al., 1999; de Wit, 1999; Perrin et al., 2001). However, there is a certain scientific value in properly accounting for the dominant biological and physical processes describing ecosystem-atmosphere interactions, even if this greatly complicates the models.

This study introduces the novel coupling of the mesoscale WRF model with the complex multilayer Advance Canopy-Atmosphere-Soil Algorithm (ACASA) model, to improve the surface and atmospheric representation in a regional context. The objectives of this study are to (1) parameterize complex land surface processes that drive local mesoscale circulations, and (2) to investigate the effects of model complexity on accuracy.

2. Models, methodology and data

2.1. The Weather Research and Forecasting (WRF) model

The mesoscale model used in this study is the Advanced Research WRF (ARW) model Version 3.1. WRF is a state-of-the-art, mesoscale numerical weather prediction and atmospheric research model developed by a collaborative effort of the National Center for Atmospheric Research (NCAR), the National Oceanic and Atmospheric Administration (NOAA), the Earth System Research Laboratory (ESRL), and many other agencies. The WRF model contains a nearly complete set of compressible and non-hydrostatic equations for atmospheric physics (Chen and Dudhia, 2000). Multiple atmospheric layers vary in vertical grid

spacing with height to simulate three-dimensional atmospheric variables. The mass-based terrain following coordinate in WRF improves the surface processes. It is commonly used to study air quality, precipitation, severe windstorm events, weather forecasts, and many other atmospheric related conditions (Borge et al., 2008; Thompson et al., 2004; Powers, 2007; Miglietta and Rotunno, 2005; Trenberth and Shea, 2006). Compared to the 2.5° (equivalent to 250 km^2) resolution of General Circulation Models (GCMs), the WRF model with high spatial and temporal resolution is more suitable to study climate conditions over California; WRF can be nested so that fine grid spacing of on the order of 1 km or less is possible.

Four different parameterizations of land-surface processes are available in the WRF model as mentioned in the introduction. WRF's more widely used and most sophisticated NOAH employs simplistic physics compared to ACASA, being more akin to the set of ecophysiological schemes that include SiB and BATS (Dickinson et al., 1993; Sellers et al., 1996). There is only one vegetated surface layer in the NOAH scheme, along with four soil layers to calculate soil temperature and moisture. The "big leaf" approach assumes the entire canopy has similar physical and physiological properties to a single big leaf. Energy and mass transfers for the surface layer are calculated using simple surface physics (Noilhan and Planton, 1989; Holtslag and Ek, 1996; Chen and Dudhia, 2000). For example, the surface skin temperature is linearly extrapolated from a single surface energy balance equation, which represents the combined surface layer of ground and vegetation (Mahrt and Ek, 1984). Surface evaporation is computed using modified diurnally dependent Penman-Monteith equation from Mahrt and Ek (1984) and the Jarvis parameterization (Jarvis, 1976). The current WRF LSMs are relatively simple, when compared to the higher order closure based ACASA model, and none of them calculate carbon flux. Hence, there is good justification for use of a fully coupled

WRF-ACASA model, which can handle carbon dioxide fluxes and the reaction of ecosystems to increased carbon dioxide concentrations.

2.2. The Advance Canopy-Atmosphere-Soil Algorithm (ACASA) model

Compared to the simple NOAH, the ACASA model is a complex multilayer analytical land surface model, which simulates the microenvironment profiles and turbulent exchange of energy, mass, CO₂ and momentum within and above ecosystems that constitute land surfaces. It represents the interaction between vegetation, soil and the atmosphere based on physical and biological processes described from the scale of leaves (microscale), which is on the order of 100 times the ecosystem vegetation height, i.e., hundreds of meters to around 1 km. The surface layer is represented as a column model with multiple vertical layers extending to the lowest planetary boundary. The model has 10 vertical atmospheric layers above-canopy, 10 intra-canopy layers, and 4 soil layers.

For each canopy layer, leaves are oriented in 9 sun-lit angle leaf classes (random spherical orientation) and 1 shaded leaf class in order to represent radiation transfer and leaf temperatures in a representative and variable array that aggregates to a representative and realistic exchanges for sensible heat, water vapor, momentum, and carbon dioxide. Within each layer, calculations are carried out for the radiation balance partitioned into nine leaf inclination angle classes and one shaded leaf class, with leaves distributed spherically. The values of fluxes at each layer depend on those from all layers, so the radiative-transfer equations are iterated until numerical equilibrium is reached. Shortwave radiation fluxes, along with associated arrays (probabilities of transmission, beam extinction coefficients, etc.), are not changed while the turbulence set of equations is iterated to numerical convergence.

Plant physiological processes, such as evapotranspiration, photosynthesis and respiration, are calculated for each of the leaf classes and layers, based on the simulated radiation field and the micrometeorological variables calculated in the previous iteration step. The default maximum rate of Rubisco carboxylase activity, which controls plant physiological processes is provided for each of the standardized vegetation types, although specific values of these parameters can be entered. Temperature, mean wind speed, carbon dioxide concentration, and specific humidity are calculated explicitly for each layer, using the higher order closure equations (Meyers and Paw U, 1986, 1987; Su et al., 1996).

In addition to the capability to calculate the carbon dioxide flux, a key advanced component of the ACASA model is its higher-order turbulent closure scheme. The parameterizations of the fourth-order terms used to solve the prognostic third order equations are described by assuming a quasi-Gaussian probability distribution as a function of second-moment terms (Paw U and Gao, 1988). Compared to lower order closure models, the higher order closure scheme increases the model accuracy through improving the description of the turbulent transport of energy, momentum, and water by both small and large eddies. While in small-eddy theory or eddy viscosity, energy fluxes move down a local gradient, large eddies in the real atmosphere can transport flux against the local gradient. Such counter-gradient flow is a physical property of large eddies associated long distance transport. For example, mid-afternoon intermittent ejection-sweep eddies that cycle deep into a warm forest canopy with snow on the ground, having sweeps originating above the canopy from regions, where air temperature ranges between the warm canopy and the cold snow, would result in overturning of eddies to transport relative warm air from above the canopy through the canopy to the snow surface below. The local gradient from the canopy to the above-canopy air would

indicate sensible heat going upwards, instead of the actual heat flow down to the snow past the canopy due to the long turbulence scales of transport. These potentially counter-gradient transports are responsible for much of land surface evaporation, heat, carbon dioxide and momentum fluxes (Denmead and Bradley, 1985; Gao et al., 1989). The ACASA model uses higher order closure transport between multiple layers of the canopy, mimicking non-local transport, allowing the simulation of counter-gradient and non-gradient exchange. However, with only one surface layer, the simple lower order turbulent closure model NOAH is limited to only down-gradient transport and not mixing within the canopy.

Both rain and snow forms of precipitation are intercepted by the canopy elements in each layer. Some of the precipitation is retained on the leaf surfaces to modify the microenvironment of the layers for the next time step, depending on the precipitation amount, canopy storage capacity, and vaporization or sublimation rate. The remaining precipitation is distributed to the ground surface, influencing soil moisture and/or surface runoff as calculated by the layered soil model. The soil model physics in ACASA are very similar to the diffusion physics set used in NOAH, but with enhanced layering of the snowpack for more representative thermal profiles throughout deep snow. The multilayer snow model allows interactions between layers and more effectively calculate energy distribution and snow hydrological processes such as snow melt when surface snow experiences higher or lower temperatures than the underlying snow layers. This is important over regions with high snow depth such as Sierra Nevada Mountain where snow is an important source of water. The multilayer snow hydrology scheme has been well tested during the SNOWMIP project (Etchevers et al., 2004; Rutter et al., 2009), where ACASA performed as well or better than many snow models by accurately estimate the snow accumulation rate as well as the timing of the snow melt in a

wide range of biomes.

The stand-alone version of the ACASA model has been successfully applied to study sites across different countries, climate systems, and vegetation types. These include a 500 year old growth coniferous forest at the Wind River Canopy Crane Research Facility in Washington State (Pyles et al., 2000, 2004), a spruce forest in the Fichtelgebirge Mountains in Germany (Staudt et al., 2011) , and a maquis ecosystem in Sardinia near Alghero (Marras et al., 2008), and a grape vineyard in Tuscany near Montalcino, Italy (Marras et al., 2011).

2.3. The WRF-ACASA coupling

In an effort to improve the parameterization of land surface processes and their feedbacks with the atmosphere, ACASA is coupled to the mesoscale model WRF as a new land surface scheme. The schematic diagram of Fig. II.1 represents the coupling between the two models. From the Planetary Boundary Layer (PBL) and above, the WRF model provides meteorological variables as input forcing to the ACASA land surface model at the lowest WRF sigma-layer. These variables include solar shortwave and terrestrial (atmospheric thermal long-wave) radiation, precipitation, humidity, wind speed, carbon dioxide concentration, and barometric pressure. Radiation is partitioned into thermal IR, visible (PAR) and NIR by the ACASA model, which treats these radiation streams separately owing to the preferential scattering of the different wavelengths by vegetation as the radiation passes through the canopy. Part of the radiation is reflected back to the PBL according to the layered canopy radiative transfer model, The remaining radiation used to drive photosynthesis and energy balance.

Differing from the single layer NOAH surface model coupled to WRF, ACASA creates a

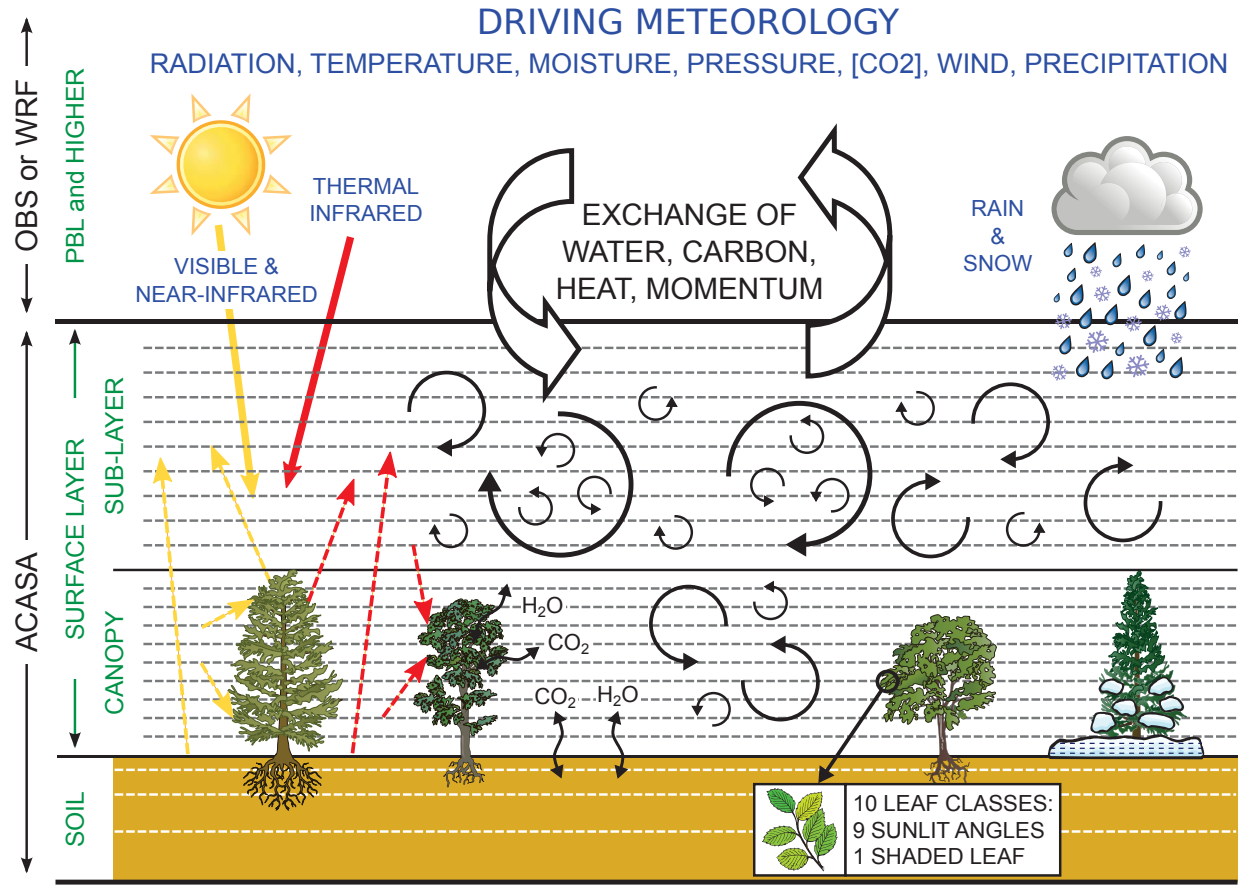


Figure II.1: The schematic diagram of the WRF-ACASA coupling.

normalized vertical LAI or LAD (Leaf Area Density) for the multiple canopy layers according to vegetation type. This is crucial because the canopy height and distribution of LAD have direct influences over the interactions of wind, light, temperature, radiation, and carbon between the atmosphere and the surface layer.

2.4. Model setup

The WRF model requires input data for prognostic variables including wind, temperature, moisture, radiation, and soil temperature, both for an initialized field of variables through the domain, and at the boundaries of the domain. In this study, these input data are provided by

the Northern America Regional Reanalysis (NARR) dataset to drive the WRF-NOAH and WRF-ACASA models. Unlike many other reanalysis data sets with coarse spatial resolution such as ERA40 (European Center for Medium-Range Weather Forecasts 40 Year Re-analysis) and GFS (Global Forecast System), NARR is a regional data set specifically developed for the Northern American region. The temporal and spatial resolutions of this data set are 3 hours and 32 km, respectively.

Simulations of both the default WRF-NOAH and the WRF-ACASA models were performed for two yearly simulations (2005 and 2006) with horizontal grid spacing of 8 km x 8 km. These two years were chosen because they provide the most extensive set of surface observation data. The model domain covers all of California with parts of neighboring states and the Pacific Ocean to the west, shown in Fig. II.2. The complex terrain, and vast ecological and climatic systems in the region make it ideal to test the WRF-NOAH and WRF-ACASA coupled model performances. The geological and ecological regions extend eastward from the coastal range shrub lands to the Central Valley grasslands and croplands, then to the foothill woodlands before finishing at the coniferous forests along the Sierra Nevada range. Further inland to the east and south includes the Great Basin and Range Chaos, an arid and complex mosaic of forests and chaparral tessellated amid the myriad fossae that erupt between dunes and playas. The contrasting moist Northern and semiarid Southern California landscapes are also represented in tandem.

Beside the differences in the land surface model, both WRF-NOAH and WRF-ACASA employ the same set of atmosphere physics schemes stemming from the WRF model. These include the Purdue Lin et al. scheme for microphysics (Chen and Sun, 2002), the Rapid Radiative Transfer Model for long wave radiation (Mlawer et al., 1997), Dudhia scheme

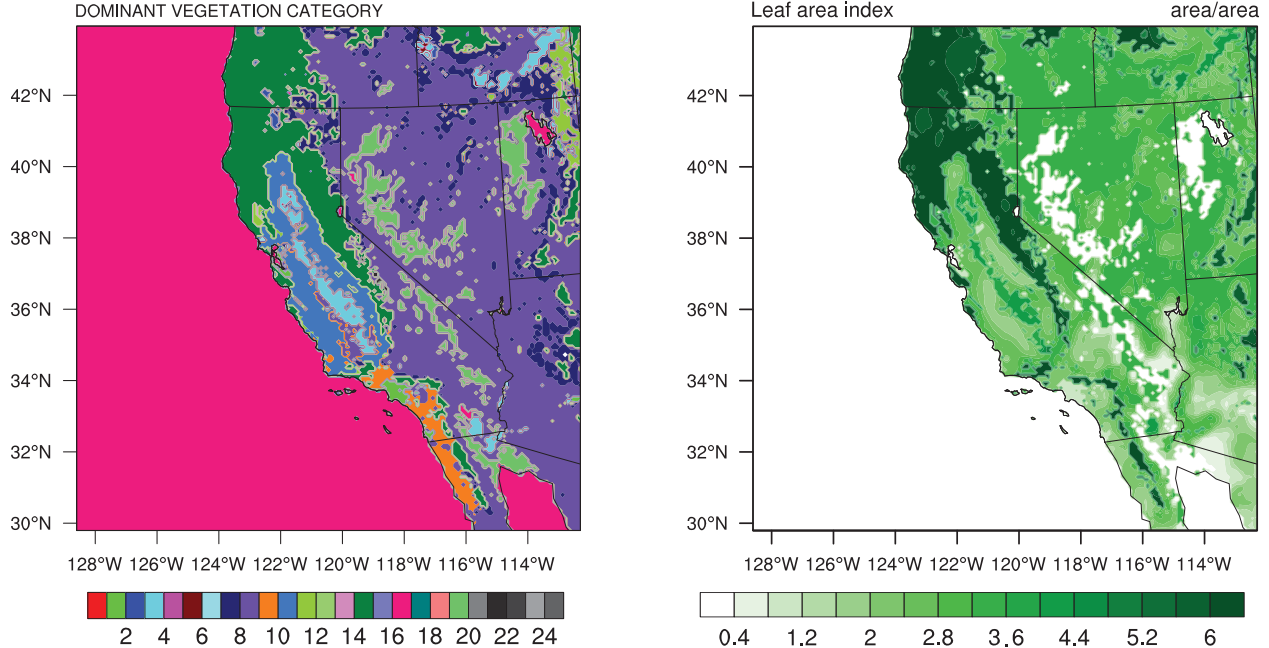


Figure II.2: The complex topography and land cover of the study domain is represented here by: (left) Dominant vegetation type and (right) Leaf Area Index (LAI) from USGS used by the WRF model. The horizontal grid spacing of 8 km is needed to resolve the major topographical and ecological features of the domain.

for shortwave radiation (Dudhia, 1989), Monin-Obukhov Similarity scheme for surface layer physics of non-vegetated surfaces and the ocean, and the MRF scheme for the planetary boundary layer (Hong and Pan, 1996). WRF runs its atmospheric processes at a 60-second time step, while the radiation scheme and the land surface schemes are called every 30 minutes. Because ACASA assumes quasi-steady-state turbulent processes, its physics are not considered advisable for shorter time intervals. Both NOAH and ACASA calculate surface processes and update the radiation balance, as well as heat, water vapor, and carbon fluxes, surface temperature, snow water equivalent, and other surface variables in WRF. Analytical nudging of four dimensional data assimilation (FDDA) is applied to the atmosphere for all model simulations in order to maintain the large-scale consistency and reduce drifting of model simulation from the driving field over time. Such nudging (FDDA) is commonly

practiced in limited-area modeling and current methods active in WRF are widely accepted through rigorous testing (Stauffer and Seaman, 1990; Stauffer et al., 1991).

2.5. Data

The main independent observational datasets used to evaluate the model simulations were obtained from the Meteorological Section of the California Air Resource Board (ARB). The NARR data were not used for the evaluation as the dataset is used for FDDA during both model simulations. The ARB meteorology dataset comprises over 2000 surface observation stations in California from multiple agencies and programs: Remote Automated Weather Stations (RAWS) from the National Interagency Fire Center, the California Irrigation Management Information System (CIMIS), National Oceanic and Atmospheric Administration (NOAA), Aerometric Information Retrieval System (AIRS), and the Federal Aviation Administration. Potential measurement error and uncertainties are expected in the ARB data because of the differences in station setups and measurement guidelines from the different agencies. For example, ambient surface air temperature is measured at various heights between 1 to 10 meters above the ground, depending on the measuring agency. Some stations are located in urban environments, while the model simulations are focused on natural vegetated environments. Therefore, some bias between the observation and simulation over densely populated area are likely. However, with hourly data from over 2000 observation stations within the study domain, the ARB dataset is a valuable dataset. Out of the 2000 surface stations in the overall current ARB database, there were about 730 stations operational during the study period of 2005 and 2006 (Fig. II.3).

The meteorological and surface conditions from the WRF-NOAH and WRF-ACASA

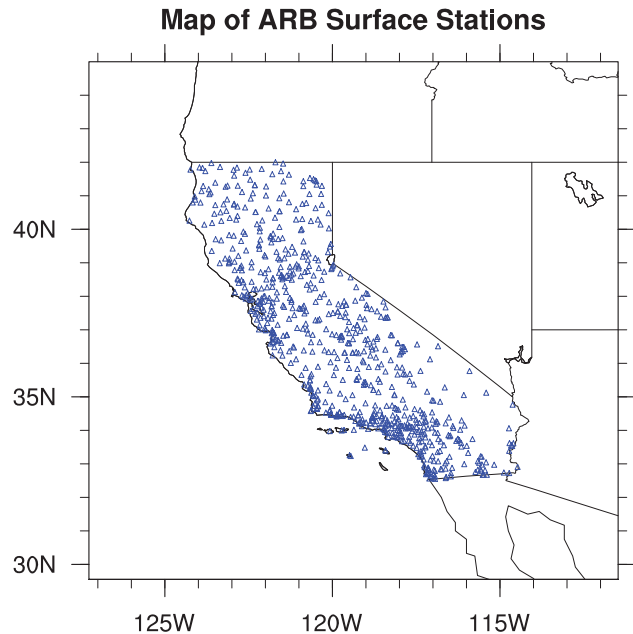


Figure II.3: Map of the location of the California Air Resources Boards surface stations.

model simulations were evaluated using the Air Resource Board data both as a dataset for the entire domain, and using specific stations for more in-depth analysis. This represents in no uncertain terms the most rigorous test of ACASA to date, in terms of the sheer number of ACASA point-simulations and the number of ACASA points linked in both space and time. This investigation is therefore represents a significant elaboration upon earlier work (Pyles et al., 2003). Meteorological variables such as surface air temperature, dew point temperature, and precipitation from the two model simulations were compared with each other and the observational data. Four basins within the study domain were selected to represent the different vegetation covers and geological locations within the domain: the Northeast Plateau (NEP) is mostly grassland that covers 32 percent of the landscape; the Mojave Desert (MJ) station located at the southeastern California is mostly shrubland with a 13.75 percent of vegetation cover; the San Joaquin Valley (SJV) is a major agricultural region, covered by irrigated cropland and pasture with about 23 percent of the land cover

by vegetation; and the Sierra Nevada Mountain County (MC) with 60 percent of the land covered by high-altitude vegetation (mainly evergreen needle leaf forest). The four basins cover a total of 240 stations. . Measurements from these basins were compared to the WRF-NOAH and WRF-ACASA simulation outputs to the nearest grid points. From each basin, one station was identified for further analysis (see Table II.1).

Table II.1: Selected sites from the Air Resources Board meteorological stations network.

Basin	Station id	Latitude	Longitude	Vegetation PFT
NEP	5751	41.959	-121.471	7 Grassland
MD	5780	33.557	-114.666	8 Shrubland
SJV	5783	35.604	-119.213	3 Irrigated Cropland and Pasture
MC	5714	38.754	-120.732	14 Evergreen Needleleaf Forest

Hourly, daily and monthly data were used for model evaluation in this study. Due to the nature of systematic errors from instrument and operation, however, data gaps are inevitable in surface observations. To avoid the missing data bias, only the days with complete sets of 24 hours of data are used for statistical analyses. The reason for this selection of data is illustrated in Fig. II.4. The black line in Fig. II.4 represents the hourly temperature observation for the Mojave Desert Station during June 2006. The red line represents the daily mean temperature from days with complete sets of 24 hours of temperature observation. The black line contains data with missing gaps, which influence the mean monthly temperature calculation. The monthly mean temperature changes if the monthly mean temperature is calculated using only days with the complete 24 hours rather than all data. This is due to significant amount of missing data during the daytime time that skews the monthly temperature toward the cooler nighttime temperature and results in a cold bias. By using only days with complete 24 hours of measurement for statistical analyses, the temperature bias

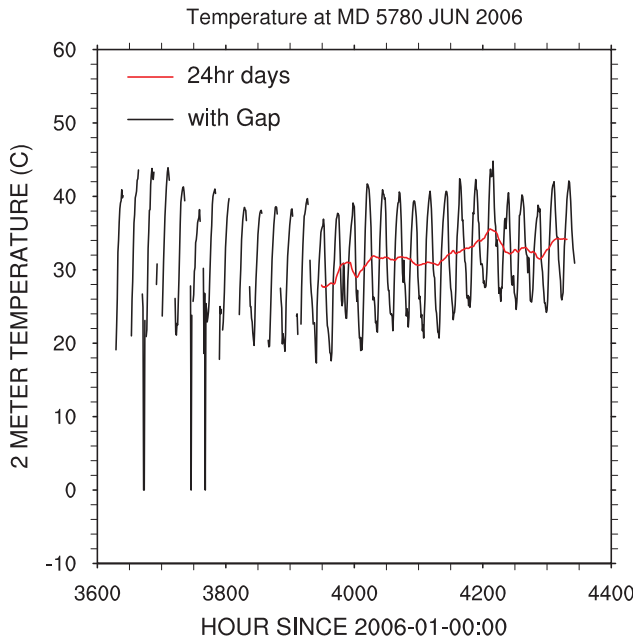


Figure II.4: Time series of the surface air temperature at Mojave Desert Station during June 2006. The black line represents the entire set of surface temperature observation with gaps presented. The red line represent the daily mean temperature calculated using only days with all 24 hours of observation available.

toward a certain period of the day is avoided.

One of the challenges in making the comparison between the simulations and the observations are the differences between the heights and station landscape of the observational stations and the heights of the simulations grid points. Many stations are within patches of specific landscape types that may differ significantly from the overall grid point landscape. Even more challenging is the fact that the WRF-ACASA simulations have outputs for the temperatures within a canopy, so for orchards or forests, the 2-meter height ("surface") simulation data are not expected to match the 2-meter height observations well. WRF-ACASA simulations at 2-meter height for the taller plant ecosystems represents temperatures within the plant canopy or in the understory; yet the observations from the ARB network are never in such locations, but rather they are over other surfaces not representative of the simulation

grid-point, and usually not even at the 2-meter height. The WRF-NOAH simulations do not suffer the same problems compared to the observations in terms of the 2-meter height falling in the understory, because the NOAH surface model is a big-leaf model, so the 2-meter height represents a height more similar in characteristics to the observations. Despite these significant shortcomings, to maximize the number of observations, the ARB data were chosen because of the large number of stations throughout the simulation domain. The results from year 2005 and year 2006 are similar, so only year 2006 is presented here.

3. Results and Discussion

The monthly mean temperatures near the surface over California from both model simulations are compared against the surface observations in Fig. II.5. The left panel shows the ARB data (gathered at approximately 10 m above the ground), where the white areas represent regions with missing observations. The WRF-NOAH and WRF-ACASA simulation outputs are represented in the center and right hand panels. The regions geographical complexity is highlighted by the spatial and temporal variations in the surface temperature. The warm summer and cool winter are typical of a Mediterranean-type climate. In addition to the seasonal variation, both WRF-ACASA and WRF-NOAH models are able to capture the distinct characteristics of the warm Central Valley and semiarid region of Southern California. The large flat Central Valley is dominated by Irrigated Cropland and Pasture, and surrounded by Cropland/Grassland Mosaic. The cold temperatures over the mountain regions are also visible from the surface temperature field. However, there are noticeable differences between the WRF-ACASA and the WRF-NOAH over the Central Valley.

During the month of February, there is a distinct feature of a colder Central Valley

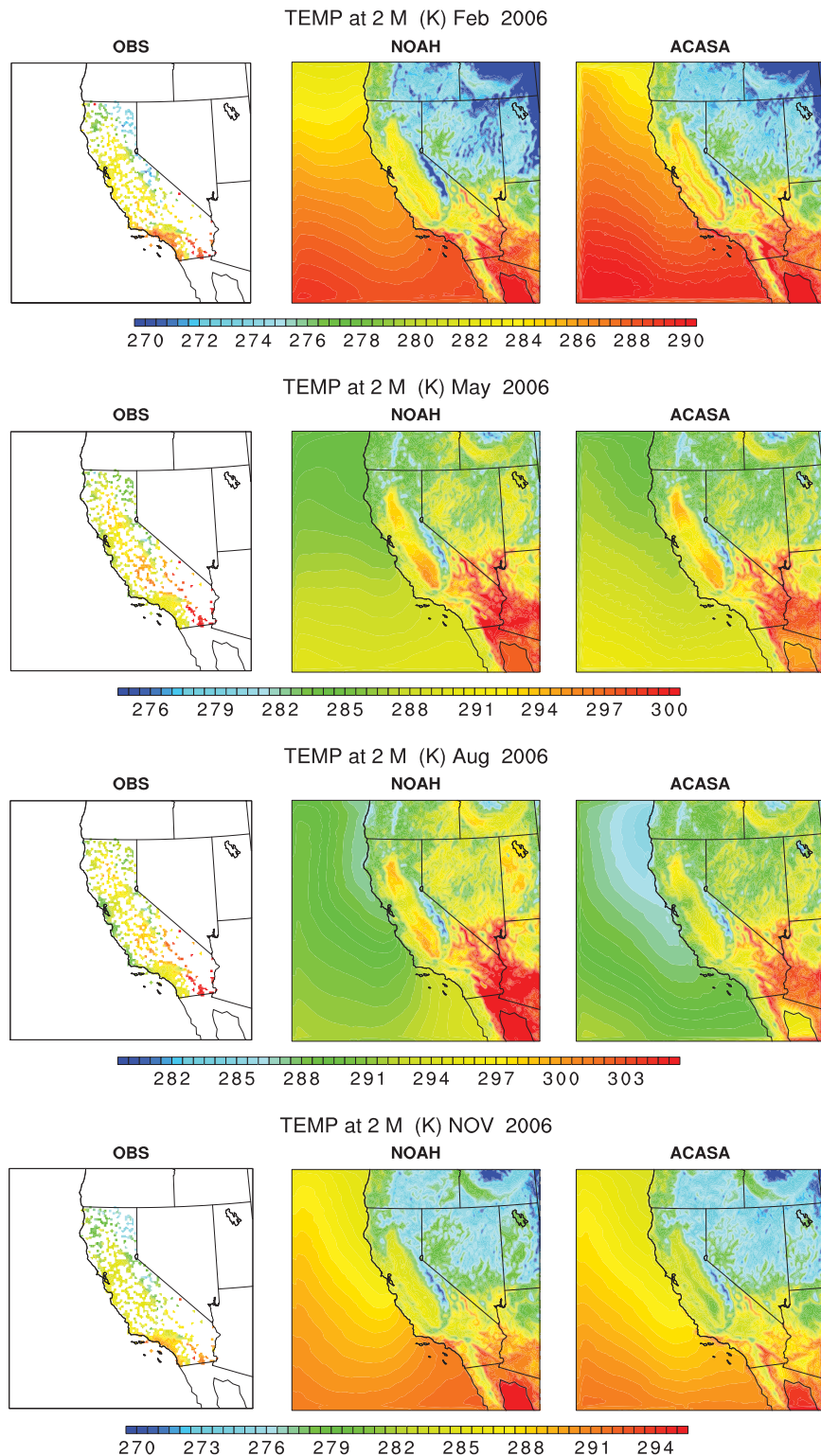


Figure II.5: Monthly mean surface air temperature simulated by WRF-ACASA and WRF-NOAH and for the surface observations for the months of February, May, August and November 2006.

surrounded by a slightly warmer region in the WRF-ACASA output. A similar effect is also visible in the month of November, when WRF-ACASA experiences a cold bias over the Central Valley. The temperature contrast of this region is mostly due to the differences in land cover type as well as leaf area index associated with the land cover (Fig. II.2). These two variables control important plant physiological processes in the WRF-ACASA model such as photosynthesis, respiration, and evapotranspiration. Lower plant leaf area index for the area surrounding Central Valley leads to less transpiration than in higher LAI Central Valley areas, which has higher partitioning of available energy to latent heat and less to sensible heat.

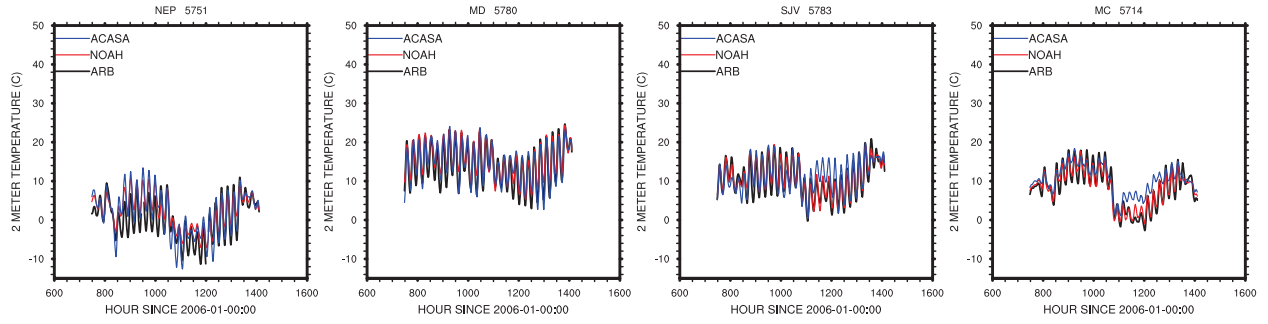
While the WRF-ACASA model is highly influenced by vegetation cover and the changes in LAI, the surface processes in WRF-NOAH rely heavily on the prescribed minimum canopy resistance for each of the vegetation type. Therefore, the contrast in temperature on over regions of different vegetation cover and leaf area index is more pronounced in the WRF-ACASA model than the WRF-NOAH model. The overall agreement between the model simulations from WRF-ACASA and WRF-NOAH agree well with the surface observation throughout the year. However, the WRF-ACASA experiences a cold bias over the high LAI region in the Central Valley during the month of August. Once again it should be noted that the WRF-ACASA output and the observations are generally not at the same height as the observation height, and the local vegetation type commonly differs from that surrounding the observation sites. The high complexity WRF-ACASA relies on the leaf area index to simulate plant physiological processes and energy budget. The unusually high LAI values, when compare to the remote sensing measured LAI, over the Central Valley during the summer months could result in overestimated of evapotranspiration over the region as

seen in the Central Valley bias. The WRF-NOAH model is less sensitive because it uses prescribed canopy resistances. This highlights the conundrum of advancing model physics—more sophisticated models become more exposed to input data quality as they become more representative of variations in land use type.

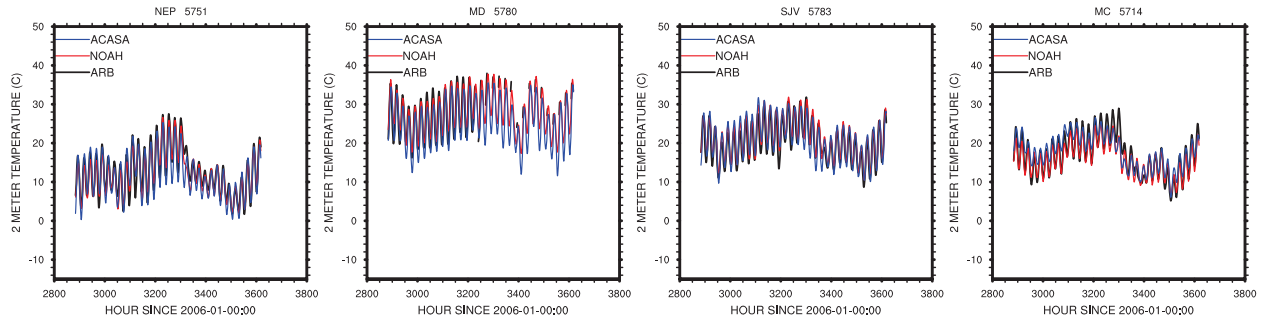
Figure II.6 shows time series of surface air temperature simulated by WRF-ACASA and WRF-NOAH as well observed at four different stations for the months of February, May, August, and November 2006. It shows that both WRF-ACASA and WRF-NOAH perform well in simulating the temporal pattern of temperature changes across the seasons and stations (four stations representing the Northeast Plateau Station, the Mojave Desert Station, San Joaquin Valley station, and the Mountain Counties Station). Even short time weather events are clearly detectable in the simulated temperature changes. One such example is the Northeast Plateau station during the month of November, when it experienced with a 20°C plunge in temperature followed by a warming of 10°C within five days. Both models are able to simulate this short time weather event.

There are differences between the WRF-ACASA and WRF-NOAH performances by time and location. While the model simulations from both models agree well with the surface observation during the cold season of February and November, they differed during the warmer months. During the month of May over the Mojave Desert station, the WRF-ACASA model started with good agreement with the surface observation but gradually differed with time. The daily minimums (or nighttime temperatures) during the month became cooler than the surface observation with time. During August, the nighttime temperatures were consistently 3 to 4°C cooler than the observed nighttime temperature. PBL heights at night using both NOAH and ACASA were the same as in minimum sigma-layer heights in

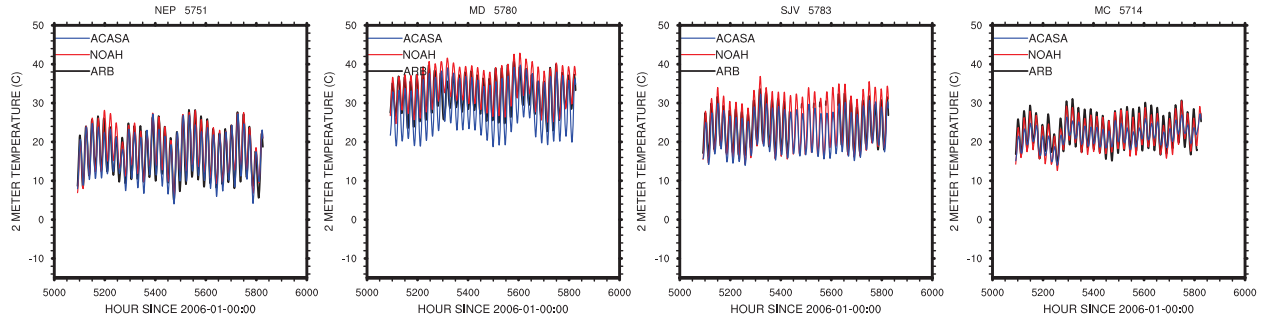
Timeseries 2 meter Temperature in Feb-2006



Timeseries 2 meter Temperature in May-2006



Timeseries 2 meter Temperature in Aug-2006



Timeseries 2 meter Temperature in Nov-2006

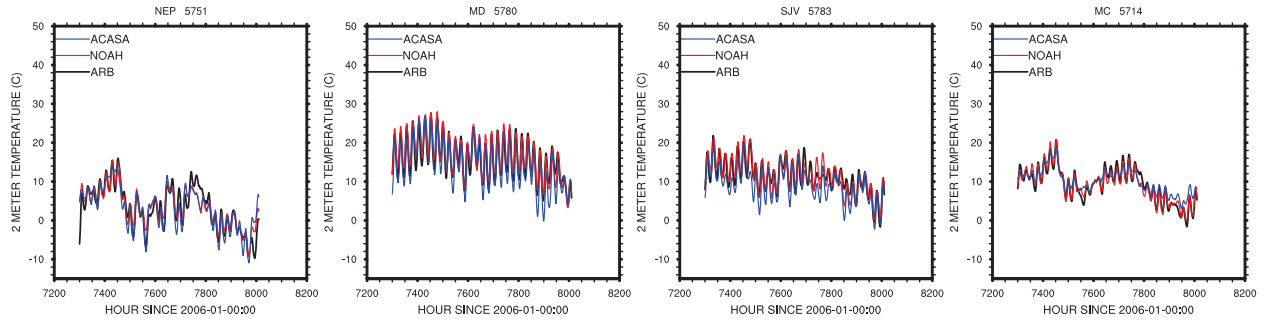


Figure II.6: Time series of surface air temperature simulated by WRF-ACASA and WRF-NOAH and for the surface observations for four different stations and for the months of February, May, August and November 2006.

WRF (Pyles, personal communication). This may be excessively shallow given observations suggesting nocturnal PBL heights over deserts to be on the order of 100 to 300 meters (Stull, 1988). ACASA results for nighttime cooling would be influenced to a cold bias if the PBL were too shallow, as the negative sensible heat flux would become "trapped" in the shallow inversion layer. ACASA is potentially more sensitive to this than NOAH and related, due to different minimum turbulent mixing thresholds for Monin-Obukhov similarity vs. higher-order turbulence calculations.

Figure II.7 examines the differences in the diurnal patterns from each station between the two land surface models over the four seasons. While the simulated diurnal temperatures from the two models fall mostly within the ± 1 standard deviation range from the surface diurnal temperature depending on the season and locations, there are some small differences in times and locations between the two. Both WRF-ACASA and WRF-NOAH perform exceptionally well over the Northeast Plateau station throughout the year, with the WRF-ACASA model performing slightly better than the WRF-NOAH model during the early winter mornings. In the summer and to lesser extent in autumn seasons over Mojave Desert, the WRF-ACASA model tended to underestimate the temperature during the early mornings. On the other hand, the WRF-NOAH model tended to predict summer temperature at 1.0 standard deviations above the mean most of the day. Further investigation shows that this morning cooling likely due to the canopy representation in the WRF-ACASA model. This might also be a factor in the slight overestimation of temperature during summer by the WRF-NOAH model. While both WRF-ACASA and WRF-NOAH assign a Shrubland plant functional type to the Mojave Desert site, the WRF-ACASA model also prescribed a 3-meter canopy height to the Shrubland vegetation type. Therefore, the WRF-ACASA

model takes longer in the morning to heat up the surface air temperatures of the Mojave Desert site, which is assumed to be within the canopy. As a result, it causes a lag of daytime temperature rise and cooler daily maximum temperatures than the observed values. As the summer ends, however, the diurnal patterns of the WRF-ACASA model once again compare well with the observation; falling within the ± 1 standard deviation range. Not visible in Fig. II.6, the diurnal patterns of WRF-ACASA over the Mountain County station show that the diurnal variations are smaller than the variations displayed by the surface measurement as well as by the WRF-NOAH simulations. As a result, the daytime temperatures during August fall below the observed temperature range. On the other hand, the WRF-NOAH model during the warmer months of May and August experiences a warm bias. The daytime temperatures of WRF-NOAH exceed the observed temperature range over San Joaquin Valley Station.

Further investigation into the temperature differences between the two models in time evolution and diurnal pattern reveals that these are results of differences in model representations of land cover type as well as canopy structure of the two models. Both models agree the best with the observation over the Northeast Plateau station. The site information indicated that this station is located over short vegetated grassland, which matches the land cover type assigned by the WRF model to that particular 8 km x 8 km grid-point. Even though the WRF-ACASA model uses a multilayer canopy representation for all its land cover types, there is no significant difference between the two models over this simple short grass canopy regardless the number of layers. However as the canopy become taller and more complex, the representations of canopy structure and plant physiology become more important. Most importantly, the correct representation of land cover is crucial. For exam-

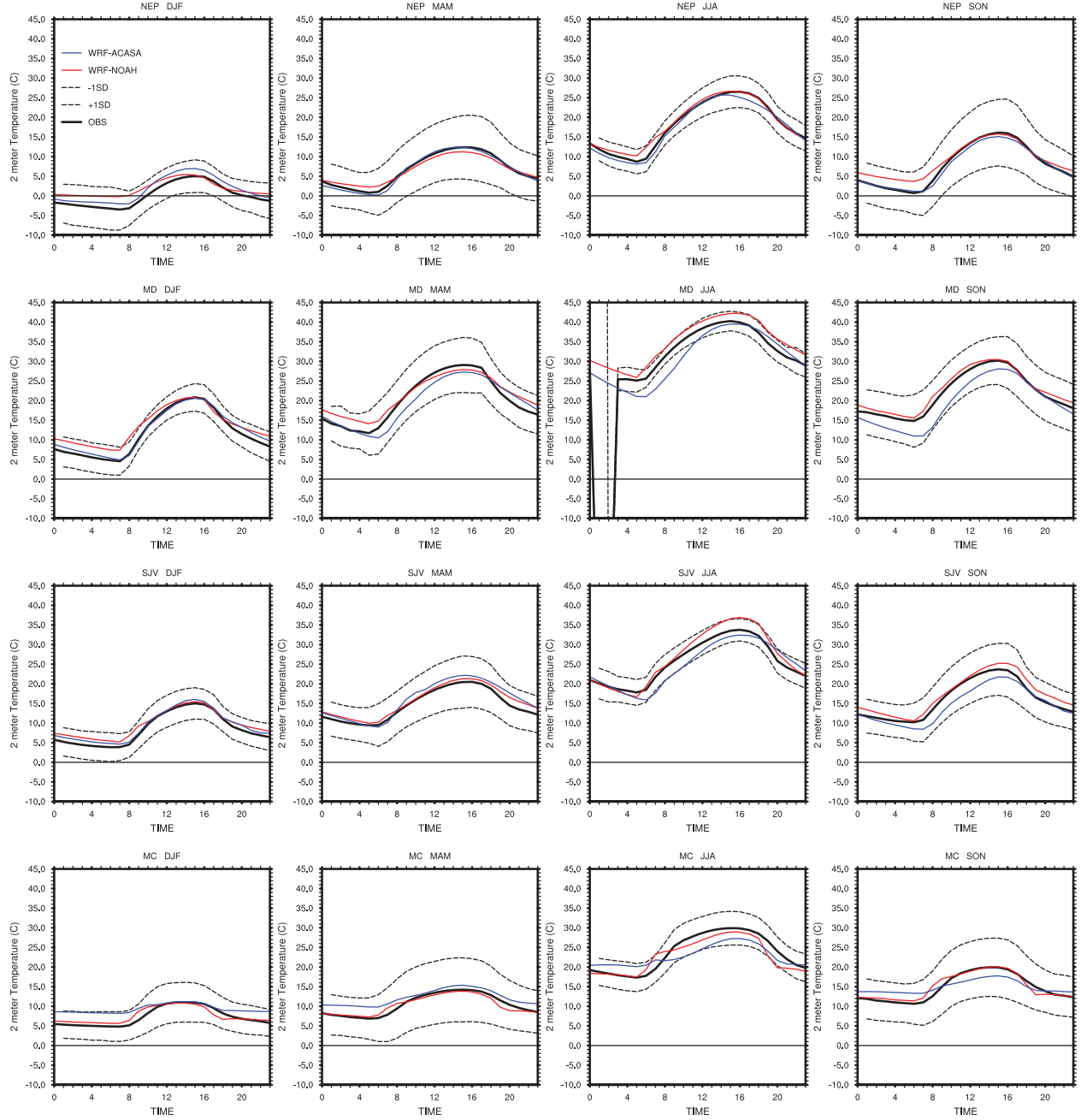


Figure II.7: Diurnal cycle of surface air temperature for each seasons for the Northeast Plateau, Mojave Desert, San Joaquin Valley, and Mountain County stations. The solid and the two dash black lines represent the surface observation and ± 1 standard deviation from the mean respectively. The WRF-ACASA results are showed in blue and the WRF-NOAH results are in red.

ple, the WRF model assigns a vegetation type of Evergreen Needleleaf Forest to the 8 km x 8 km grid point of the Mountain County Station. However, a closer look at the MC station

shows that the stations is actually located at the edge of the forest over a large clear-cut short grass area instead of within the forest as assumed by the WRF-ACASA model, and above a single big leaf rough surface by the WRF-NOAH model. This mismatch of land cover type seems to be more problematic to the WRF-ACASA model than the WRF-NOAH model in its temperature simulations, probably because the single-leaf NOAH description is closer to a short grass area for observed air temperatures at this site, than temperatures in the understory of a forest as in ACASA.

While a single layer land surface model is used in the WRF-NOAH, the WRF-ACASA assumes a 17-meter canopy height with 10 vertical layers for this vegetation type. The surface air temperature simulated by the WRF-ACASAs multilayer canopy structure and its radiation transfer scheme is therefore a surface air temperature within the canopy with overhead shading from tall trees, and with the microclimatic influences of understory temperature and humidity. Due to less direct heating from shortwave radiation, the daytime temperatures within the canopy layers as simulated by the WRF-ACASA model during the warm seasons of May and August are respectively lower than the surface air temperature measured over a short grass area near the forest. In addition, the Needleleaf forest land cover type used in the WRF-ACASA model experiences turbulent transport and mixing of energy, moisture, gas, and momentum within the canopy layers as results from the higher-order turbulent closure scheme. Therefore, unlike environmental condition at the station at 2-meter height above the short grass area, the air parcel at 2-meter height within the WRF-ACASA tall canopy experiences a drastic reduction in nighttime heat loss. Hence, the surface air temperatures of the WRF-ACASA simulation are higher than the surface observation during the nights of February and November. Such details of canopy structures and their associated thermody-

namic processes, however, are lacking from the single layer WRF-NOAH model, and do not match the observational site characteristics.

As mentioned before, the WRF-ACASA model tends to underpredict temperature observations during early summer morning in the Mojave Desert and the WRF-NOAH model tends to overpredict temperature all day. The prolonged cooling in the morning simulated by the WRF-ACASA model is associated with the low vegetated cover over shrublands. In this situation, more energy is lost from the surface to the atmosphere. In general, the model performances from WRF-ACASA and WRF-NOAH vary depending on the season and the vegetation cover. The cool biases seen in desert regions may also be due to the nocturnal inversion issue described earlier.

Figure II.8 shows scatter plots of simulated monthly surface air temperature from the WRF-ACASA and WRF-NOAH model versus observations sorted by seasons for the four basins defined previously. Each of the points represents a monthly average for one station in the specified basin, and the colors indicate seasons. Least squares regression of the seasonal data shows that both model simulations approach a 1:1 line relationship with the observations. There are some small differences in performances between the two models depending on seasons and locations. This collective analysis of all stations from the four basins shows that although there are some cold biases over the Mojave Desert station the models perform well across the entire basin.

Table II.2 and Fig. II.9 present the statistical analysis of the WRF-ACASA and WRF-NOAH near-surface temperature outputs for each of California's 13 basins. Statistical values of R-square value, Root Mean Square Error (RMSE), and Degree of Agreement are calculated for each of the basin for each of four seasons. The Coefficient of Determination or (R-square)

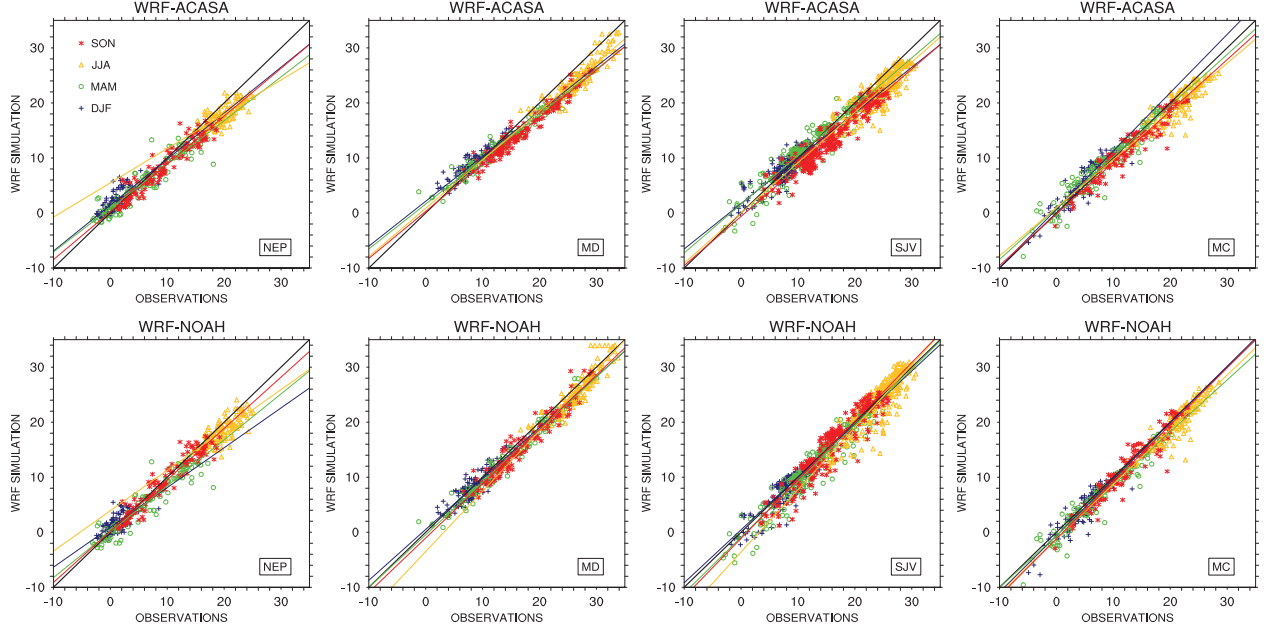


Figure II.8: Time series of surface air temperature simulated by WRF-ACASA and WRF-NOAH and for the surface observations for four different stations and for the months of February, May, August and November 2006.

represents the correlation of the model simulation with the surface observation. The RMSE shows the relative errors of the model simulation against the observation, while the Degree of Agreement is a statistical method to assess the agreement between the model simulations with the surface observation.

Overall, both of the models have a high degree of agreement with all 700 observation stations within the 13 ARB basins during Winter, Spring, and Autumn. The dry summer season is more problematic than the other seasons for both of the models and more so for the WRF-ACASA model over coastal regions such as South Coast, San Diego, and San Francisco basins. This is most noticeable in the RMSE values for WRF-ACASA over the low vegetated regions of Great Basin Valley (GBV), Salton Sea (SS), and San Diego (SD), which increased dramatically during the warm season. While the degree of agreement for the San Francisco Basin (SFB) during the wintertime is high with values above 0.8 for both models, the R-

Table II.2: Statistical between the models and observations for the 13 ARB basins by season: December, January and February (DJF); March, April and May (MAM); June, July and August (JJA); September, October and November (SON).

Season	Basin	Degree of				Degree of	
		R-square	RMSE ($^{\circ}\text{C}$)	Agreement	R-square	RMSE ($^{\circ}\text{C}$)	Agreement
WRF-NOAH WRF-NOAH WRF-NOAH WRF-ACASA WRF-ACASA WRF-ACASA							
DJF	SCC	0.831671	1.73878	0.91687	0.716923	2.46986	0.821745
MAM	SCC	0.98397	1.32221	0.987497	0.806324	2.09018	0.910685
JJA	SCC	0.603668	2.03934	0.93101	0.532604	2.2107	0.899527
SON	SCC	0.817867	1.79367	0.934533	0.8446	1.7037	0.951894
DJF	SJV	0.996713	1.49348	0.996796	0.944033	1.55048	0.969605
MAM	SJV	0.989379	1.81218	0.991555	0.983285	1.70317	0.991714
JJA	SJV	0.981085	2.24522	0.97525	0.790353	2.77545	0.71053
SON	SJV	0.995999	1.9562	0.997329	0.836214	2.83981	0.88651
DJF	NCC	0.738797	1.4336	0.885708	0.624952	2.15347	0.703579
MAM	NCC	0.977027	1.21572	0.98831	0.804917	1.65924	0.952791
JJA	NCC	0.891338	1.91748	0.968166	0.796365	1.78896	0.947152
SON	NCC	0.945243	1.53172	0.96535	0.961512	1.16758	0.986446
DJF	SC	0.967272	1.88247	0.966178	0.913497	1.64677	0.948648
MAM	SC	0.993072	1.55349	0.993048	0.981621	1.37131	0.990378
JJA	SC	0.588722	2.06404	0.831568	0.580935	3.4954	0.595515
SON	SC	0.980249	1.89105	0.988638	0.710668	2.40559	0.831628
DJF	SV	0.986383	1.1287	0.991035	0.925806	1.28074	0.964948
MAM	SV	0.980696	1.29392	0.98801	0.981402	1.21403	0.992255
JJA	SV	0.99783	1.64352	0.997999	0.752783	2.453	0.67696
SON	SV	0.997573	1.46927	0.99837	0.881367	2.09812	0.919228
DJF	SD	0.951017	1.46921	0.96677	0.764242	1.9857	0.85756
MAM	SD	0.966413	1.15405	0.975935	0.926948	1.26534	0.973743
JJA	SD	0.487301	2.05678	0.768834	0.554737	3.64936	0.612857
SON	SD	0.875988	1.47285	0.946929	0.564617	2.1236	0.800983
DJF	GBV	0.813173	2.7741	0.952817	0.754106	3.40534	0.908663
MAM	GBV	0.93591	2.36249	0.962156	0.936978	2.20798	0.969805
JJA	GBV	0.853203	2.64441	0.856085	0.804406	3.01706	0.739935
SON	GBV	0.92474	2.2518	0.966767	0.917856	2.34017	0.963998
DJF	SFB	0.185791	1.77587	0.876986	0.284025	2.0497	0.886728
MAM	SFB	0.913346	1.51517	0.976113	0.63263	2.0793	0.941796
JJA	SFB	0.743593	1.93917	0.924286	0.495629	3.10351	0.768198
SON	SFB	0.950796	1.4078	0.981719	0.629486	1.98632	0.848947
DJF	SS	0.496889	1.86463	0.876449	0.727061	2.19616	0.901978
MAM	SS	0.994308	1.2895	0.996386	0.910398	1.67741	0.964686
JJA	SS	0.679887	2.58393	0.790626	0.391227	2.63565	0.684046
SON	SS	0.991819	1.59417	0.996416	0.769102	3.04378	0.865084
DJF	NEP	0.813234	1.46407	0.947417	0.762997	1.81746	0.897551
MAM	NEP	0.926788	2.14003	0.968855	0.928542	1.96821	0.976753
JJA	NEP	0.743007	2.09303	0.861164	0.59725	2.52024	0.769247
SON	NEP	0.987654	1.54218	0.99447	0.936724	1.83687	0.972525
DJF	MD	0.991988	1.37581	0.996475	0.904003	1.27348	0.971514
MAM	MD	0.969527	1.62038	0.982023	0.921582	1.88437	0.969443
JJA	MD	0.957873	1.99593	0.960473	0.74645	2.84406	0.72887
SON	MD	0.948833	1.90569	0.966272	0.824341	2.55955	0.884061
DJF	MC	0.983341	1.61558	0.982671	0.945083	1.75623	0.952361
MAM	MC	0.965586	1.87782	0.977757	0.991983	1.76668	0.996098
JJA	MC	0.898993	2.1299	0.893741	0.830306	2.39603	0.834615
SON	MC	0.982515	1.81802	0.987068	0.963089	1.81886	0.977584
DJF	NC	0.890632	1.45055	0.96326	0.751115	1.89727	0.919472
MAM	NC	0.677484	3.47913	0.872094	0.64897	3.17359	0.911504
JJA	NC	0.631845	2.60202	0.7467	0.631316	2.92231	0.629611
SON	NC	0.948986	1.76809	0.976128	0.876387	1.87418	0.951667

square values show that there is little correlation between the model simulations and the surface observations. It could be due to the small range of observation data. Overall, the temperature simulations from both models agree well with the observations where the degree of agreement is high. Previous examination on a station-by-station basis also reveals that there is a mismatch in vegetation cover between the WRF models and the actual surface station, such as the Mountain Counties station. These mismatches introduce errors that are not due to model physics, and they contribute to some of the low R-square and high RMSE values in the collective study.

Figure II.10 shows time series of surface dew point temperature over the same four stations. The dew point temperature is another important variable that influences the land surface interaction with the atmosphere because it indicates condition for condensation. The disparities between the WRF-ACASA and WRF-NOAH models are more distinct in the dew point temperature than in the surface temperature. While both models perform well with the surface temperature simulation, the WRF-ACASA model outperforms the WRF-NOAH in simulating the dew point temperature especially over the San Joaquin Station and during May for the Mojave Desert station. This could be due to the complex physiological processes in the WRF-ACASA model that allow a better simulation of the hydrological conditions. Although the vegetation covers over these two regions are sparse, the multilayer canopy structure in the WRF-ACASA model is likely to retain moisture longer within the canopy. Therefore, the dew point temperature from WRF-ACASA is better simulated than the WRF-NOAH model, which is a single canopy layer model. However, both models have difficulty over the Mojave Desert Station where they underestimated the dew point temperature as much as 15°C during February and November. Similar to the surface temperature

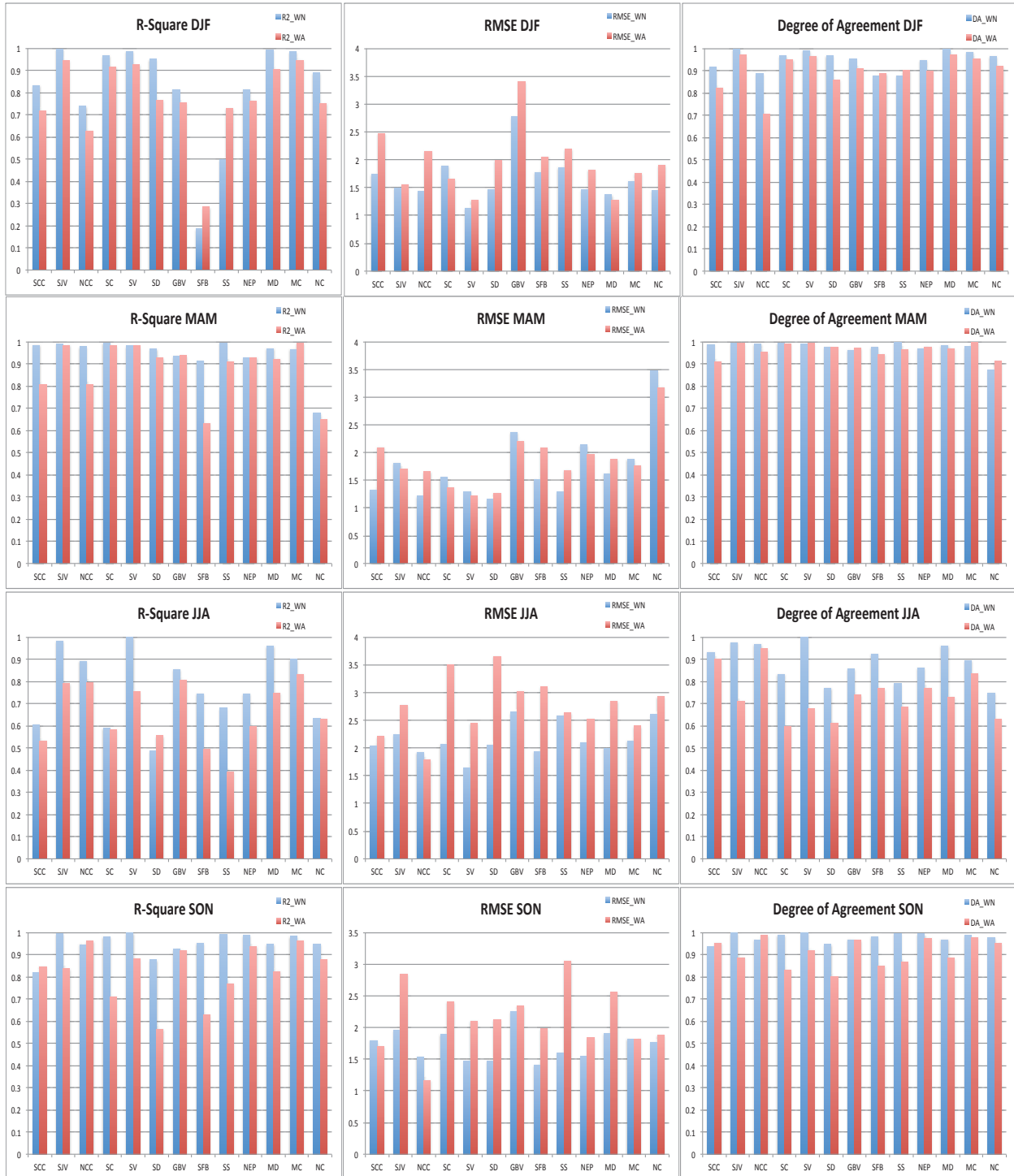


Figure II.9: Statistical analysis of two model simulations versus observed for R-square, Root Mean Square Error (RMSE), and Degree of Agreement for the four different seasons.

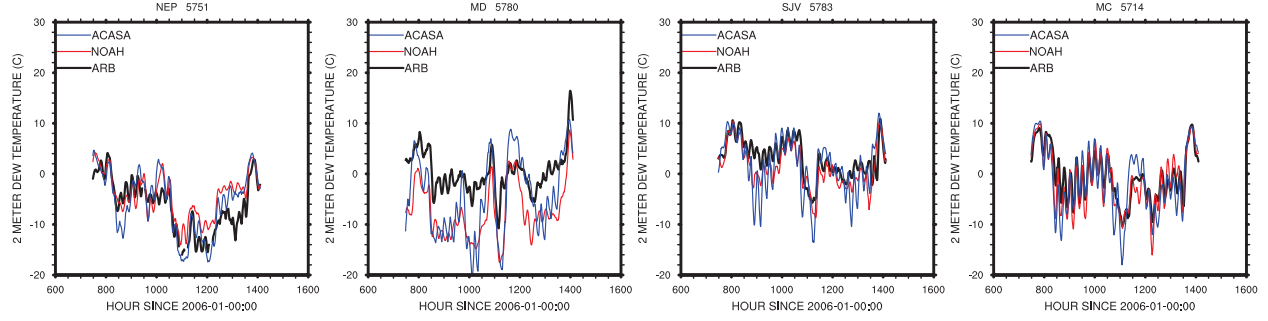
analysis, both models performed best over the Northeast Plateau station with well-matched land cover type and simple canopy structure of a short grass. In general, the dew point temperature simulations from the WRF-ACASA model match closely with the observations in magnitude and timing.

Figure II.11 presents diurnal patterns of surface dew point temperature for the four different seasons. Unlike for the surface air temperature, there is relatively little diurnal variation in the surface dew point temperature throughout the seasons and locations. The simulated dew point temperatures in both WRF-ACASA and WRF-NOAH are functions of surface pressure and surface water vapor mixing ratio. Since the surface pressure does not change dramatically throughout the day, changes in dew point temperature are mainly due to fluctuations in water vapor mixing ratio. Once again, the dry arid and low vegetated Mojave Desert site is problematic for both WRF-ACASA and WRF-NOAH models.

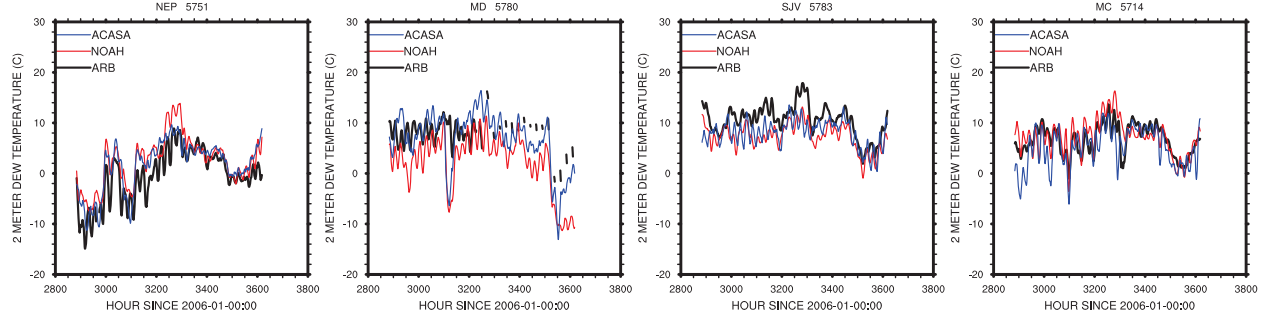
Figure II.12 shows scatter plots of Compared to the surface temperature, Fig. II.12 shows that the model simulations on dew point temperature exhibit more scatter than for other observational sets examined thus far. Although Fig. II.10 seems to indicate that for Mojave Desert Station, WRF-ACASA has a better agreement with surface observations, the seasonal patterns for the entire Mojave Desert Basin show that both WRF-ACASA model and WRF-NOAH performances are comparatively poor in this sparsely vegetated region. The choice of land surface model did not affect the model simulation, hence the problem could be in the atmospheric processes in WRF and not in the land surface processes.

This could be the result of the assumption of horizontal homogeneous in each of the 8 km x 8 km grid cell used in both WRF-ACASA and WRF-NOAH model. A single model grid cell that is not representative of all stations could be representing several observation stations

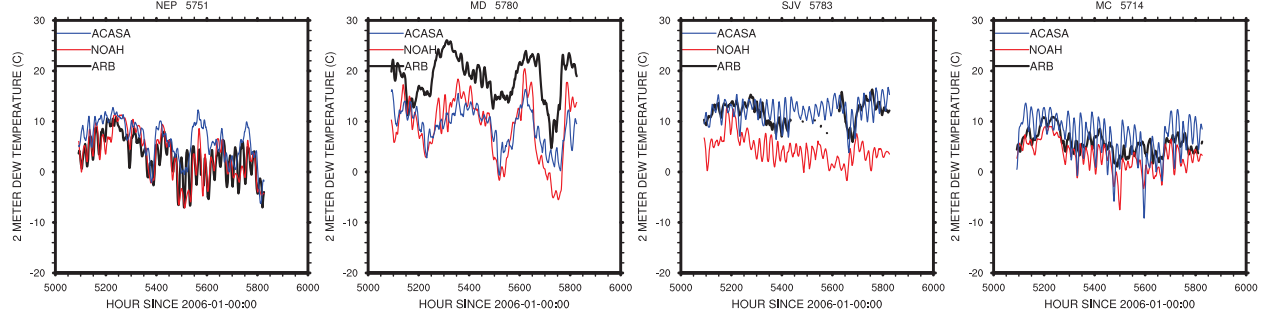
Timeseries 2m Dew Point Temperature in Feb-2006



Timeseries 2m Dew Point Temperature in May-2006



Timeseries 2m Dew Point Temperature in Aug-2006



Timeseries 2m Dew Point Temperature in Nov-2006

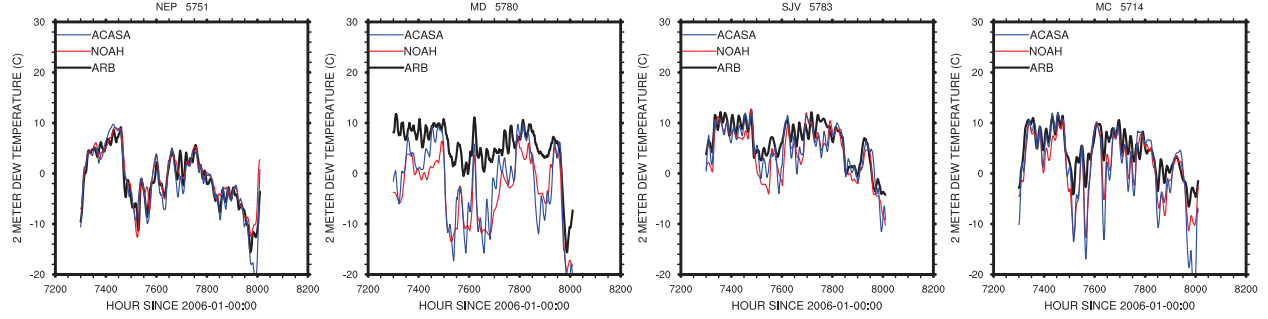


Figure II.10: Time series of Dew point model predictions and observations for four basins during February, May, August, and November.

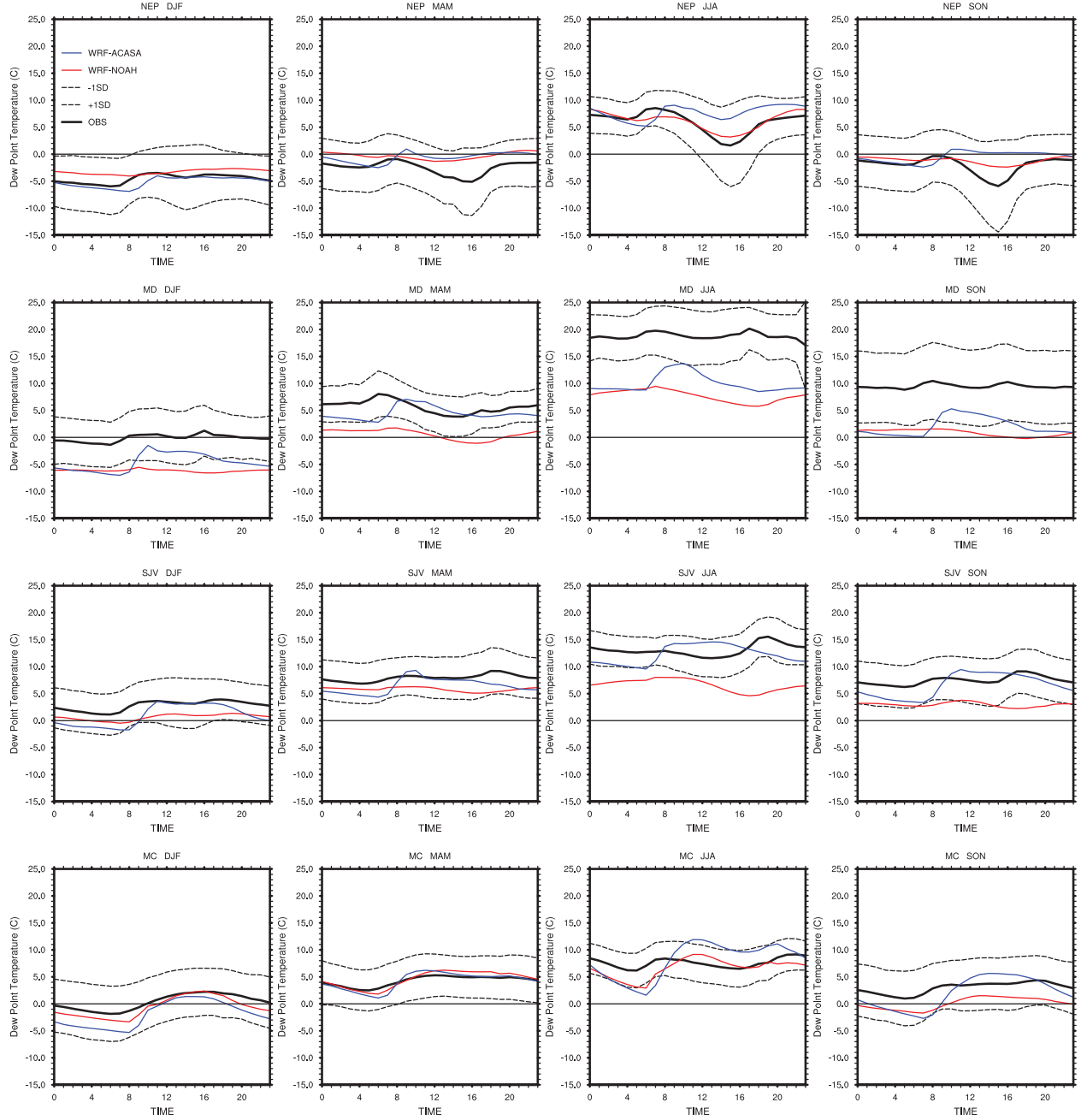


Figure II.11: Mean diurnal dew point temperature trends for the four seasons and the four air basins: Northeast Plateau, Mojave Desert, San Joaquin Valley, and Mountain County stations.

with different microclimatic conditions. This is especially important when the shrublands in the Mojave Desert Basin have different degree of canopy openness. Surprisingly, unlike the previous analysis, Fig. II.12 shows that the WRF-ACASA model underperforms relative

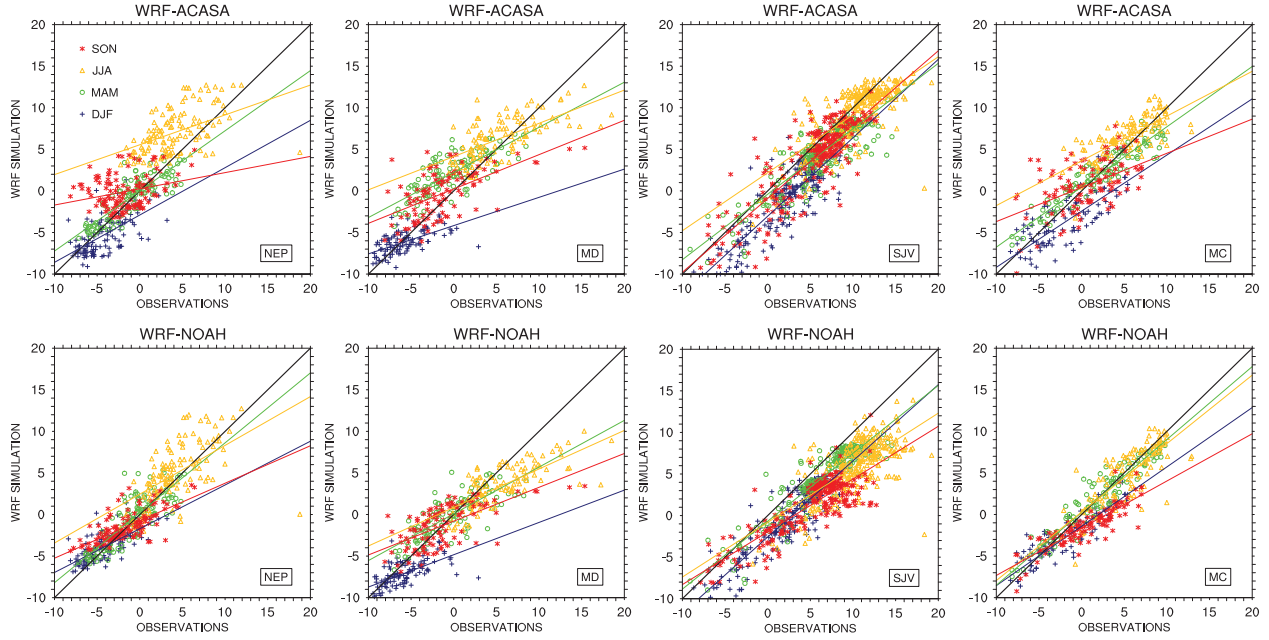


Figure II.12: Same as Fig. II.8 but for surface dew point temperature.

to WRF-NOAH over the Northeast Plateau basin, with the correlation between the model simulation and the observations lower than WRF-NOAH.

Figure II.13 compares the relative humidity from both WRF-ACASA and WRF-NOAH with the surface observation for four different locations during February, May, August and October of 2005. Except for Mountain Counties station, both models fall mostly within the 1 standard deviation range with the WRF-ACASA model showing somewhat better agreement than the WRF-NOAH model over the Mojave Desert Station. The WRF-NOAH model underestimates the relative humidity for Mojave Desert and San Joaquin Valley throughout the year. Although there is a land cover mismatch between the actual station and the model, the higher relative humidity values in the WRF-ACASA simulation compared with WRF-NOAH during the warm season reinforce that the multi-layer canopy structure and higher order turbulent closure scheme help the vegetation parameterization to simulate the retention of more moisture within the canopy layers.

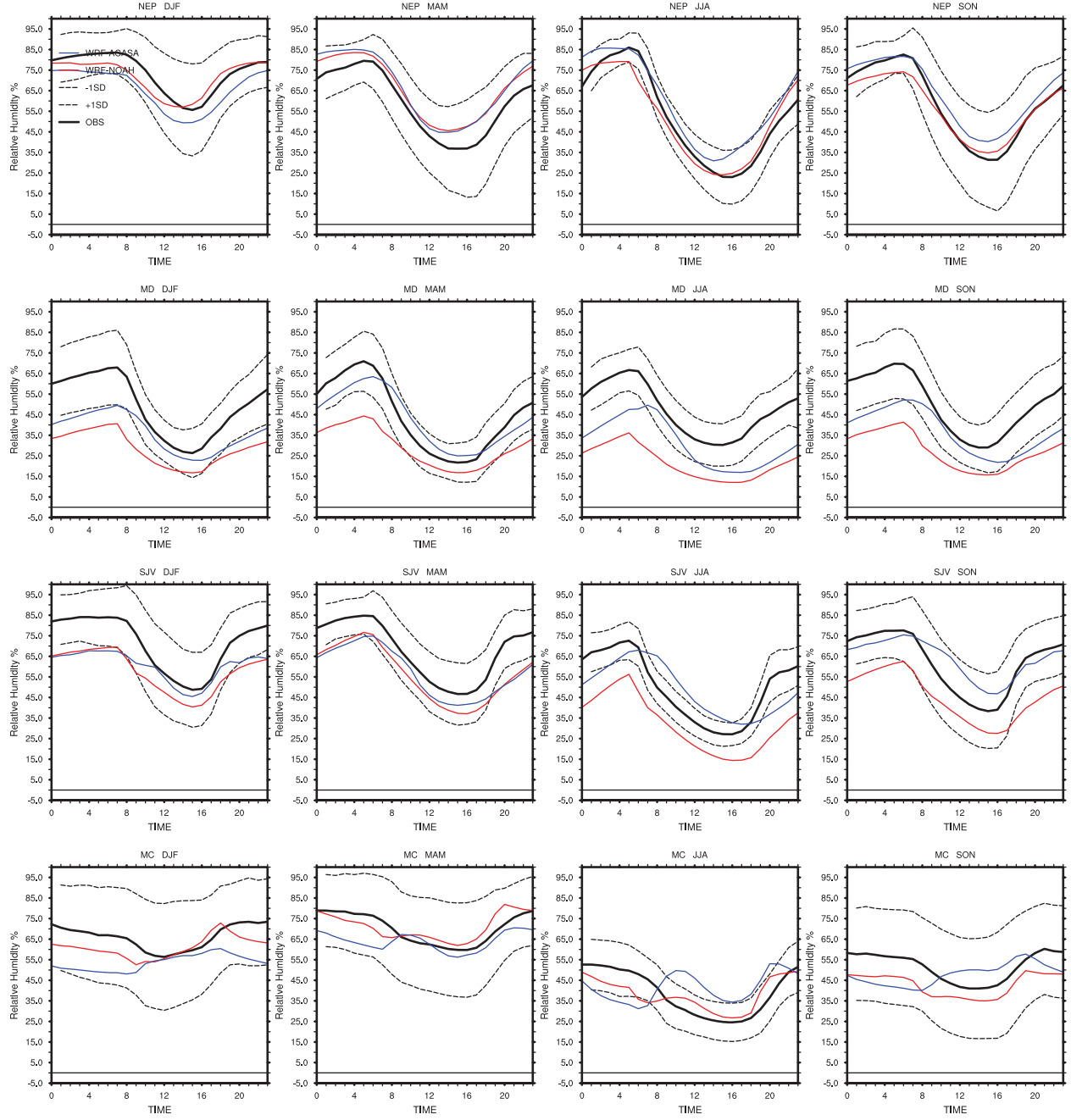


Figure II.13: Same as Fig. II.8 but for surface relative humidity.

The land cover mismatch in the model could lead to overestimation of the relative humidity in areas of low vegetation cover. The high LAI values over the Central Valley and the assumption of horizontal homogeneous with one dominant vegetation cover cause the WRF-ACASA model to allow too much water to be preserved within the canopy layers dur-

ing the warm August conditions instead of evaporating the water rapidly. As a result, it overestimated the daytime relative humidity.

Figure II.14 shows a Taylor diagram of monthly mean surface air temperature, dew point temperature, relative humidity, wind speed, and solar radiation simulated by WRF-ACASA and WRF-NOAH for all 730 stations in California. Except for the wind speed, the Taylor diagrams for the four different seasons shows that simulations from both models agree well with the surface measurement. The surface air temperature, with high correlations, low RMSEs, and matching variability, is most accurately simulated by both models when compared to the surface observations. While the WRF-NOAH model is slightly better in standard deviation for the air temperature, the WRF-ACASA is slightly better for dew point temperature. Relative humidity, on the other hand, shows low correlation and high root mean square error from both models. These high root mean square errors and poor correlations could be attributed to model assumption of homogenous vegetation and leaf area cover for each grid cell, especially over low vegetated regions as previously mentioned.

4. Conclusion

This study compares and evaluates the two different approaches and complexity of land surface models ACASA and NOAH embedded in the state-of-art mesoscale model WRF as they simulate the surface conditions over California on a regional scale. With vast differences in land cover, ecological and climatological conditions, the complex terrain of California provides an ideal region to test and evaluate the two land surface models. Analysis of model simulations for 2006 from both WRF-ACASA and WRF-NOAH were compared with hundreds surface observation stations from the California Air Resources Board network. While

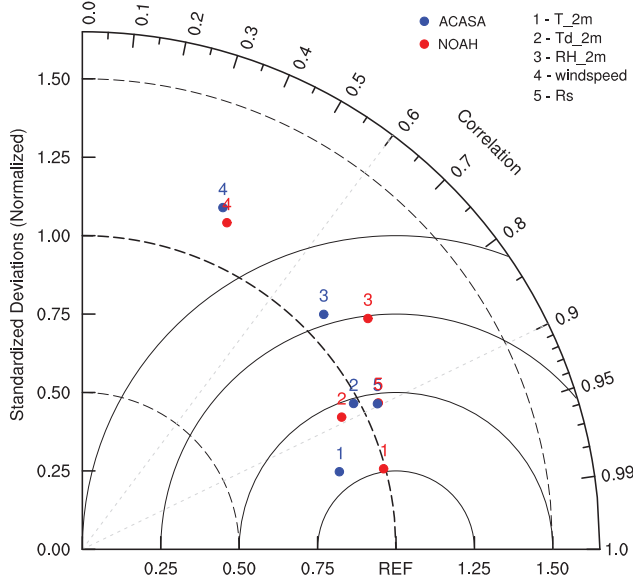


Figure II.14: Taylor diagram of monthly mean surface air temperature, dew point temperature, relative humidity, wind speed, and solar radiation for both WRF-ACASA and WRF-NOAH for all ARB stations. WRF-ACASA is represented by blue dots and WRF-NOAH by red dots.

both ACASA and NOAH land surface models use four soil layers for below ground representation, the WRF-NOAH uses a single layer "big leaf" to represent the surface layer for all land cover types. In all single-layer models such as NOAH, there is no interaction and mixing within the canopy regardless of the specified vegetation type. As a result, the NOAH land surface model assumes that the entire canopy has similar physical and physiological properties as a single big leaf. In contrast, the ACASA land surface model use multi-layer canopy structure that varies according to different land cover type. The complex physically based model includes the intricate surface processes such as canopy structure, turbulent transport and mixing within and above the canopy and sublayers, and the interactions between the canopy elements and the surrounding air. Light and precipitation from the atmospheric layers above are intercepted, infiltrated, and reflect within the canopy layers and along with other meteorological and environmental forcings to drive plant physiological responses. In ad-

dition, the higher order closure scheme in the model allows both down- and counter-gradient transport of carbon dioxide, water vapor, heat, and momentum within and above the canopy layers and interact with the atmosphere. Through plant evapotranspiration, photosynthesis, respiration, and roughness length, the surface ecosystem transforms the environmental conditions and influences the atmosphere processes above such as modifications on surface temperature, dew point temperature, and relative humidity. Therefore, compared to the WRF-NOAH with simplified surface and ecosystem representation, the WRF-ACASA coupled model presents a detailed picture of the physical and physiological interactions between the land surface and the atmosphere. However, when compared to 2-meter near surface observations, WRF-ACASA simulation output may have the qualification that it could be simulating understory microclimate, compared to WRF-NOAHs big leaf with no understory, and the ARB stations that are usually over short grasses or bare surfaces.

The comparisons between model simulations and surface observations show that the WRF-ACASA model is able to soundly simulate surface and atmospheric conditions. Its simulation of temperature, dew point temperature, and relative humidity agree well with the surface observations overall. While overall both WRF-ACASA and WRF-NOAH simulations agree well with the surface observations, model performances vary between the two approaches of land surface representations depending on surface and atmosphere conditions. For example, during the cold and wet winter, surface temperature, dew point temperature and relative humidity from both models have high degree of agreement as well as high correlation with the surface observations. However, as the season starts to warm up, a temperature bias for WRF-ACASA in certain regions begin to increase. Maximum daytime temperatures in the WRF-ACASA simulations are systematically lower than the observed daily maximum

during the warmer months over low vegetated regions such as the Mojave Desert. This temperature bias is likely due to the surface representation in the WRF-ACASA model producing too much evaporative cooling from high leaf area index. For the shrubland vegetation with low leaf area index, the leaf area indices for each of the sub-canopy layers are further reduced. The higher order turbulent closure scheme more effectively reflects the energy transport away from the surface level to induce heat loss. These thermodynamically processes in the WRF-ACASA model allow describing the prolonged period of cooling in early mornings. As a result, the high daytime temperature is underestimated in the multi-layer model.

The analysis of dew point temperature and relative humidity on the other hand shows that these more detailed physical processes in WRF-ACASA seem to improve the dew point temperature and relative humidity simulations compared to the WRF-NOAH model. The process parameterizations appear to allow the retention of more moisture within the canopy layers as well as the distribution of moisture within and above the canopy. Compared to the WRF-NOAH model, the WRF-ACASA model has a more complex and detailed canopy and plant physiological process parameterizations to more realistically represent the ecosystem-atmosphere interactions. The model simulations of the two models agree well with the surface observations through time and space as showed in temperature, dew point temperature and relative humidity.

Overall, when compared to the simple single layer WRF-NOAH model, the WRF-ACASA model has greater model complexity to present a more detailed picture of how the atmosphere and ecosystems interact including ecophysiological activities such as photosynthesis and respiration without decreasing the quality of the output. Finally, this study describes the newly coupled WRF-ACASA model and its performance in simulating the surface conditions over

the complex terrain and vegetated regions of California. The physical and physiological processes in the WRF-ACASA model highlight the effect of different land surface components and their overall impacts on atmospheric conditions. In addition, the WRF-ACASA model provides the opportunities to study more questions involving the ecosystem responses to the atmospheric impacts such as the contribution of irrigation on canopy energy distribution, land use transformations, climate change, and other dynamic and biosphere-atmospheric atmosphere interactions.

Chapter III

The Role of Surface Representations: Leaf Area Index, Land Use

Covers, and Model Complexity in Calculating Evapotranspiration

1. Introduction

The land surface is well recognized to be a crucial component that governs the evolution of atmospheric processes. Complex interactions between the atmosphere and land surface drive energy, momentum, heat, water, and gas exchanges that ultimately modify the atmospheric motions. Much of these effects are attributed to the presence of vegetation in the surface layer (Potter et al., 1993; Dickinson and Henderson-Sellers, 2006; Dirmeyer et al., 2010). Vegetation is an extensive and dynamic component of the land surface layer, representing 99% of the mass of surface biota. Effects of climate on vegetation phenology have long been a research focus in the ecology and plant science communities (Levitt et al., 1980; Jones, 1992). Climate conditions such as temperature, humidity, and radiation strongly influence plant physiological responses in photosynthesis, respiration, transpiration, and energy flux. However, the influences of vegetation on the climate and atmospheric processes are less well understood. Reasons for this include numerical complexity and related challenges that arise from properly representing the exchanges between the physiologically active vegetated land surface and the atmosphere. In the recent years, research interests in land and atmospheric interactions have grown considerably, benefitting from the developments of atmosphere and land surface models as well as advanced instrumentation and field campaigns. Because of the importance of vegetation in the land surface layer, land surface parameterization in

atmospheric models must emphasize the processes associated with vegetation.

There are two important and potentially related factors that characterize the biosphere-atmosphere interactions: land cover type and the amount of vegetation. Differences in land use cover ecosystem types can dramatically influence land surface processes through such features as surface roughness, canopy transmission of light, physiological responses to environmental controls, and interception of precipitation. The second factor is leaf area index, which is a representation of the areal amount of vegetation over a given area of land. Leaves provide surface area for photosynthesis, respiration, and transpiration that control the moisture and energy exchanges with the atmosphere. Specifically, the leaf area index (LAI) strongly influences the amount of absorbed solar radiation and its transmutation into other energy exchanges such as sensible and latent energy. Studies using General Circulation Models (GCMs) have demonstrated the importance and influence of LAI on the short- and long-term evolution of surface hydrology, including snowpack evolution, soil wetness, and evapotranspiration (Chase et al., 1996; Pitman et al., 1999; Bounoua et al., 2000; Hales et al., 2004). Gao et al. (2008) further examined the sensitivities of land surface climate to the changes in spatial distribution of LAI from different treatments of surface properties: natural inter-annually varying vegetation versus a 10-year climatological annual cycle. Overall, the study showed that observed inter-annually varying vegetation properties led to improvement in estimations of surface fluxes such as latent heat and surface evapotranspiration, regional surface temperature, and spatial distribution of precipitation.

Reference evapotranspiration and actual evapotranspiration are the potential and actual losses of water to the atmosphere by transpiration from plants and evaporation from both soil and vegetation, respectively. The accurate estimations of these two variables are crucial

for optimal water management practices as well as drought monitoring. They are especially important for regions with limited water availability and high water demand, such as the Central Valley of California. Water availability has been and will continue to be one of the most important issues facing California for years and perhaps decades to come. Standardized reference evapotranspiration (ETo) is independent of vegetation type, leaf area index and canopy structure because it is an estimate of the evapotranspiration from a virtual surface of vegetation with known canopy and aerodynamic resistance (Allen et al., 2005). Although ETo is technically defined for a virtual surface, it provides a good estimate of the evapotranspiration from a surface covered by 0.12 m tall cool-season grass with adequate water supply. Therefore, vegetation representations of most plants are by definition not directly included in estimating ETo. However, the response of ETo to environmental variables is closely linked to the response of actual evapotranspiration. Reference evapotranspiration therefore provides a type of environmentally controlled physiological standard model that is useful in assessing potential environmental controls on actual evapotranspiration. In reality, the land surface is covered by diverse vegetation ranging from grasslands to mixed woodlands, to forests; their existence at any location is a result of the complex interaction of anthropogenic activity, ecological constraints, and environmental controls including water availability. Hence, the actual evapotranspiration (ETa) often differs from the reference evapotranspiration (ETo), mainly from differences in the transpiration component of ET.

Transpiration from vegetated surfaces accounts for significant amounts of water entering the atmosphere. For example, 70% of the total precipitation on the continental United States and 85% of total evapotranspiration from the Amazon rainforest are cycled at least once through leaf transpiration (Shuttleworth, 1984). In addition to environmental conditions, the

canopy vegetation also controls the overall transpiration rate physiologically and physically, by opening and closing stomata to regulate energy and gas exchanges and by the sheer amount of leaf area available for this activity in response to light and water stress. Many processes and interactions in the atmosphere and the biosphere influence plant and soil water losses by evapotranspiration. The need to improve representation within of surface-atmosphere interactions remains an urgent priority within the modeling community.

Motivated by Gao et al. 2008 and previous studies, this research extended the earlier works involving coarse resolution GCMs to examine the impacts of land surface representations in regional models (Abramowitz et al., 2008; Henderson-Sellers et al., 1996; Chen et al., 1997). The mesoscale Weather Research and Forecasting model (WRF) is used here with two land surface models (LSMs) having two distinct levels of complexity: the intermediate complexity NOAH and the complex Advanced Canopy-Atmosphere-Soil Algorithm (ACASA), to simulate evapotranspiration over California's diverse terrain and ecosystems. The objective of this paper is to investigate how the variability of reference and actual evapotranspiration is influenced by the surface representation, such as leaf area index, and the land surface model complexity. Both reference and actual evapotranspiration are important to an understanding of the hydrologic cycle, vegetation dynamics, and surface energy balances in the surface layer. They are also important variables for use in water management, drought monitoring, agricultural production, and fire hazard management. The effects of leaf area index and model complexity on reference evapotranspiration represents the vegetated controls on the atmosphere that can feedback to the land surface, as reference evapotranspiration is completely dependent on the atmospheric conditions; whereas the simulated actual evapotranspiration represents the complete interaction between the atmosphere and the vegetation

and includes the feedback process.

2. Models, Methodology and Data

2.1. Models

In this study, the Advanced Research WRF (ARW) model Version 3.1 is used to perform climate simulations over California. WRF is a state-of-the-art, mesoscale numerical weather prediction and atmospheric research model developed by a collaborative effort of the National Center for Atmospheric Research (NCAR), the National Oceanic and Atmospheric Administration (NOAA), the Earth System Research Laboratory (ESRL), and many other agencies. The WRF model contains a nearly complete set of compressible and non-hydrostatic equations for atmospheric physics (Chen and Dudhia, 2000). The high spatial and temporal resolution of the WRF model is essential for simulating climate over the intricate terrains and land covers of California. The physical parameterizations used in this study are described in more details in Chapter 1.

Two different land surface models are used in this study: the NOAH model (Mahrt and Ek, 1984; Chen and Dudhia, 2000) and the ACASA model (Meyers, 1985; Meyers and Paw U, 1987; Pyles, 2000; Pyles et al., 2000). The two land surface models differ significantly in the complexity of the representation of plant physiology and biometeorological processes. While NOAH is widely used for both climate studies and weather forecasting, it is an intermediate complexity model with multiple soil layers but only a single canopy layer. It scales the single leaf-based physical and physiological processes to represent the whole canopy using bulk similarity assumptions. The ACASA model is a higher complexity model that includes many

plant physiological and biometeorological processes, i.e., photosynthesis and respiration, that are not represented in the NOAH model. It uses multilayer canopy structures and multi-sun angles within each layer to represent the canopy. These subsequently allow variables such as LAI, air and canopy temperature, wind speed and humidity to also vary vertically. The surface layer is divided into 10 canopy layers and 10 above-canopy layers. Within each canopy layer there are 10 leaf angle classes, i.e., 9 sunlit at 10-degree intervals and one shaded, to represent differential illumination of canopy surfaces. A third order turbulent closure scheme used in the ACASA model allows both down- and counter-gradient transport that are not presented in the NOAH land surface model. Of particular importance is the role of Leaf Area Index (LAI) in controlling the surface processes in the two land surface models. LAI in the NOAH model is primarily used to calculate the bulk canopy resistance of the single surface layer. Canopy resistance for vegetation transpiration and energy partitioning is estimated using the Jarvis parameterization, where canopy resistance R_c is a function of $R_{c,min}$ (a single prescribed minimum canopy resistance specified by plant functional type), LAI, and F1, F2, F3, and F4, which account for the effects of radiation, temperature, humidity, and soil moisture (Jacquemin and Noilhan, 1990; Chen and Dudhia, 2001a,b).

$$R_c = \frac{R_{c,min}}{LAI(F_1F_2F_3F_4)} \quad (\text{III.1})$$

On the other hand, LAI in the ACASA model affects the light and precipitation interceptions and alters the energy budget in the canopy and the surface layer above accordingly. Depending on land use cover, the LAI values are used to create vertical profiles for multilayer canopy structures. The model calculates canopy resistance and stomatal resistance at the

leaf surface of each vertical layers using a combination of the Ball-Berry stomatal conductance (Leuning, 1990; Collatz et al., 1991) and the Farquhar et al. (1982) photosynthesis equation used in (Su et al., 1996).

$$g_{s,w} = m \frac{A_n}{c_s} rh_s + b \quad (\text{III.2})$$

$$rh_s = \frac{g_b q_A + g_{s,w} q_s(T_L)}{g_b + g_{s,w} q_s(T_L)} \quad (\text{III.3})$$

$$c_s = c_A - \frac{A_n}{g_b} \quad (\text{III.4})$$

where $g_{s,w}$ is the leaf stomatal conductance to water vapor, A_n is the net CO₂ uptake rate at the leaf surface, c_s and rh_s are the CO₂ concentration and the fractional relative humidity at the leaf surface, m and b are empirical regression coefficients; c_A is the CO₂ concentration in air, $q_s(T_L)$ is saturated mixing ratio of water vapor at leaf temperature T_L , g_b is the leaf boundary layer conductance, q_A is the mixing ratio of water vapor in the air. Because evapotranspiration is an inevitable result of plant physiological processes, oversimplifying the linkage between moisture and carbon dioxide fluxes in land surface processes can lead to the loss of vital information that impact climate simulations (Zhan and Kustas, 2001; Houborg and Soegaard, 2004).

2.2. Data

In this study, WRF simulations are forced by the Northern America Regional Reanalysis (NARR) dataset, which provides input data such as wind speed and direction, temperature, moisture, radiation, and soil temperature to drive the initialization and boundary conditions

of the WRF models. The NARR is a regional data set specifically developed for the Northern American region. The temporal and spatial resolutions of this data set are 3-hour intervals and 32-km respectively (Mesinger et al., 2006).

Two leaf area index datasets are used to drive the surface processes. The default USGS LAI data used by the WRF model prescribes the maximum and minimum LAI values for each point according to prescribed plant functional types. Monthly LAI is extrapolated linearly between the maximum and minimum LAI values with monthly Green Vegetation Fraction, which is the fraction of the grid cell covered by active vegetation (Gutman and Ignatov, 1998). The MODIS (Moderate Resolution Imaging Spectroradiometer) dataset is measured daily to provide high spatial and temporal resolution LAI (Knyazikhin et al., 1999). The USGS LAI and MODIS LAI are shown in Fig. III.1 for different seasons of the year 2006. The USGS LAI values are significantly higher than those of the MODIS LAI dataset, especially during the summer months. There is no inter-annual variability in the WRF USGS LAI, in contrast to the satellite measured MODIS LAI. Both LAI datasets display temporal and spatial differences among the different time of the year over California.

The main independent observational datasets used to evaluate the model simulations were obtained from the California Irrigation Management Information System (CIMIS) for reference evapotranspiration, and the AmeriFlux network for both reference evapotranspiration and actual evapotranspiration (Fig. III.2). The CIMIS stations are sparsely located, mostly in the Central Valley and Southern Coastal areas. There are only six AmeriFlux sites in California for the study period, chosen to be the period with the most active stations. However, because three stations were close to the other three, only three distinct markers are visible in Fig. III.2. The combined coverage of the two datasets still leaves much of California

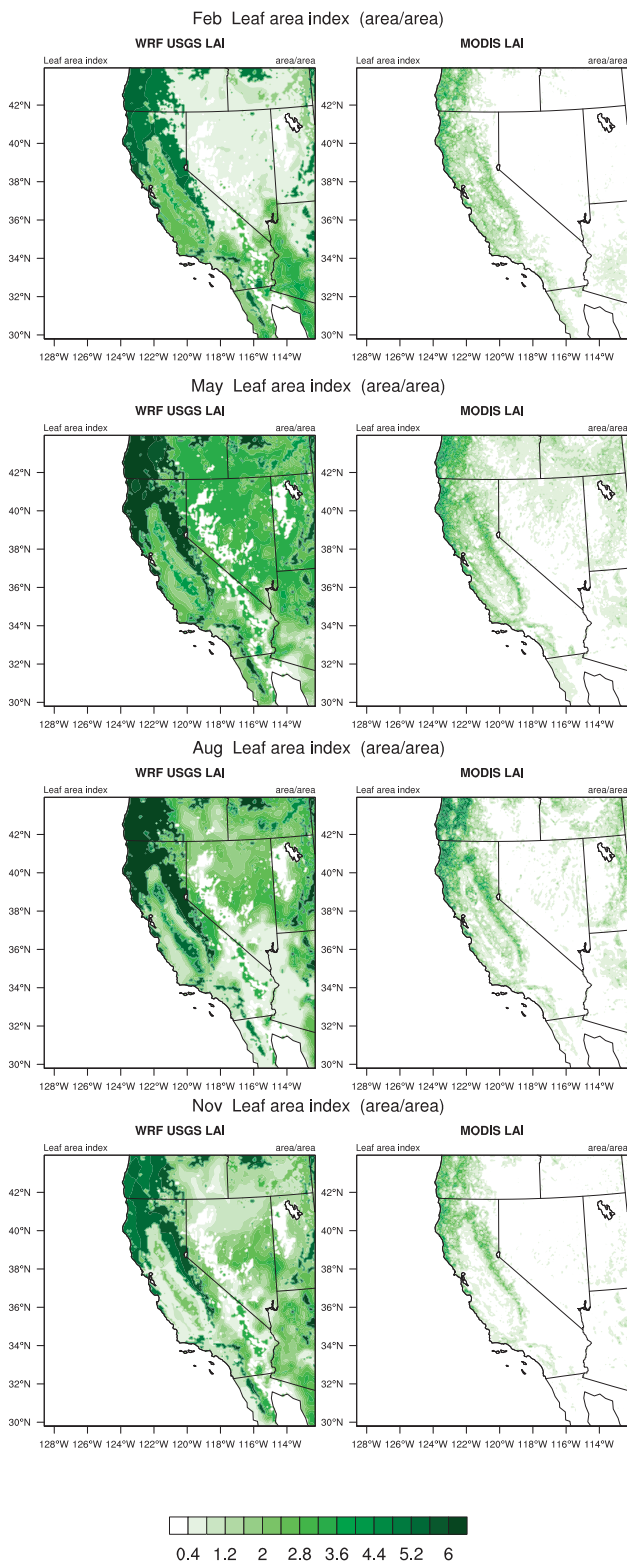


Figure III.1: Maps of MODIS LAI and USGS LAI for the months of February, May, August and November 2006.

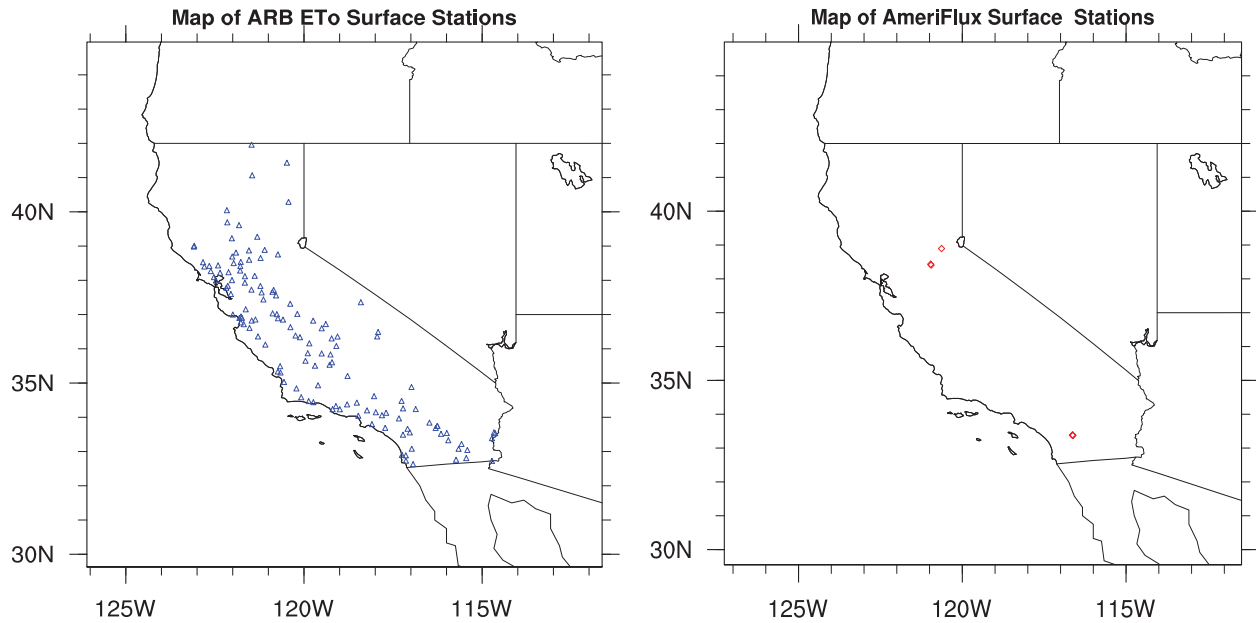


Figure III.2: Maps of the location of the (left) 120 CIMIS stations (part of the ARB network) and of the (right) 6 AmeriFlux stations used in this study.

underrepresented for flux observations. As a result, the mesoscale model can be a powerful tool to fill in the temporal and spatial gaps of the surface observations. Furthermore, the WRF model can also be used as a forecasting tool for policy making and agricultural and resource management practices.

Only the dominant vegetation types or plant functional types (PFTs) are used in both ACASA and NOAH models to represent each grid cell. However, these PFTs do not necessarily represent the observed vegetation type at each of the stations, as shown in Table III.1. For example, the three Sky Oak sites (USSO2, USSO3, and USSO4) are identified as Evergreen Needleleaf Forest by WRF, instead of the savannas and shrublands that actually surround the sites (observed PFT).

Table III.1: Selected sites from the Air Resources Board meteorological stations network.

Station	Site Name	WRF Plant Functional Type (PFT)	WRF-ACASA Canopy height (m)	Measured height (m)	Site observed PFT
NEP	Northeast Plateau	Grassland	1	1.2	Irrigated Grassland
MD	Mojave Desert	Shrubland	3	1.2	Irrigated Grassland
SJV	San Joaquin Valley	Irrigated Cropland and Pasture	1.5	1.2	Irrigated Grassland
MC	Sierra Nevada Mountain	Evergreen Needleleaf Forest	17	1.2	Irrigated Grassland
USBLO	Blodgett Forest	Evergreen Needleleaf Forest	17	12.5	Evergreen Needleleaf Forest
USVAR	Vaira Ranch	Savanna	10	1	Grasslands
USTON	Tonzi Ranch	Savanna	10	23	Woody savannas
USSO2	Sky Oak Old	Evergreen Needleleaf Forest	17	4.2	Woody Savannas
USSO3	Sky Oak Young	Evergreen Needleleaf Forest	17	1	Closed Shrublands
USSO4	Sky Oak New	Evergreen Needleleaf Forest	17	1.5	Closed Shrublands

2.3. Model setup

Four model simulations with the combination of the two land surface models and two LAI representations were used to simulate ETo and ETa over all of California with its vast and diverse terrains and ecosystems. The four simulations were: WRF-ACASA with default USGS LAI, WRF-ACASA with high resolution MODIS LAI, WRF-NOAH with USGS LAI, and WRF-NOAH with MODIS LAI. Simulations were performed for the years 2005 and 2006 with horizontal grid spacing of 8 km x 8 km. Besides the differences in the land surface model, all simulations employed the same set of atmospheric physics schemes stemming from the WRF model. These include the Purdue scheme for microphysics (Chen and Sun, 2002), the Rapid Radiative Transfer Model for long wave radiation (Mlawer et al., 1997), Dudhia scheme for shortwave radiation (Dudhia, 1989), Monin-Obukhov similarity scheme

for surface layer physics of non-vegetated surfaces and the ocean, and the MRF scheme for the planetary boundary layer (Hong and Pan, 1996). WRF runs at a 60-second time step (this time step is larger than 6 delta x and may cause instability), while the radiation scheme and the land surface schemes are called every 30 minutes. Boundary conditions are specified using NARR. Reference evapotranspiration was calculated using Penman-Monteith equation (Allen et al., 2005) with simulation outputs of surface air temperature, dew point temperature, solar radiation, and wind speed at 2-meter height. Actual evapotranspiration was calculated within the WRF-ACASA and WRF-NOAH models.

Reference evapotranspiration and actual evapotranspiration for the four simulations were compared with surface observations to test the hypothesis that terrestrial representations in land surface model influence the simulated evapotranspiration on both local and regional scales. Hourly, daily, monthly and annual temporal scales were used to evaluate the variability of model performance. The comparison between surface observations and model simulations were similar for 2005 and 2006. However, due to the large amount of missing data during year 2005, mainly results from 2006 are presented here.

One of the challenges in making the comparison between the simulations and the observations are the differences between the heights and station landscape of the observational stations and the heights of the simulations grid points. Many stations were within patches of specific landscape types that may differ significantly from the assigned overall grid point landscape, one example being the PFTs of the three Sky Oak sites. In addition, the surface measurement heights for the AmeriFlux sites varied from site to site (Table III.1). This becomes even more challenging when considering that the WRF-ACASA simulations have outputs for the temperatures within a canopy, abd so for orchards or forests, the 2-meter

height ("surface") simulation data are not expected to match the various heights from observations well. WRF-ACASA simulations at 2-meter height for the taller plant ecosystems represent temperatures within the plant canopy or in the understory; yet the observations from the CIMIS were generally taken over well-watered grass; while those from the AmeriFlux network were also over other surfaces not representative of the simulation grid-point, and furthermore are usually not even recorded the standard 2-meter height. The WRF-NOAH simulations do not suffer the same problems compared to the observations in terms of the 2-meter height falling within the understory, because the NOAH surface model is a big-leaf model, so the 2-meter height represents a height more similar in characteristics to the observations.

3. Results and Discussion

The seasonal diurnal patterns of ETo from the four WRF simulations are compared with the CIMIS surface observations in Fig. III.3. The seasonal diurnal patterns of the model simulations generally compare well with the surface measurements with little differences between the two LAI datasets. The Northeast Plateau station with the same observed plant function type as the WRF model shows the best model comparisons, where all simulations of ETo are closely followed the diurnal patterns of the measurements throughout the four seasons. However, over the sparsely vegetated areas of the Mojave Desert stations and the San Joaquin Valley Stations where the observed plant function types do not match well with the model plant functional types, both models overestimate the ETo values during daytime of the warmer seasons. The two different LAI datasets do not have a significant impact on the ETo simulations, though usage of the MODIS LAI slightly improve the WRF-ACASA

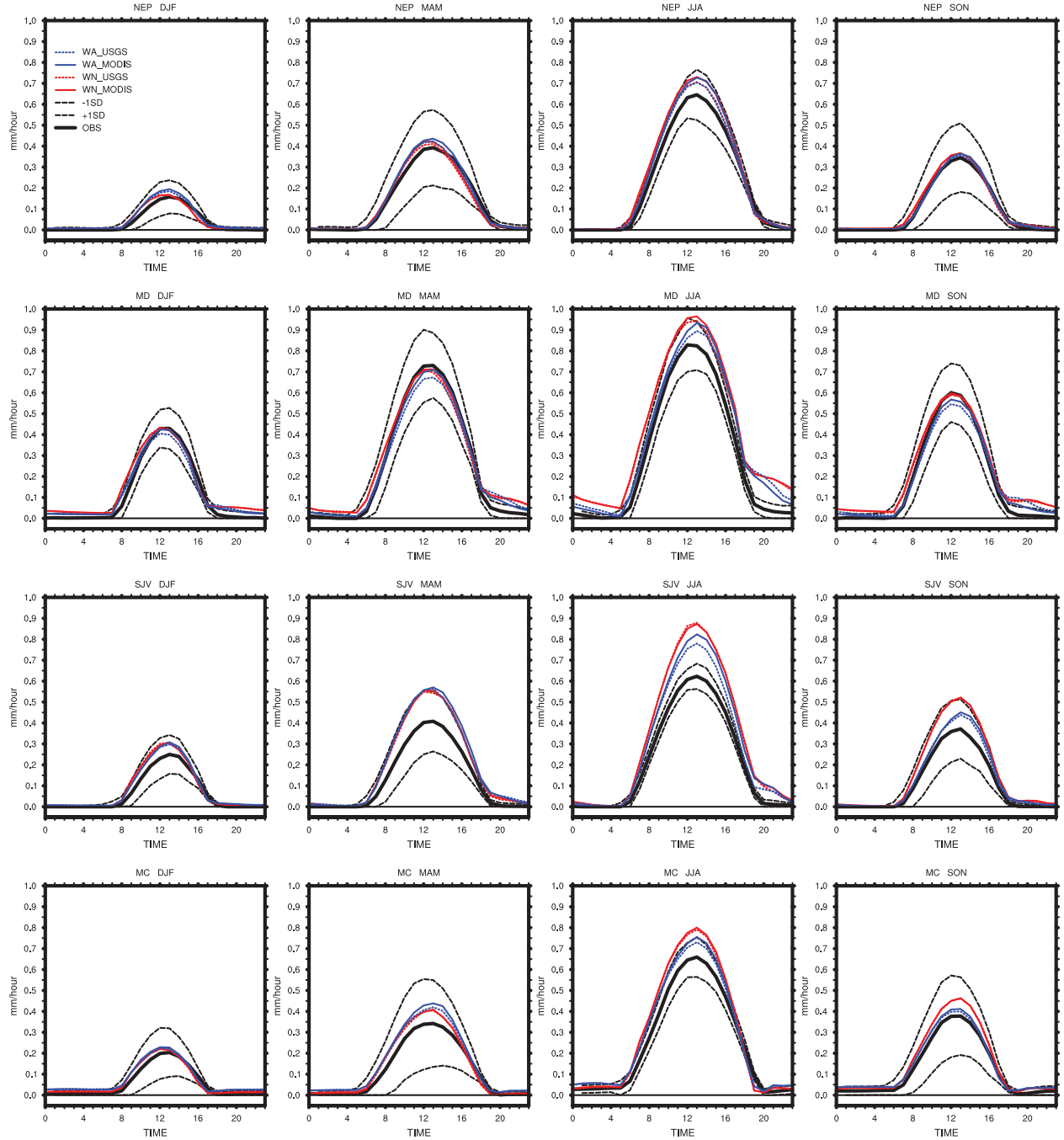


Figure III.3: Seasonal diurnal patterns of reference ETo for the four model simulations for the CIMIS sites. The black lines are CIMIS ETo measurements with two dash lines representing one standard deviation above and below the mean diurnal patterns. The red lines are WRF-NOAH simulations and the blue lines are WRF-ACASA simulations with MODIS LAI. The dashed lines are for simulations with USGS LAI. Winter is assumed to be December, January, and February (DJF) spring is March, April, and May (MAM) summer is June, July, and August (JJA), and autumn is September, October, and November (SON).

simulations for the San Joaquin Valley station. While both models overestimate the ETo for the San Joaquin Valley station, the WRF-ACASA model results exhibit a reduced bias during the daytime.

Similar seasonal diurnal pattern of ETo for the AmeriFlux sites are shown in Fig. III.4. Overall, regardless of the model complexity and leaf area index dataset, ETo from all four simulations agree well with the surface observations. The graph also shows that the effect of the two LAI datasets on ETo calculation is smaller than the effect of model complexity. This is evident because the WRF-ACASA simulations with or without MODIS LAI perform slightly better than the two WRF-NOAH simulations during the summer and autumn for the Vaira Ranch and Tonzi Ranch stations. The differences between the four simulations are small and all simulated ETo are within one standard deviation of the surface measurements.

The time series of the daily ETo of the CIMIS surface observations as well as the four model simulations are compared in Fig. III.5 for year 2006. In general, the WRF simulations of daily ETo during the summer are poor compared to surface observations. The sparsely vegetated Mojave Desert and San Joaquin Valley stations are most problematic for the model simulations. The overestimation of daily ETo in the time series results from the daytime bias of ETo from Fig. III.3. Although the diurnal patterns of ETo from Fig. III.3 overestimate by only a few tenths of millimeter per hour of during the daytime, such a bias accumulates. Like the results from Fig. III.3, the model simulations over the Mojave Desert and the San Joaquin Valley stations experience the biggest bias. There is no clear evidence in Fig. III.5 to show the impact of using different LAI datasets on daily ETo. However, as in Fig. III.3, the more complex WRF-ACASA model reduces the daily bias slightly. This is due to the improvement of dew point temperature from the WRF-ACASA model where higher complexity in plant

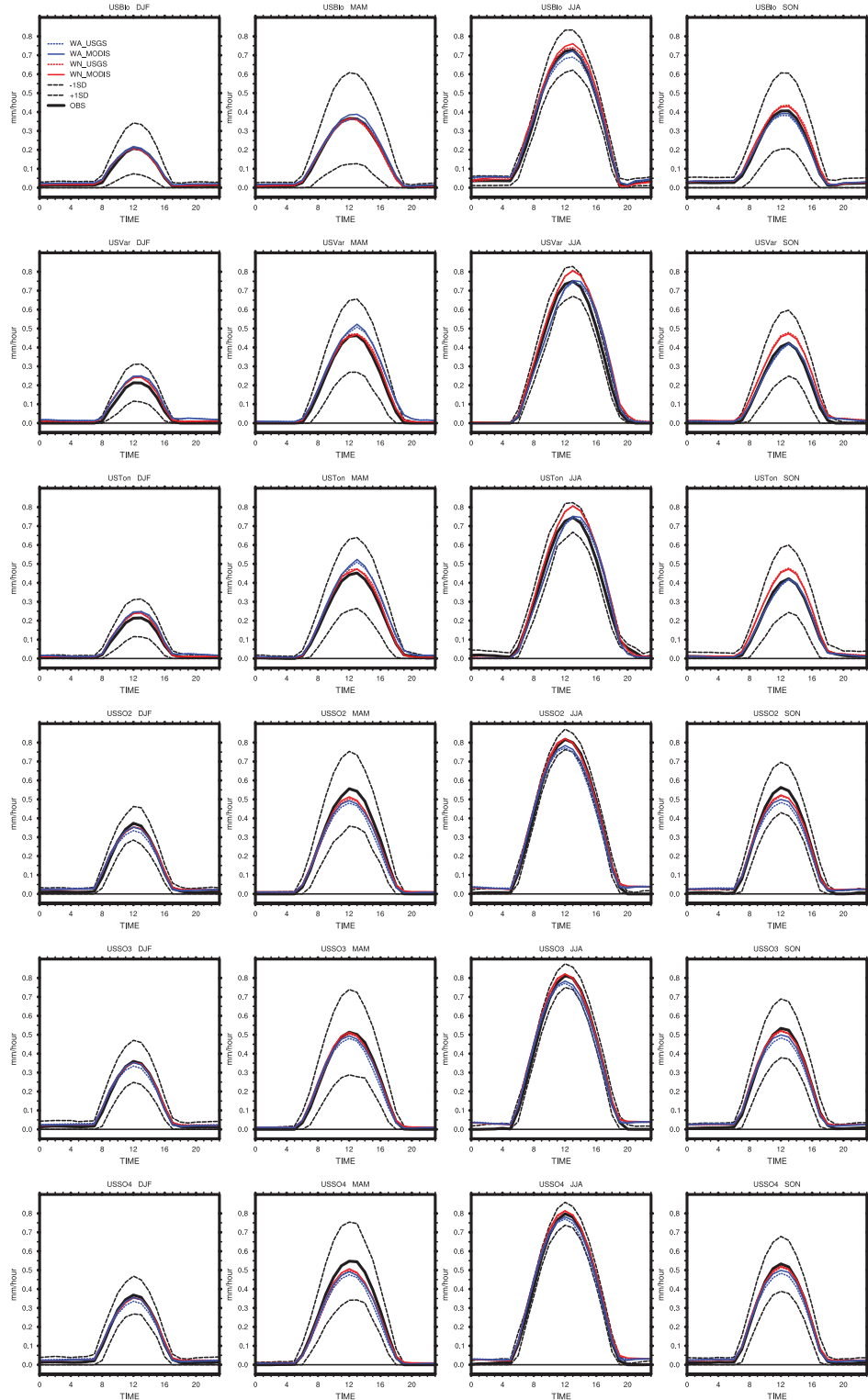


Figure III.4: Same as Fig. III.3 for the AmeriFlux sites.

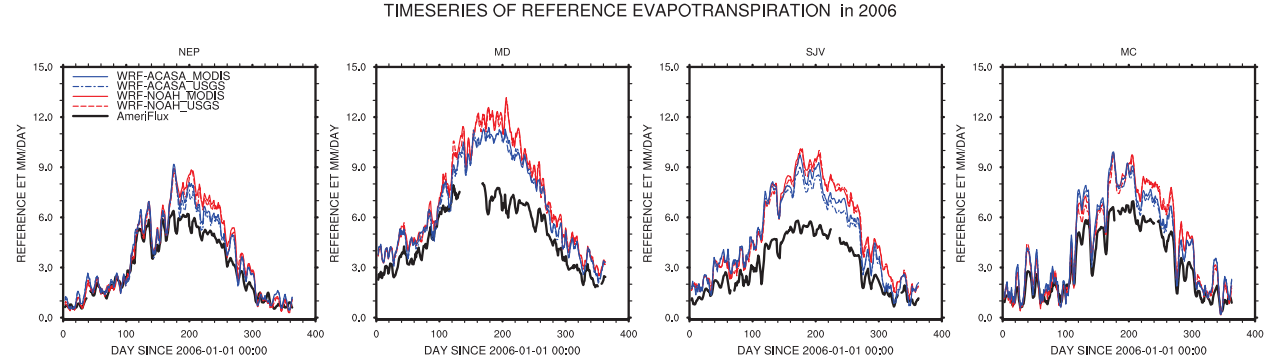


Figure III.5: Time series of reference evapotranspiration for the CIMIS sites. The solid black line represents observation. The blue lines are for WRF-ACASA, and the red lines are for WRF-NOAH. The solid lines are simulations with MODIS LAI, and the dashed lines are simulations with USGS LAI.

physiology representation and multilayer canopy structure improve the moisture exchange within and above the canopy, as shown in Chapter 1.

The time series of daily reference evapotranspiration for the year 2006 are shown in Fig. III.6 for the observations of the six AmeriFlux sites along with the four WRF simulations for the surface. Compared to the time series of Fig. III.5 over managed CIMIS stations, the timing as well as the magnitude of the four WRF simulations agrees well with the surface observations. This reaffirms the results shown in Fig. III.4, where simulated diurnal patterns of ETo match closely of the surface observations. Once again, the impact of different LAI is not noticeable on ETo calculations. However, there are smaller differences between the WRF-ACASA and WRF-NOAH models. The WRF-ACASA simulated daily ETos over Vaira Ranch and Tonzi Ranch stations during the summer and autumn match more closely to observations than WRF-NOAH as indicated in Fig. III.6.

The daily cumulative ETo values from the four model simulations are plotted against the AmeriFlux stations for four seasons in Fig. III.7 and III.8. Most of the scatter plots of both WRF-ACASA and WRF-NOAH show good correlations with the surface observations

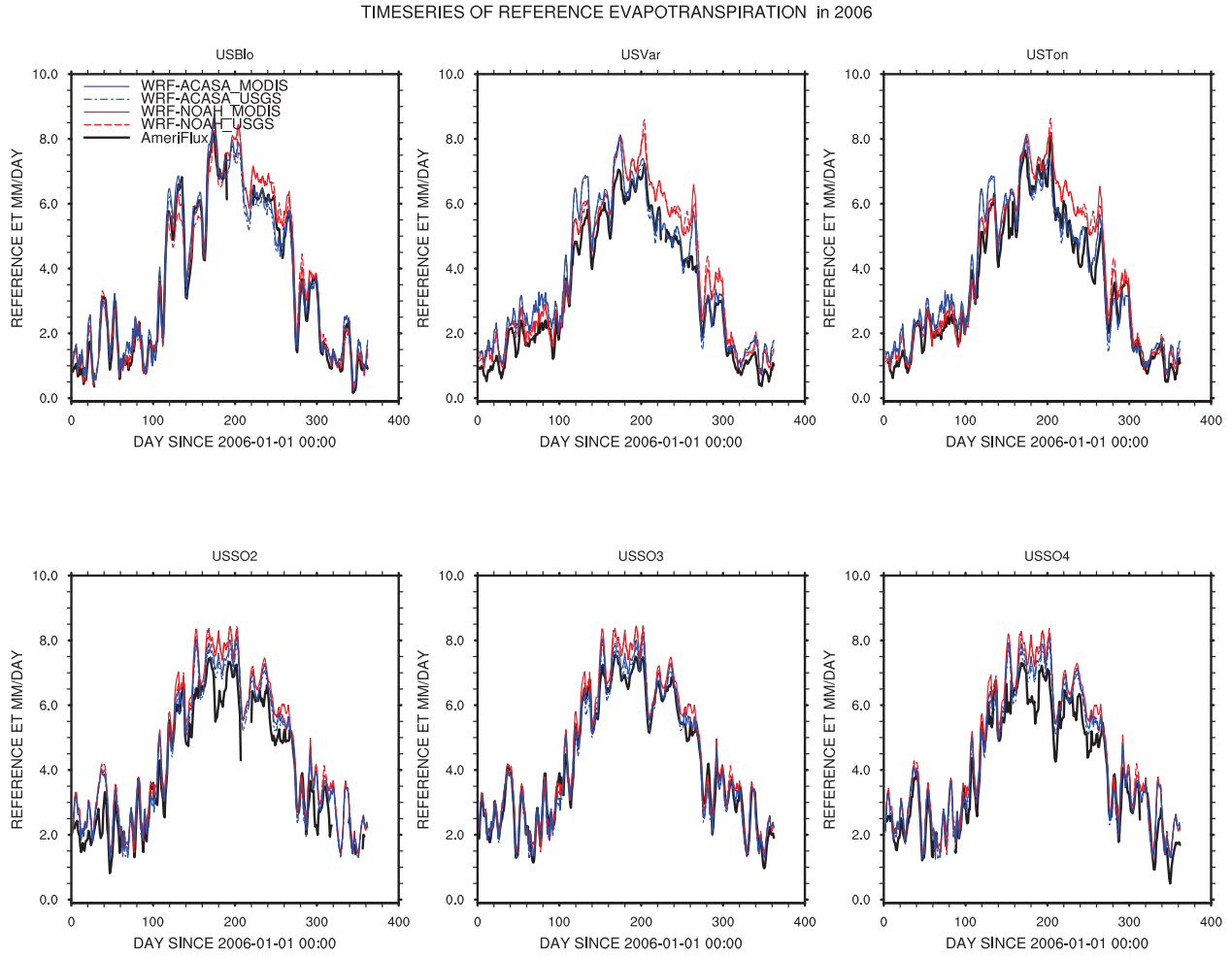


Figure III.6: Same as Fig. III.5 for for the AmeriFlux sites.

expect during the summer season, where both models overestimate the daily ETo slightly, especially over the Old and New Sky Oak sites. This could be caused by the misrepresentation of the surface conditions more so than model physics. The dominant PFT as well as the horizontal homogeneity assumption used in both models for the grid cell misrepresent these sites diversity in surface conditions, including stand ages, disturbance histories, and terrains variations. These heterogeneous surface conditions create differentiation in microclimatological environments, which in turn would trigger different plant physiological responses that the WRF model cannot simulate with its dominant vegetation type arrays.

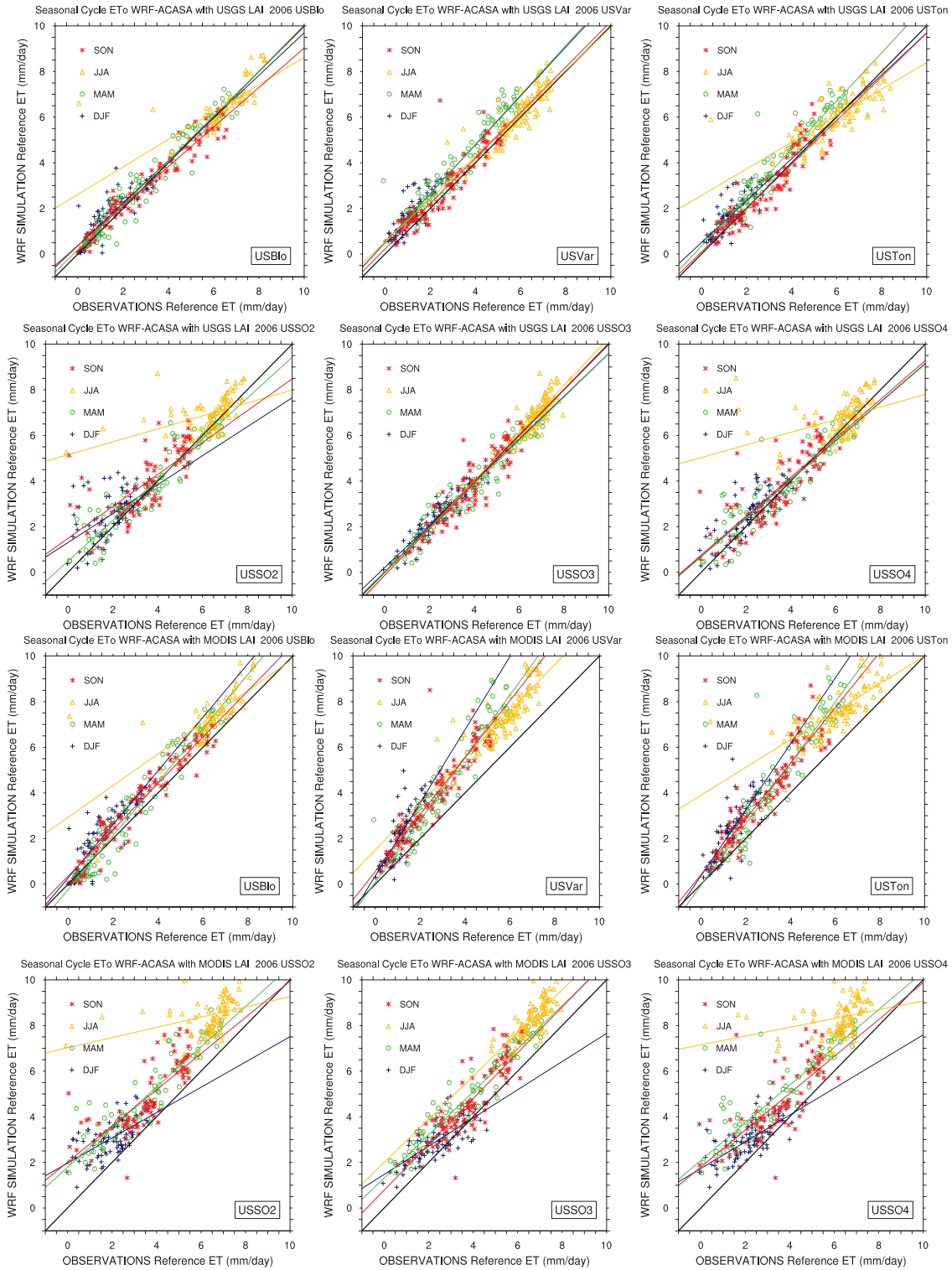


Figure III.7: Scatter plots of daily ETo simulated by WRF-ACASA with both MODIS and USGS LAI over the six AmeriFlux locations. The daily ETo are sorted by seasons.

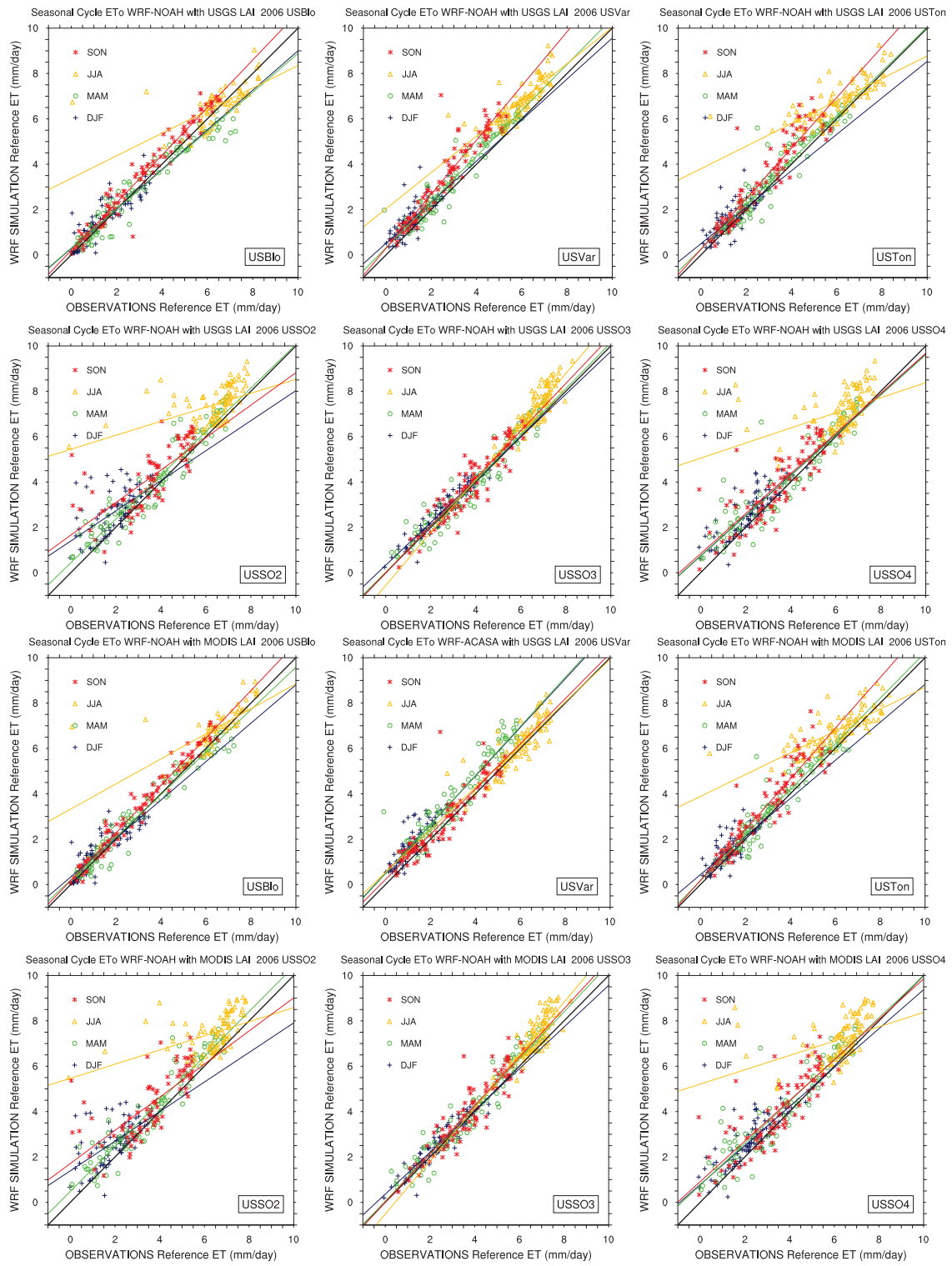


Figure III.8: Same as Fig. III.7 but for WRF-NOAH.

The choice of LAI datasets appears to reveal no significant impact on model results on of ETo. Usage of the MODIS LAI slightly increases the daily ETo in the WRF-ACASA model over the WRF-NOAH model. This is a result of lower LAI values in the MODIS dataset increasing the surface air temperature in the WRF-ACASA model and as well as slightly decreasing the relative humidity, thusly increasing the evaporative demand. The annual cumulative reference evapotranspiration over the entire domain for WRF-ACASA with MODIS LAI, WRF-ACASA with USGS LAI, WRF-NOAH with MODIS LAI and WRF-NOAH with USGS LAI are shown in Fig.III.9. The two leaf area indexes do not have a large effect on the annual cumulative reference evapotranspiration when the same model is used. The differences are more results of model complexity between WRF-ACASA and WRF-NOAH. Over the southern Central Valley and southern California, where the San Joaquin Valley and Mojave Desert stations from the CIMIS network are located, the WRF-ACASA simulations have lower annual ETo values than the WRF-NOAH simulations. These differences are evident from the previous results. Although both WRF-ACASA and WRF-NOAH models overestimate the daytime reference ET over these two sites during the spring and summer seasons, the biases in the WRF-ACASA simulations are smaller than the WRF-NOAH simulations. The time series graphs in Fig.III.5 and Fig.III.6 also show the WRF-ACASA simulations closer to the observed values. Consequently, the WRF-NOAH model overestimates the annual cumulative reference evapotranspiration as compared to that estimated by the WRF-ACASA model.

The Taylor Diagram in Fig.III.10 illustrates the relative accuracy of the WRF-ACASA and WRF-NOAH models to the observational data for daily ETo, 2-meter temperature, dew point temperature, relative humidity, wind speed and solar radiation in each of the four

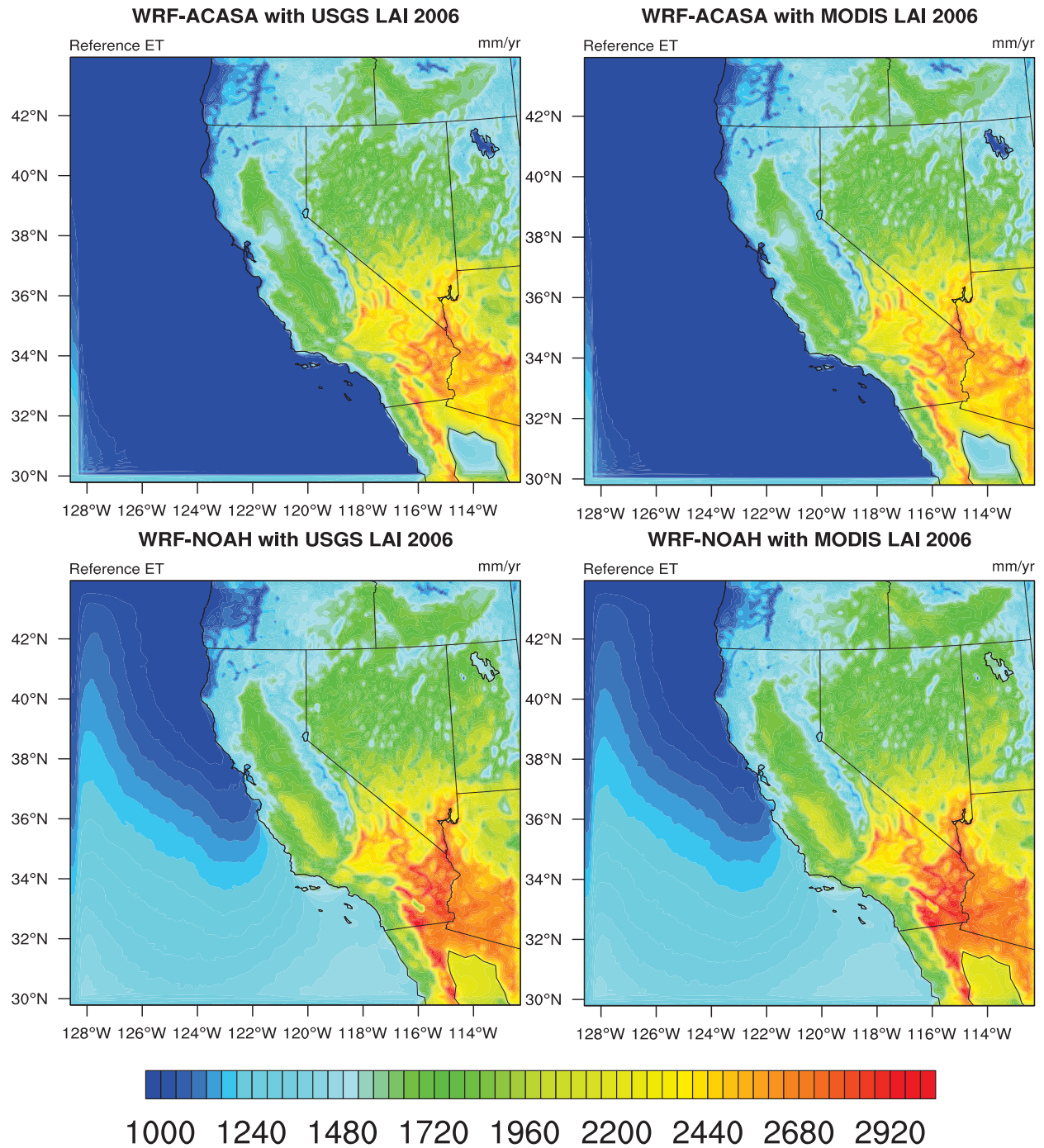


Figure III.9: Maps of ETo.

seasons. Using three non-dimensional statistical parameters (the ratio of the variances, the correlation between the two fields, and the RMSE), the Taylor Diagram quantifies how well the two models with the two LAI datasets simulate an observed meteorological field. Even

though the differences in the LAI values shown in Fig. III.1 are large, the impact of LAI on surface variables appears small. The largest impact is from model complexity. Generally in all four seasons, the 2-meter air temperatures are well simulated by both WRF-ACASA and WRF-NOAH models. However, both models are comparatively poor at simulating wind speed throughout the year. This disparity in wind speed simulation could be due to the difference measurement heights and more generally model and station discretization. The wind speeds from the WRF models are simulated at 10-meter height whereas the observed wind speeds are measured at 2-meter height. Therefore, surface measurements of wind speed do not identically match with the standard output from the WRF models. Despite the empirical relationship used to estimate the 2-meter wind speed from the simulated 10-meter wind speed values, the correlations are still low (Allen et al., 2005).

$$u_2 = u_z \left(\frac{4.87}{\ln(67.8 \cdot z - 5.42)} \right) \quad (\text{III.5})$$

During the winter, the ETo simulations from both models have reasonable correlations with the surface observation but the RMSEs are high with a large amount variability in the standard deviations. This could be due to the bias from the wind speed and dew point temperature simulations used in the Penman-Monteith equation to calculate ETo. The reduction in both dew point temperature variability and RMSE of wind speed during the spring seems to improve ETo simulations. The sudden reduction across all statistical variables in the ETo simulations seems to be caused by the poor performance of net downward shortwave radiation. This could be due to a possible shift of timestamp in the CIMIS stations where daylight saving time appear to be used in some stations, where downward shortwave radia-

tion is unrealistically above zero before 5am, and peak radiation occurs at 1 pm instead of the expected near-noon time. This potential major mismatch of time stamps between the WRF models and CIMIS measurements during the summer month contribute to the poor performance of ETo simulations.

Figure III.11 and III.12 show the seasonal diurnal patterns of actual evapotranspiration, ET_a, of the four WRF simulations and of the six AmeriFlux stations. Due to the large amount of missing data in the Sky Oak sites during 2005, no diurnal observation is displayed for these sites. While the differences in model complexity and leaf area index data do not have major influence on the reference evapotranspiration simulation among the four model runs, the actual evapotranspiration graphs show otherwise. The lower leaf area index in the MODIS LAI dataset systematically lowers the simulated actual evapotranspiration for all four AmeriFlux stations throughout the seasons. Compared to WRF-NOAH model, the leaf area index has a larger impact on WRF-ACASA model, since the WRF-ACASA model relies on the leaf area index in multiple ways: in the radiation transfer equations, as a direct multiplier times the physiologically determined latent energy flux density per leaf class, and as multipliers to the leaf drag elements affecting the simulated turbulence; while the NOAH model uses the LAI only to reduce the canopy resistance through an inverse relationship. In addition to LAI, the plant functional type also plays an important role the WRF-ACASA model. At the three Sky Oaks sites, the combination of the PFT mismatch and the USGS LAI dataset, caused WRF-ACASA to overestimate the actual evapotranspiration. However, when the MODIS LAI is used instead, the more accurate LAI values greatly reduce the bias although the wrong PFT still has a large effect. The WRF-NOAH model also benefits from the more accurate MODIS LAI representation, but not as strongly as WRF-ACASA.

Taylor Diagram: Model vs. CIMIS 2006

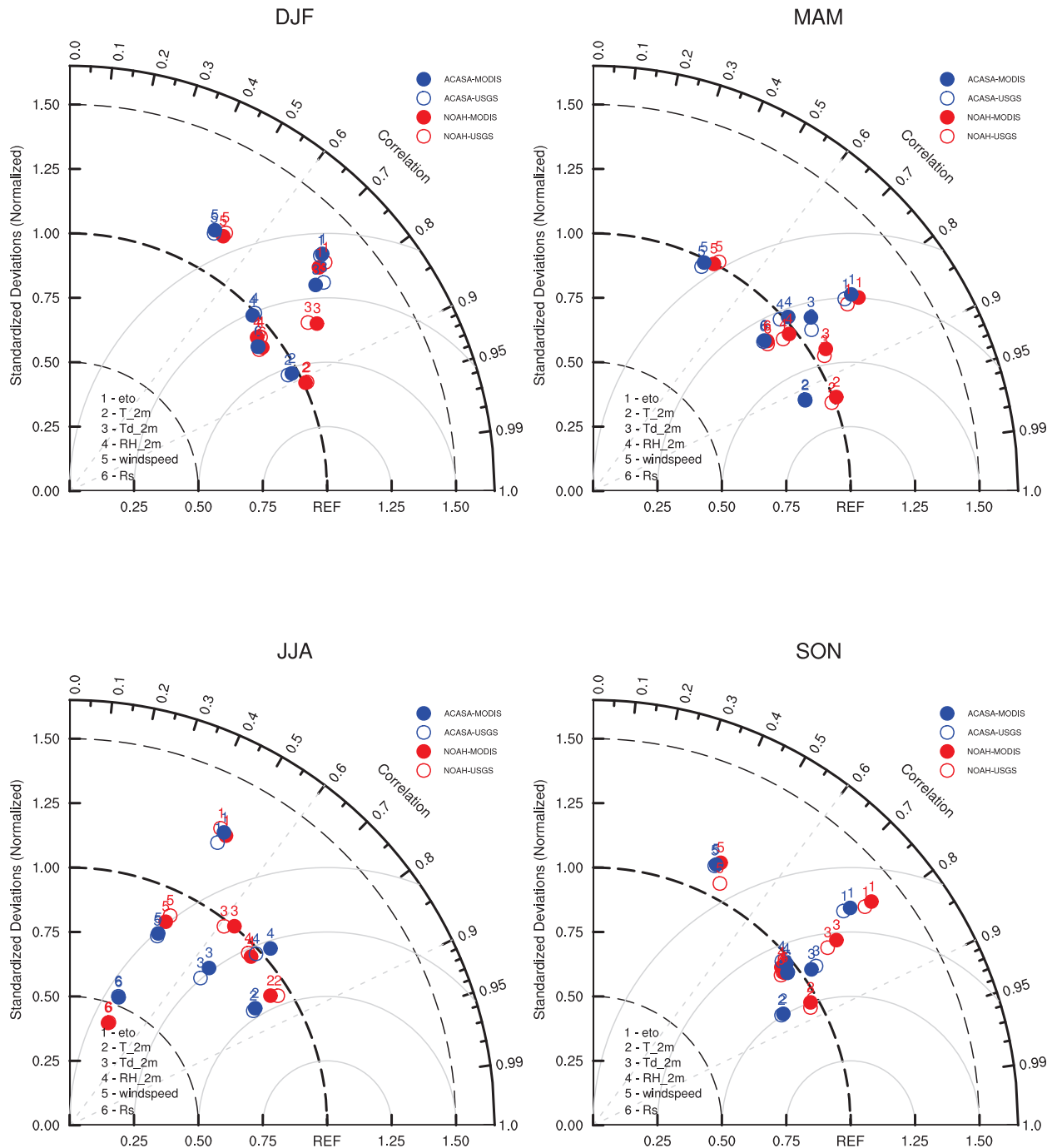


Figure III.10: Taylor Diagram for the four WRF simulations vs. CIMIS station measurements.

This difference in WRF sensitivity using ACASA vest NOAH with MODIS LAI could be due to the differences in surface representation between the WRF-ACASA and WRF-

DIURNAL ACTUAL EVAPOTRANSPIRATION in 2005

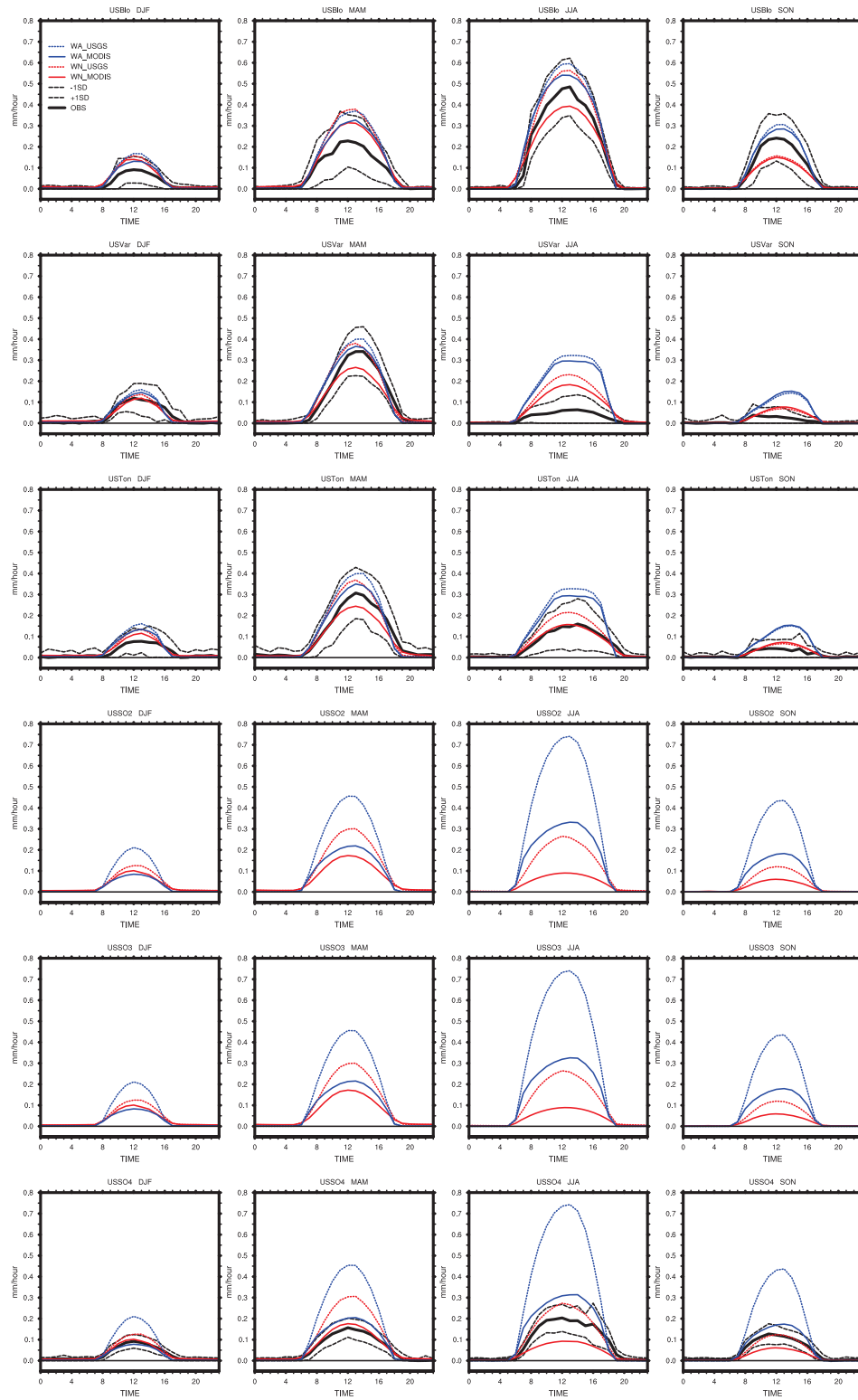


Figure III.11: Diurnal patterns of the actual evapotranspiration for 2005.

DIURNAL ACTUAL EVAPOTRANSPIRATION in 2006

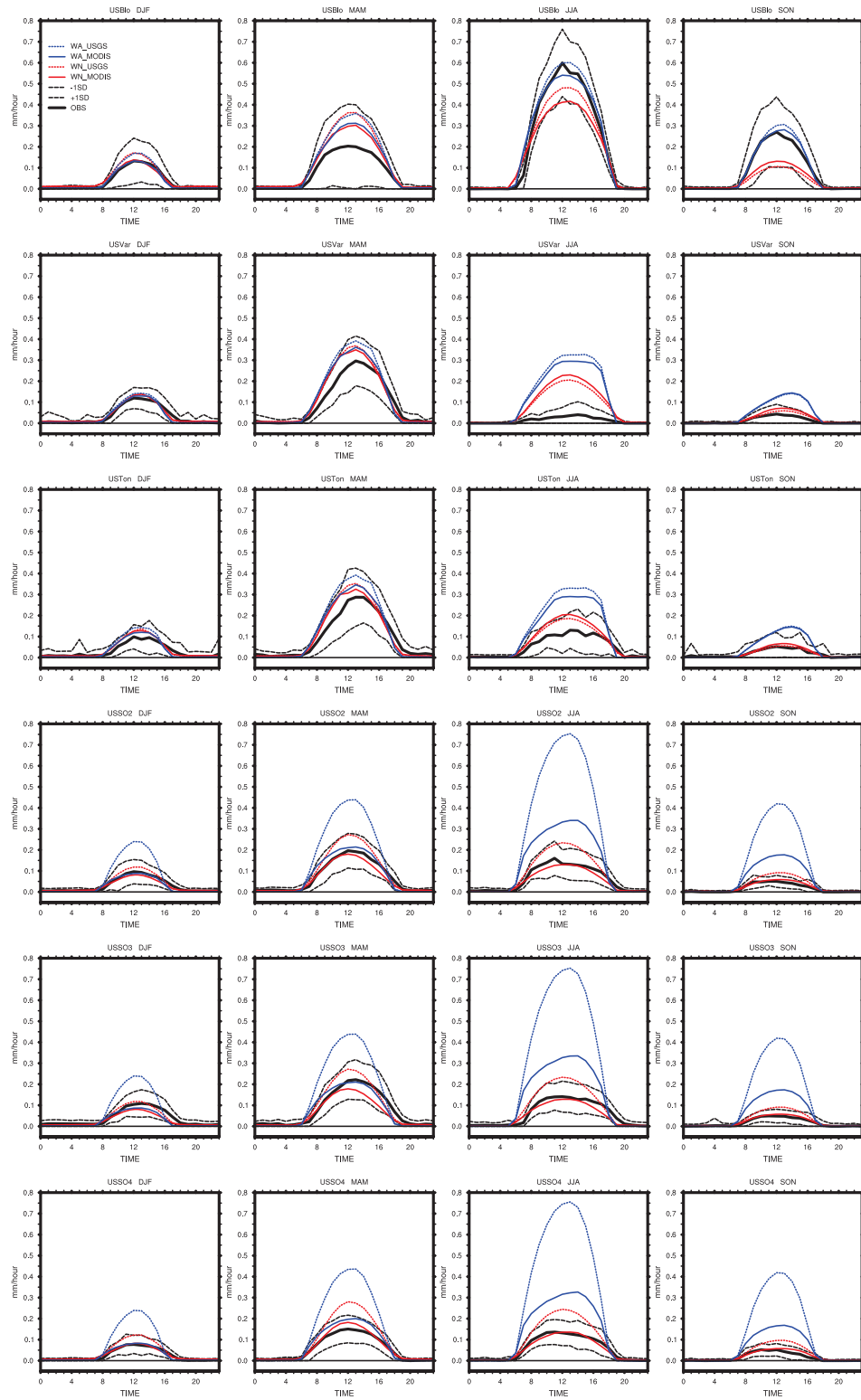


Figure III.12: Same as Fig. III.11

NOAH models. Unlike the single layer "big leaf" model of the WRF-NOAH, each of the plant functional types in the WRFACASA model is associated with a different multilayer canopy structure. While the representation of each PFT with specific canopy structures and plant physiological process allows a more realistic surface representation, these complex relationships more are dependent on the quality of input variables such as land cover type and leaf area index. It is problematic when the basic PFT is not well matched with the surface station as evident in the three Sky Oaks sites. Therefore, WRF-ACASA overestimates actual ET because the WRF land surface PFT identifies Sky Oaks as physiologically active (throughout the year) evergreen needle leaf forests, when in reality they are low LAI, seasonally inactive, vegetated savanna and shrublands. The WRF-NOAH model, on the other hand with a single canopy layer, is less restricted by the land cover representation and is therefore less sensitive to changes in land surface type designation. Therefore, improvements in surface representations such as LAI and PFT would greatly improve the WRF-ACASA accuracy because many of the models physiological processes rely on them.

Figure III.13 shows the time series of daily cumulative ET_a from the four WRF model runs and the AmeriFlux measurements. Similar effects of LAI and PFT on the diurnal pattern of ET_a in Fig. III.11 and III.11 are also seen in the time series of Fig. III.13 . The mismatching PFTs over the three Sky Oak sites amplified the overestimation of daily ET_a in the WRF-ACASA model. The time series also show the impacts of the model complexity and canopy structure on the results. Over the Blodgett forest where both PFTs from the model and surface observation match well, the more complex WRF-ACASA model generally outperforms the WRF-NOAH model. The tall and dense canopy of the Blodgett forest is ideal for using the multilayer structure of the WRF-ACASA model. The complex canopy

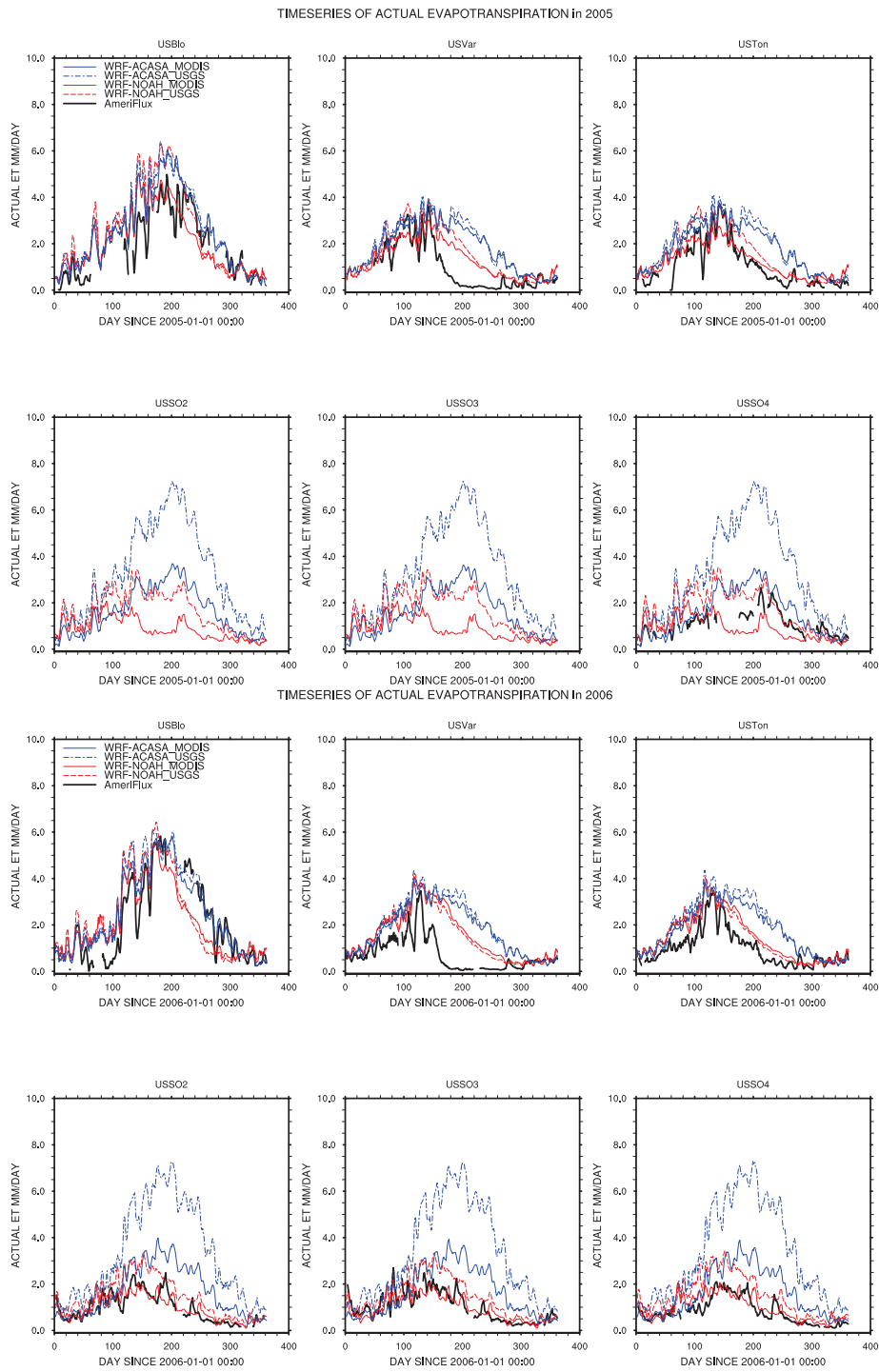


Figure III.13: The time series of cumulative daily ET_a for the six AmeriFlux sites during year 2005 and 2006. The black lines are surface measurement of daily ET_a, the blue lines are WRF-ACASA simulations, and the red lines are WRF-NOAH simulations. The model simulations with MODIS LAI are presented using solid lines and the dash lines are WRF models with USGS LAI.

representation and their plant physiological processes better describe the light penetration and inter-canopy mixing, resulting in a better ET_a simulation. The same does not seem to apply to the Tonzi Ranch due to underestimation of canopy openness when the WRF-ACASA model assumes horizontal homogeneity of closed forest in each grid cell. At the same time and over the same grid cell as the Tonzi Ranch, both models overestimated the ET_a during the summer for the Vaira Ranch site, where the grassland growing season is confined only to the wet season from October to early May. The differences in surface conditions and vegetation types of the Vaira Ranch and Tonzi Ranch sites resulted in very different ET_a values even though they are close to each other, thus sharing the same model grid cell. These emphasize the importance of surface representations such as land cover type and leaf area index in model simulations.

The scatter plots of ET_a from the four simulations are shown in Fig. III.14 and Fig. III.15. Unlike the scatter plots for ET_o in Fig. III.7 and III.8, the ET_a scatter plots show more disparities between model results when model performances are generally poor. The impacts of LAI differ according to the specific sites and models. The largest impact of MODIS LAI is over the three Sky Oak sites for the WRF-ACASA model. The MODIS LAI greatly reduces the overestimation of these three sites for the Spring and Summer, but less so in Winter and Autumn. This effect of LAI is not obvious in the WRF-NOAH simulations. The impact of PFT is also larger in the WRF-ACASA simulations than in the WRF-NOAH simulations. When the PFT is appropriate with the actual ecosystem at the Blodgett forest site, the daily ET_a simulations from the WRF-ACASA model have good correlation and covariance with the surface observations. Both models perform poorly over the Vaira Ranch site due to a poor description of the effect of the growing season as previously mentioned.

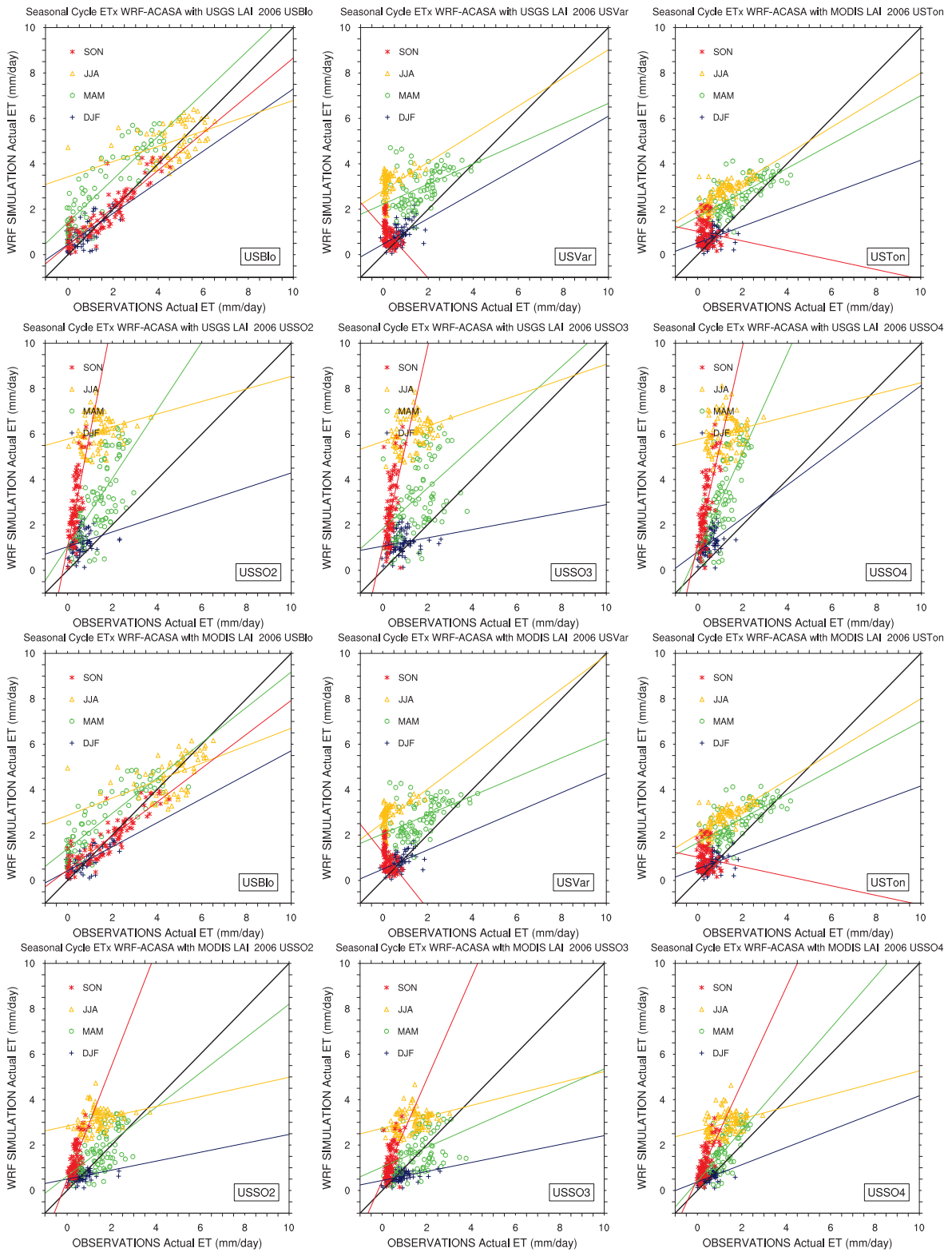


Figure III.14: Scatter plots of daily ET_a simulated by WRF-ACASA with both MODIS and USGS LAI over the six AmeriFlux locations. The daily ET_o are sorted by seasons.

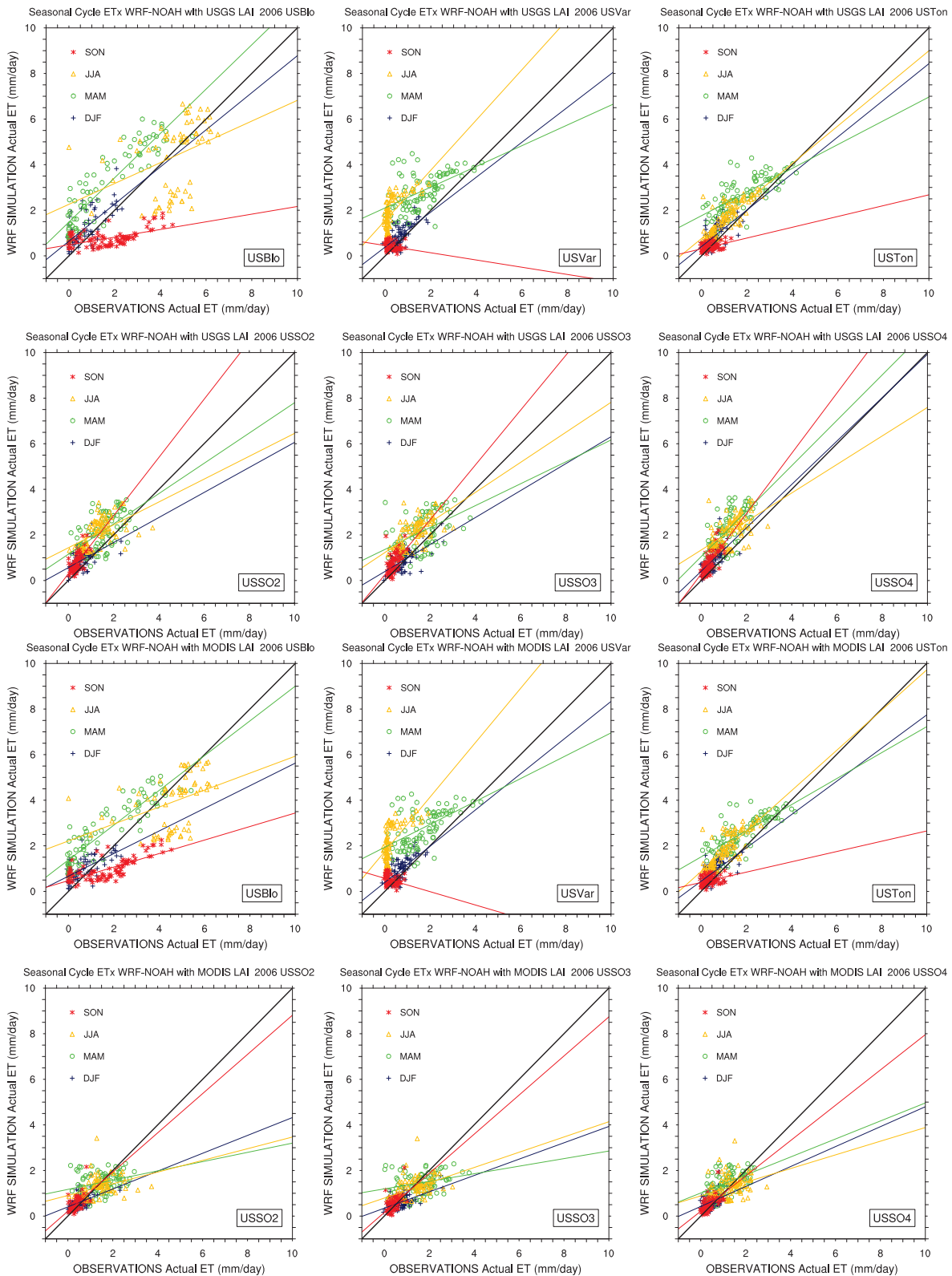


Figure III.15: Same as Fig. III.14 but for WRF-NOAH.

The WRF-ACASA model seems to underestimate of stomatal closure as shown in Fig. III.16; the stomatal resistance simulations in both WRF-ACASA with MODIS LAI and WRF-ACASA with USGS LAI are too low during the dry summer season for the sparsely vegetated sites, so the simulated evapotranspiration was too great. When sparse canopy morphology becomes more thoroughly addressed in future ACASA versions, this problem will likely diminish.

The simulated annual cumulative ET_a are showed in the panel graph of Fig. III.17. There are large differences in the WRF-ACASA with MODIS LAI compares to WRF-ACASA with USGS LAI, but such differences between the two LAI dataset is not visible in the WRF-NOAH simulations. The most significant differences in ET_a occur over the Central Valley, and northern California, which follow closely to the differences in LAI showed in Fig. III.1. This is expected since LAI is included in several processes in the WRF-ACASA model, in contrast to the WRF-NOAH model where it is only used in the scaling of the canopy resistance. An overestimation of LAI will cause WRF-ACASA to simulate too much the actual evapotranspiration, from a variety of processes. The stomatal closure issues shown in the previous graphs are also persistent in the annual timescale, where ET_a values over the southern regions are over estimated compared to corresponding values from the WRF-NOAH simulations. Thresholds in soil moisture for stomatal closure were probably set too high and led to unrealistic stomatal opening over warm and dry regions of the Mojave Desert. The difference between WRF-NOAH with MODIS LAI and WRF-NOAH with USGS LAI is small, as noted earlier, related to the fact that NOAH uses LAI only to modify the canopy resistance term, rather than to change any other processes.

The seasonal diurnal patterns of the total surface energy budget of all six AmeriFlux

DIURNAL CANOPY RESISTANCE in 2006

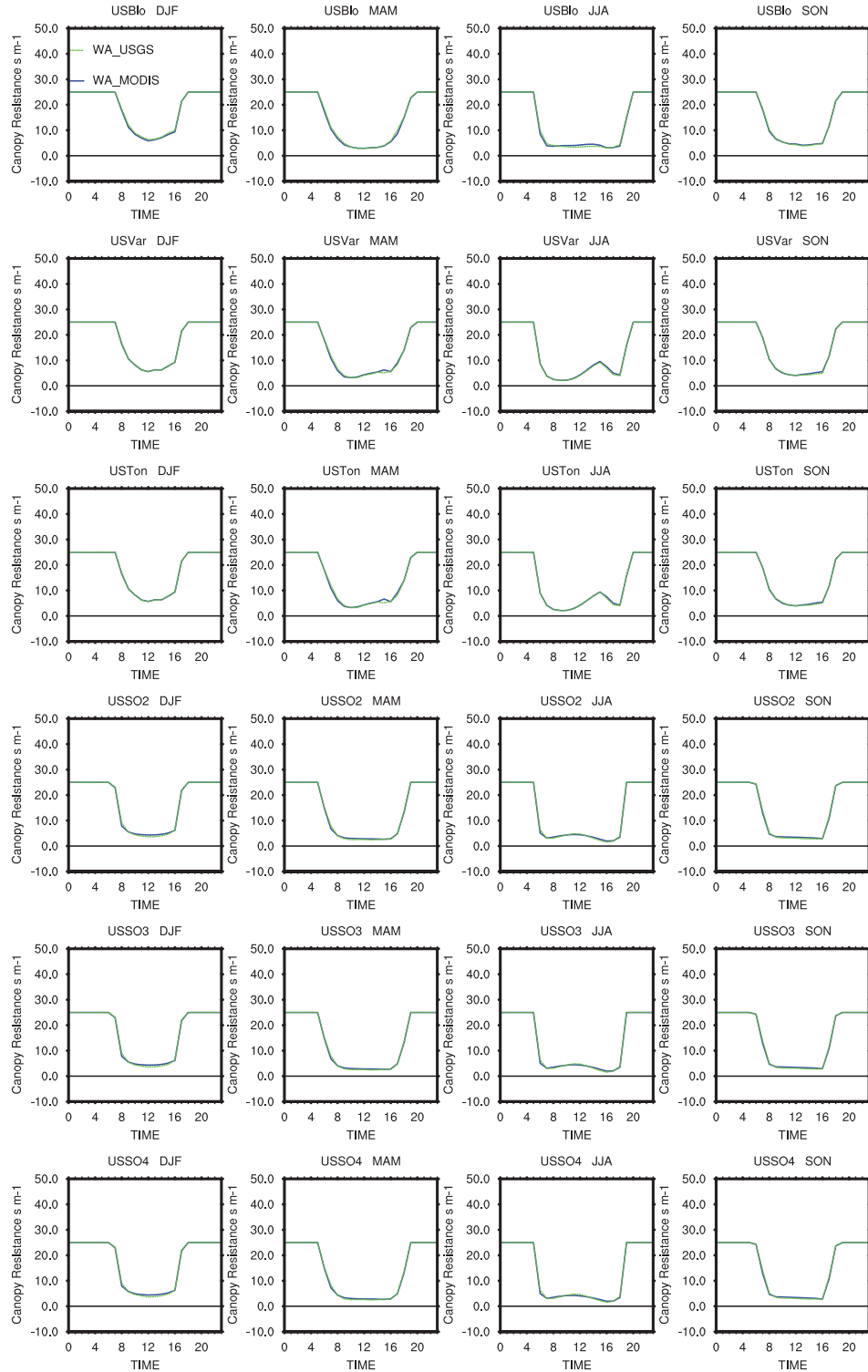


Figure III.16: The diurnal pattern of stomatal resistances. The blue line is WRF-ACASA with MODIS, the green line is WRF-ACASA with USGS.

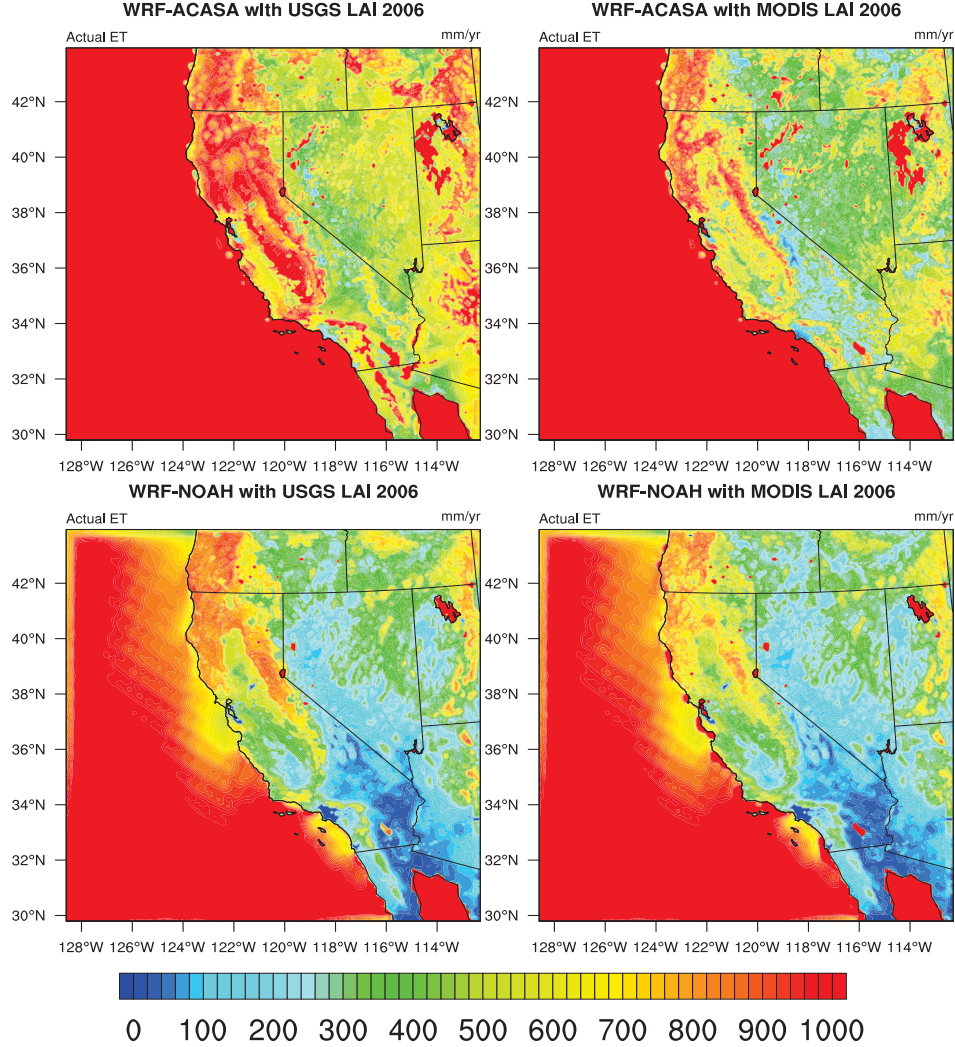


Figure III.17: Maps of ET_a.

sites are shown in Fig. III.18, III.19, III.20 and III.21 for the surface observations as well as the four model simulations. In general, the MODIS LAI helps improve latent heat fluxes in all simulations. The energy budget of the WRF-ACASA model is more sensitive to the LAI representation than the WRF-NOAH model. For example, when USGS LAI is used in the WRF-ACASA model, the latent heat fluxes over the three Sky Oak sites are greatly overestimated due to the overestimates of available leaf areas for transpiration (Figure 5a). The improvement of LAI with the MODIS data improved the energy budgets in the WRF-

ACASA model even when PFTs are mismatched (Figure 5b). In WRF-NOAH, the impact of MODIS LAI is only limited to reduction of latent heat flux over the three Sky Oak sites during the spring and summer seasons from the influence of LAI on the canopy resistance. Performances of both WRF-ACASA and WRF-NOAH models are poor over the Vaira Ranch during the summer months, when there is no active vegetation at the time and the dominant PFT does not represent this seasonal phenological inactivity of vegetation. However, the improvement in surface representation to include the leaf senescence will improve the WRF-ACASA simulations.

The Taylor diagram in Fig. III.22 summarizes the performances of the four simulations over the six AmeriFlux sites. The figure shows that the impacts of LAI on land surface models depend on the complexity of the model. While the effect of LAI is most profound in the ETa simulations, the high complexity WRF-ACASA model benefits the most from the increase in leaf area index accuracy. One example is where the LAI impacts model performance on simulating ETa during the spring and autumn seasons. The WRF-ACASA simulations of ETa using USGS LAI show poor correlations with surface observation. However, when MODIS LAI is used to improve the surface representation, the WRF-ACASA simulations of ETa also improved. There are some improvements of ETo when MODIS LAI is used for both model during the summer months, but differences are not significant in the remaining time periods.

In addition to the leaf area index, model complexity also has an impact on actual ET calculations. The WRF-ACASA model, either with or without MODIS LAI, performs better than the WRF-NOAH model during spring, summer as well as autumn seasons. Disparities between the surface observation and the WRF-ACASA simulations of air temperature, dew

WRF-ACASA with USGS LAI 2006

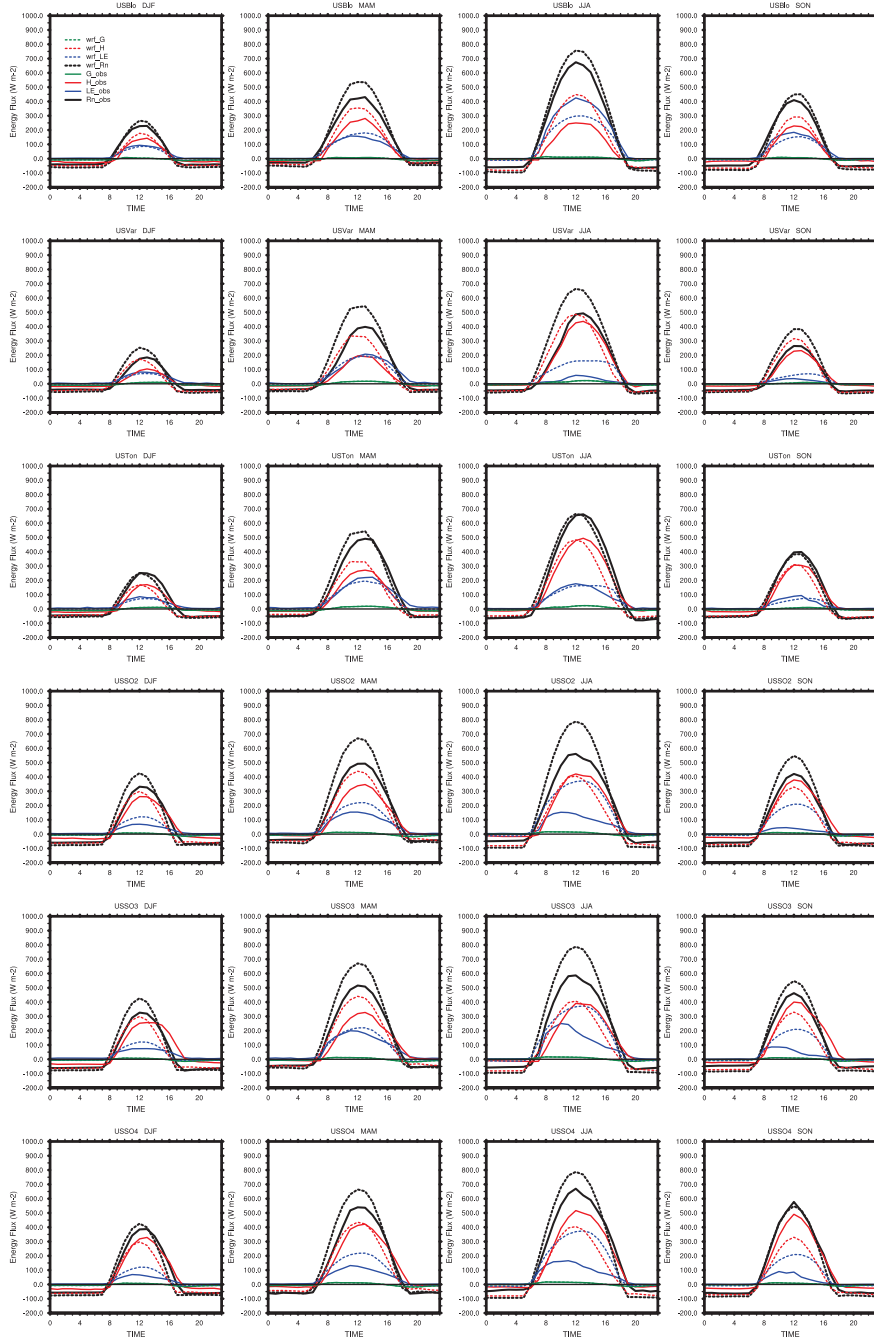


Figure III.18: The energy budget of WRF-ACASA with USGS LAI. The solid lines are for AmeriFlux station measurements, and the dash lines are for WRF-ACASA with USGS LAI simulations. Black is net radiation (R_n), red is sensible heat (H), blue is latent heat (LE), and green is ground heat flux (G).

WRF-ACASA with MODIS LAI 2006

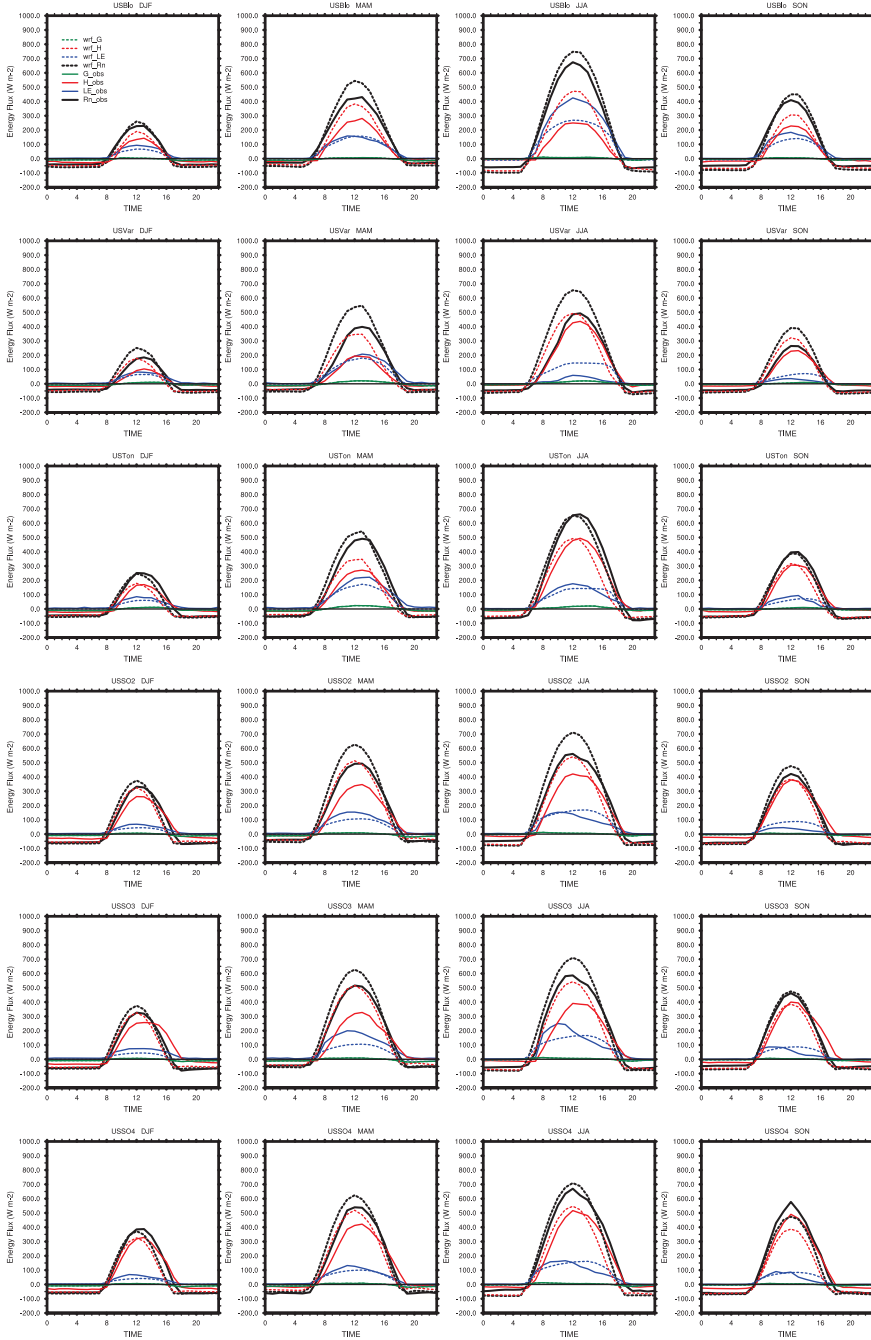


Figure III.19: Same as Fig. III.18 but for WRF-ACASA with MODIS LAI.

point temperature, and relative humidity at 2-meter height could be partially due to the differences in surface measurement heights and the assumed heights of the model outputs. This inconsistency between the observed and model simulation heights has a larger impact

WRF-NOAH with USGS LAI 2006

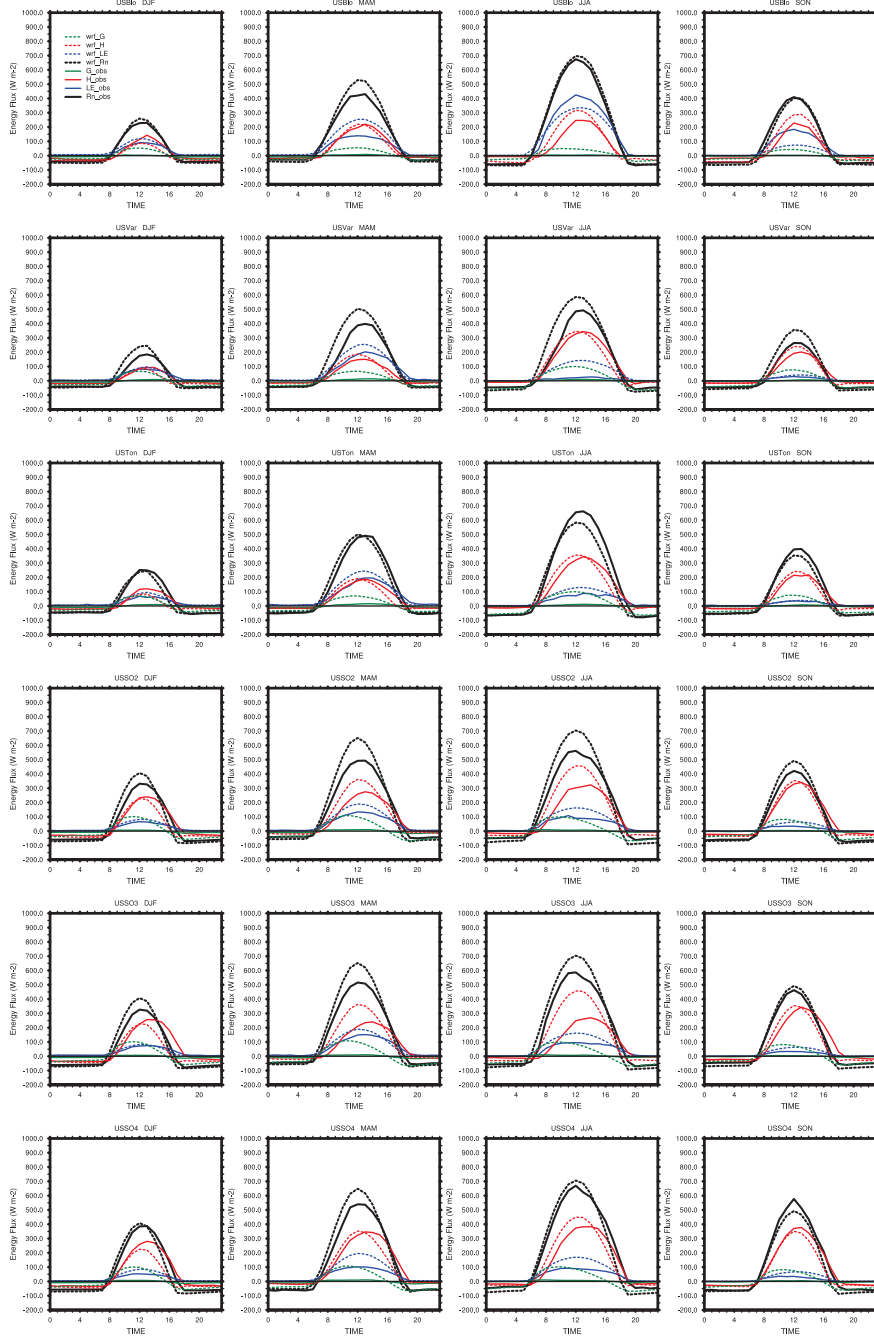


Figure III.20: Same as Fig. III.18 but for WRF-NOAH.

on the WRF-ACASA model, due to its multilayer canopy structure, than the single layer "big leaf" WRF-NOAH model. The three Sky Oak sites with mismatched PFTs are included in the Taylor diagram, and they also affect the model performance of WRF-ACASA due to

WRF-NOAH with MODIS LAI 2006

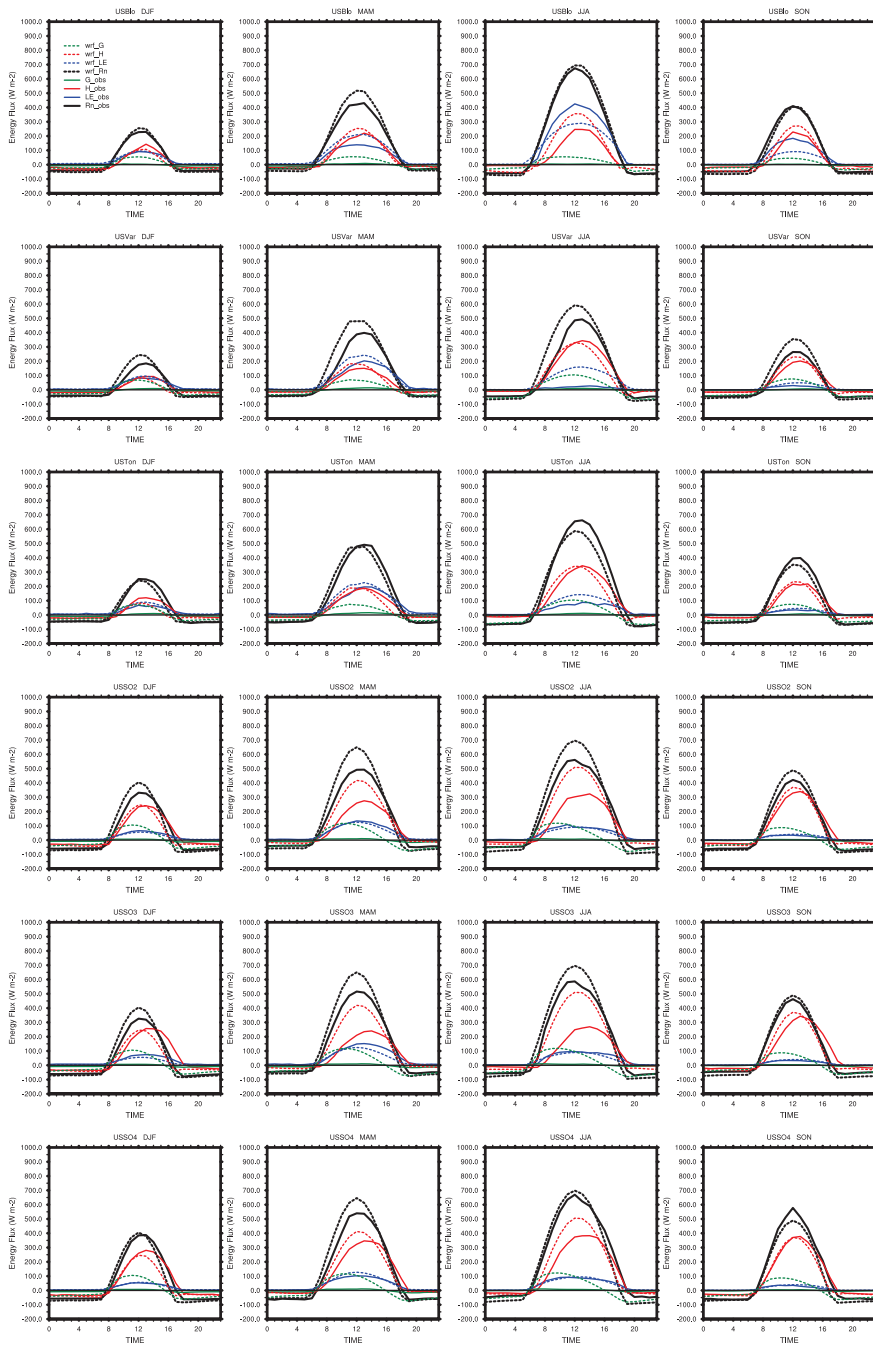


Figure III.21: Same as Fig. III.19 but for WRF-NOAH.

its sensitivity to PFT.

Taylor Diagram: Model vs. AmeriFlux 2006

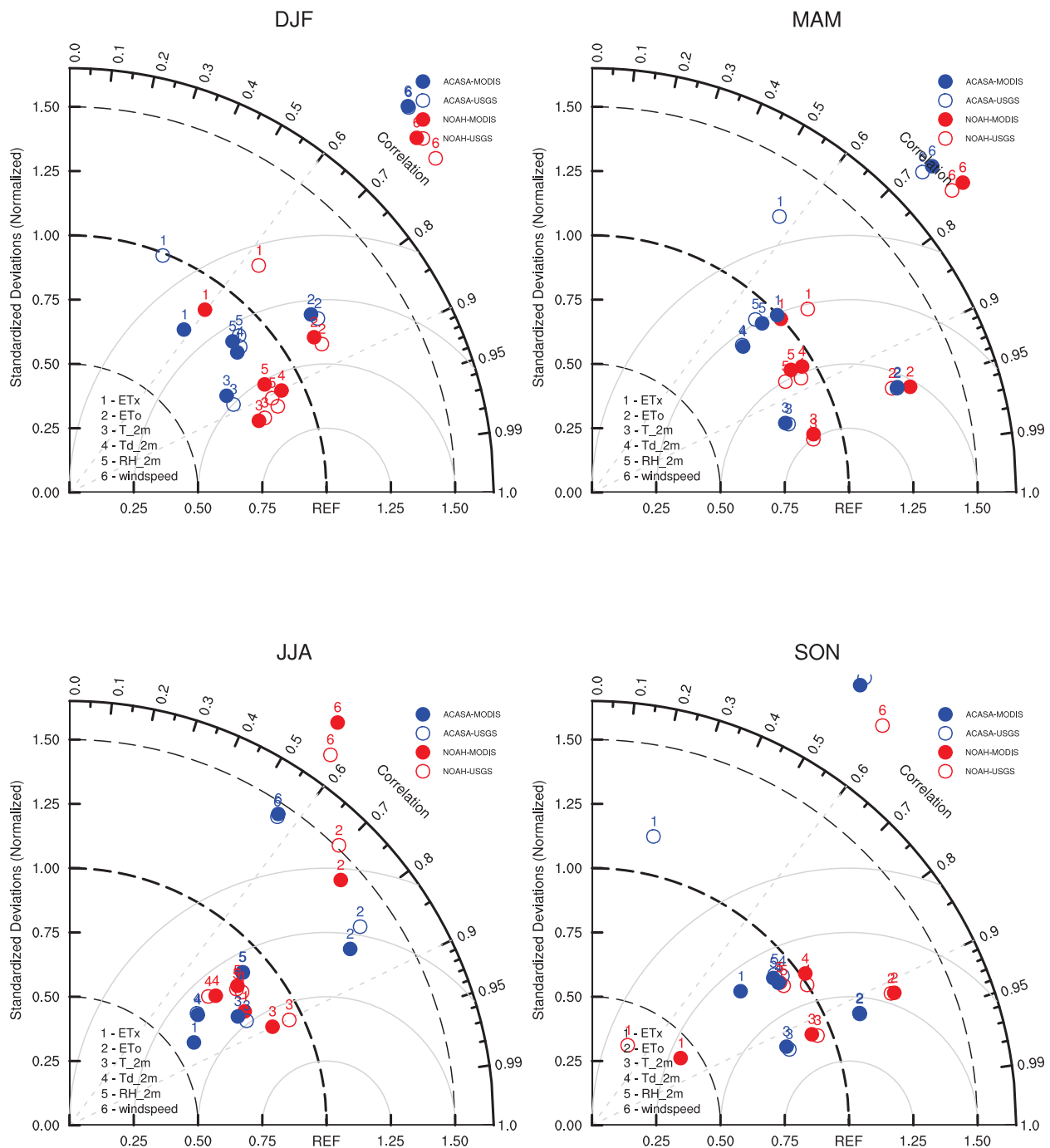


Figure III.22: Taylor diagram for model simulations and surface measurements of: air temperature, dew point temperature, and relative humidity for all six AmeriFlux sites. The order of the variables represented on the graphs is: actual evapotranspiration (ET_a), reference evapotranspiration (ETo), 2-meter air temperature (T_{2m}), 2-meter dew point temperature (Td_{2m}), 2-meter relative humidity (RH_{2m}), and 10-meter wind speed (windspeed).

4. Summary and Conclusion

In this study, the mesoscale model WRF was used to simulate ETo and ETa for locations with different combinations of land surface models and leaf area index datasets to examine the impacts that surface representations and model complexity have on ETo and ETa. The two land surface models included the intermediate complexity NOAH land surface model and high complexity ACASA model. The two LAI datasets used in the models were from the USGS and MODIS. There were four model simulations: WRF-ACASA with USGS LAI, WRF-ACASA with MODIS LAI, WRF-NOAH with USGS LAI, and WRF-NOAH with MODIS LAI. Each simulation was run for year 2005 and 2006, and covered all of California and adjacent terrain. The model results were evaluated using surface observations from the 120 CIMIS network stations for ETo and from the six AmeriFlux stations for both ETo and ETa. Sensitivity tests were employed to evaluate the impacts of differences in surface representations in both leaf area index and land cover type as well as model complexity on simulated ETo and ETa in diverse environmental conditions.

The results from these four simulations show that an increase in leaf area index accuracy generally improves estimates of ETa for both the WRF-ACASA and WRF-NOAH models, but it has little effect on ETo. Compared to the remotely-sensed measurements of LAI (MODIS), the climatological LAI dataset from USGS overestimates the leaf area index. When LAI is overestimated, there is more surface area for evapotranspiration to occur than in reality, and more radiation interception by the vegetative canopy. Therefore, there is a strong relationship between the leaf area index and the rate of evapotranspiration. The MODIS LAI helped improve the ETa calculation by increasing the accuracy of LAI representation.

This improved LAI helped to reduce the RMSE of model simulation by an average of 0.516 mm/day (Table III.2). Overall, the impact of LAI is larger on the WRF-ACASA model than the WRF-NOAH model because of the manner in which LAI impacts multiple processes and layers in ACASA compared to the single layer and simplified processes of NOAH .

Table III.2: ETa RMSE from LAI bias. Difference = RMSE (MODIS) - RMSE(USGS).

RMSE	Average	WRF-ACASA	WRF-NOAH
USGS	1.39073425	1.922467333	0.859001167
MODIS	0.874610708	1.043131917	0.7060895
Difference	-0.516123542	-0.879335417	-0.152911667

In addition to the leaf area index, the land use cover also impacts on simulations of ETa. The observed land use cover and the model land use cover for the six AmeriFlux sites are not well matched (Table III.1). When the land use cover is matched between surface observation and model assumption, WRF-ACASA had great accuracy in its ETa simulations, whereas the bias for the WRF-NOAH model increased (Table III.3). In the more complex WRF-ACASA model, the plant functional type determines the multilayer canopy structure as well as plant physiological parameters. As a result, it is more sensitive to the land cover type than the single layer WRF-NOAH models.

Table III.3: The ETa RMSE for WRF-ACASA and WRF-NOAH models from land use cover bias. Bad PFT (plant functional types) do not match between the observed and the models (the three Sky Oak sites). Good PFT are matched between the observed and the models for the Blodgett forest and the Tonzi Ranch.

RMSE	Average	WRF-ACASA	WRF-NOAH
Good PFT	0.964260656	0.998825063	0.92969625
Bad PFT	1.226428479	1.843054375	0.609802583
Difference	-0.262167823	-0.844229313	0.319893667

The accuracy in PFT, however, does not improve the model performance in the WRF-NOAH model. The WRF-NOAH simulation of ET_a for the Blodgett and Tonzi Ranch sites actually have higher RMSE values than the three Sky Oak sites, where PFTs are mismatched between observation and model. This is mostly due to the high bias in ET_a simulation over Blodgett forest, where the complex canopy physics, such as inter-canopy mixing and turbulent exchange, are underrepresented in the single layer WRF-NOAH model.

Model complexity determines the how surface representations effect ET_a estimates. For the more complex WRF-ACASA model, the combined effect of surface representations of leaf area index and land use cover is greater than the individual effect of either one (Table III.4). This is especially true over the tall Blodgett needleleaf forest, which provided ideal conditions to use the multilayer canopy structure and the third-order turbulent closure scheme of the WRF-ACASA model. The single layer WRF-NOAH model, however, experienced a slight reduction in ET_a simulations with the combined effect of surface representations. This is mostly due to the impact of PFT as mentioned above, where the single layer "big leaf" model has difficulty with tall and complex vegetated ecosystems such as the needleleaf forest.

In conclusion, surface representations such as leaf area index and land use cover appear to impact the detailed plant physiological processes calculations such as ET_a. How the overall representation affects surface processes, however, depends on the model complexity. As the model complexity increases, the model sensitivity to surface representation also increases. The surface processes of the WRF-ACASA model are more sensitive to the leaf area index than the simple, single layer WRF-NOAH model. The WRF-ACASA model is also sensitive to land use cover, whereas the WRF-NOAH model is not. The two Taylor diagrams for CIMIS stations and AmeriFlux stations do not show significant improvement in ETo or

Table III.4: The combined effect of surface representations (LAI and PFT) on the RMSE for WRF-ACASA and WRF-NOAH simulations.

WRF-ACASA	USGS	MODIS	MODIS-USGS
RMSE	LAI	LAI	
Good PFT	1.070249875	0.92740025	-0.142849625
Bad PFT	2.655658333	1.030450417	-1.625207917
Good-Bad	-1.585408458	-0.103050167	-1.728258083
WRF-NOAH	USGS	MODIS	MODIS-USGS
RMSE	LAI	LAI	
Good PFT	0.984426875	0.874965625	-0.10946125
Bad PFT	0.73622	0.483385167	-0.252834833
Good-Bad	0.248206875	0.391580458	0.138745625

other meteorological variables with improved LAI. There is, however, a small improvement of ETo in the WRF-ACASA when MODIS LAI is used instead of the USGS LAI.

While the high complexity of WRF-ACASA increases the realism of the plant physiological processes, it must be coupled with high accuracy in land surface representation in both leaf area index as well as land use cover. Consequently, there is a linear relationship between the model complexity and data quality in surface representation. The lower complexity land surface model is less restricted, thus providing more flexibility when high accuracy data is not available. Higher complexity models, however, perform better over more diverse ecosystems such as forests. Depending on the target variables and study areas of interest, the model complexity and surface representation requirements vary.

Further improvement in simulating surface processes such as the evapotranspiration can be achieved by improving the model grid cell representation. Both WRF-ACASA and WRF-NOAH models assume one dominant plant functional type in each grid cell. The AmeriFlux data, then again, show that such homogeneous representation of PFT is inaccurate. For

example, the Vaira Ranch and the Tonzi Ranch share the same grid cell while the actual surface and environmental conditions of the two sites are different. This error in grid cell representation is also true for the three Sky Oak sites. Instead of using only one dominant PFT in each grid cell, future simulations of land surface processes can be improved by using a combination of PFTs in each grid cell. Although the impact of heterogeneous land use cover in each grid cell might not have a large impact on low or even moderate complexity models such as WRF-NOAH, this could benefit models such as the WRF-ACASA model.

Chapter IV

Tracing the Carbon Dioxide Exchanges over California's Complex Ecosystems and Terrains using the WRF-ACASA Coupled Model

1. Introduction

Carbon dioxide is widely recognized as a major contributor to the current climate change phenomenon. Its emission to the atmosphere intensifies the atmospheric ability to absorb and re-emit energy and consequently increases surface temperature. Although carbon dioxide is not the most efficient greenhouse gas on a molecule-to-molecule basis, its concentration and large increases since the pre-industrial period, make it the most important anthropogenic greenhouse gas.

Fortunately, not all of the anthropogenic carbon dioxide emissions contribute to increases in the global mean carbon dioxide concentration. The Global Carbon Project (2010) shows that only 47% of the anthropogenic carbon dioxide emissions from 2000 to 2009 remain in the atmosphere. Oceans uptakes about 26% of the emissions and the remaining 27% is attributed to the terrestrial ecosystems, referred to as the "missing sink" of anthropogenic carbon emissions (Wigley and Schimel, 2005). The influence of the terrestrial carbon processes is visible in the atmospheric carbon dioxide concentration. The sinusoidal variation in the annual atmospheric carbon concentration is mainly due to the terrestrial growing season in the northern hemisphere, which has more land surface area than the southern hemisphere. Although it accounts for a significant amount of carbon dioxide exchange with the atmosphere and anthropogenic carbon uptake, there are large uncertainties in esti-

mating this terrestrial carbon flux. The terrestrial carbon sink of anthropogenic CO₂ in the Global Carbon Project is estimated as the residual of the atmospheric carbon concentration increase and the model ocean carbon uptake. Furthermore, the latest IPCC assessment report also points out that the uncertainties in climate change may be a result of uncertainties in carbon cycle (Collins et al., 2006). Hence, quantifying the carbon dioxide flux between the atmosphere and the biosphere remains a major challenge to the climate research community.

The exchange of carbon dioxide between the terrestrial system and the atmosphere is controlled by complex spatial, temporal and plant physiological variations. The eddy covariance method (EC) is regarded as the most accurate and widely used method to directly measure the carbon dioxide exchange between the atmosphere and the terrestrial system. It estimates the carbon dioxide flux through high frequency measurement of vertical wind velocity and carbon dioxide density. However, this method is not without problems and limitations. The EC method is most appropriate over large horizontally homogeneous vegetation and flat terrain. Flux is only applicable to the area of interest under turbulent conditions. The expensive instrumentation, long periods of measurement, and extensive maintenance and calibration requirements tend to limit the widespread adoption of carbon dioxide flux measurement. Therefore, it is difficult to assess the regional scale carbon dioxide flux between the terrestrial system and the atmosphere over a complex region such as California using only the EC method.

In order to fill in the gaps where EC measurements are not available or applicable, numerical models have been developed to simulate the effects of land surface on climate and atmosphere conditions and to calculate carbon dioxide fluxes. These models are referred to as the Land Surface Models (LSMs). Carbon dioxide, however, is not simulated in many

of the LSMs. For example, the land surface models in the mesoscale Weather Research and Forecasting model (WRF) do not include carbon dioxide exchange. Widely used LSMs with carbon calculations in climate studies differ greatly in their model complexities and their atmosphere-biosphere interaction. For example, the low complexity "big leaf" model oversimplify plant physiological processes and atmosphere-biosphere interactions (Paw U, 1997). The lack of multiple vegetation layers in a big leaf model renders it unable to resolve turbulence and vertical gradients that drive CO₂ fluxes (Wohlfahrt et al., 2001; Baldocchi and Meyers, 1998). Thus, they tend to overestimate of CO₂ uptake by plants as suggested by Paw U (1997). High complexity models that include the different vegetation covers, multiple canopy layers and interactive physiological processes in a land surface model is crucial in estimating carbon sequestration and the overall climate system through energy balances (Potter et al., 1993; Sagan and Khare, 1979; Anthes, 1984; Bougeault, 1991; Mihailovic et al., 1993). Furthermore, the importance of the terrestrial carbon sink is not limited to its amount of carbon uptake. The spatial and temporal distributions of the carbon sources and sinks have increasingly been the topic of discussion. Numerous studies from the AmeriFlux network using eddy covariance methods have shown that terrestrial carbon sinks vary in time, location, and weather conditions (Baldocchi et al., 2001; Falge et al., 2002; Law, 2007). Thus, the distribution of carbon is crucial in understanding the mechanisms and sustainability of the current terrestrial carbon sink.

In this study, the atmosphere-biosphere carbon dioxide exchange over the complex region of California is investigated using the mesoscale Weather and Research Forecasting model (WRF) coupled with the high complexity land surface model UC Davis Advanced Canopy-Atmosphere-Soil Algorithm (ACASA). In addition to simulating the carbon fluxes between

the two systems, the WRF-ACASA coupled model also changes the atmospheric carbon dioxide concentration according to the terrestrial carbon production and sequestration, as well as atmospheric carbon transport. Therefore the coupled model is capable of tracking the atmospheric carbon dioxide concentration to identify the spatial and temporal distribution of carbon sources and sinks on a regional scale. With all the tools in place, the objective of this study are to (1) quantify the biosphere-atmosphere exchange of carbon dioxide on a regional scale and (2) investigate the effect of atmospheric interactions between the adjacent ecosystems on the plant physiological processes at local and regional scales.

2. Models, methodology and data

2.1. Model description

The WRF model is a state-of-the-art mesoscale weather model developed for both operational forecasting and atmospheric research. The model physics and dynamic features include an Eulerian solver for the fully compressible non-hydrostatic equations with mass vertical coordinate, third-order Runge-Kutta time-integration, and fully conservative flux divergence integration. The high spatial and temporal resolution is ideal for studying the complex region of California. However, because carbon dioxide is not simulated by any of its land surface models and its default land surface models are relatively simplistic, the microscale land surface model: Advanced Canopy-Atmosphere-Soil Algorithm (ACASA) model is introduced as a submodel of WRF.

ACASA represents the interaction between vegetation, soil, and the atmosphere based on physical and biological processes described at the leaf or field scale (microscale). It is a

complex multilayer analytical land surface model that simulates both the microenvironment profiles and turbulent exchange of energy, mass and momentum within the surface-layer. The surface layer is represented as multiple vertical layers within and above the canopy into the lowest planetary boundary layer. The model also incorporates the higher third order turbulent closure scheme based on Meyers and Paw U (1986) and Meyers and Paw U (1987) to allow turbulent kinetic and thermodynamic processes to transport energy, mass, and carbon fluxes in both down gradient and counter gradient directions which many lower-order models are unable to directly simulate. Surface processes such as moisture, heat, momentum, and carbon dioxide fluxes are calculated for each of the interactive layers and integrated to represent the canopy level. In addition to the turbulent processes, the fourth-order technique from Paw U and Gao (1988) is used in the model to calculate the non-linear energy budget and surface energy temperature.

Carbon dioxide flux within the model is calculated from a combination of the Ball-Berry stomatal conductance (Leuning, 1990; Collatz et al., 1991) and the Farquhar et al. (1982) photosynthesis equation:

$$g_{s,w} = m \frac{A_n}{c_s} rh_s + b \quad (\text{IV.1})$$

$$rh_s = \frac{g_b q_A + g_{s,w} q_s(T_L)}{g_b + g_{s,w} q_s(T_L)} \quad (\text{IV.2})$$

$$c_s = c_A - \frac{A_n}{g_b} \quad (\text{IV.3})$$

$$A_n = V_c - 0.5V_0 - R_d = \min(A_R, A_E) - R_d \quad (\text{IV.4})$$

$$V_c - 0.5V_0 = \min(W_c, W_j) \left(1 - \frac{\Gamma}{C_i}\right) \quad (\text{IV.5})$$

where $g_{s,w}$ is the leaf stomatal conductance to water vapor, A_n is the net CO₂ uptake rate at the leaf surface, c_s and rh_s are the CO₂ concentration and the fractional relative humidity at the leaf surface, m and b are empirical regression coefficients; c_A is the CO₂ concentration in air, $q_s(T_L)$ is saturated mixing ratio of water vapor at leaf temperature T_L , g_b is the leaf boundary layer conductance, q_A is the mixing ratio of water vapor tin the air, V_c , V_0 and R_d are the carboxylation, oxygenation (photorespiration) and dark respiration rates of CO₂ exchange between the leaf and the atmosphere (in $\mu\text{mol m}^{-2} \text{s}^{-1}$), A_R is the Rubisco activity limit of CO₂ assimilation rate at lower intercellular CO₂ concentration when ribulose biophosphate (RuBP) is saturated, A_E is the CO₂ assimilation rate when the whole chain electron transport limits RuBP regeneration; W_c and W_j are the rates of carboxylation when RuBP is, respectively, saturated and limited by election transport (in $\mu\text{mol m}^{-2} \text{s}^{-1}$), Γ is the CO₂ compensation point in the absence of dark respiration and C_i is the intercellular CO₂ concentration ((in $\mu\text{mol m}^{-3}$).

Because carbon fixation and respiration vary significantly across vegetation types, meteorological inputs and additional species specific physiological parameters such as leaf area index, maximum rates of carboxylation, and biochemical photosynthetic coefficients are required by the model. This important feature allows ACASA to be coupled to the mesoscale model WRF and calculate carbon flux to and from any vegetation cover as long as the physiological parameters are available or can be estimated. More details on the stand-alone ACASA model can be found in Pyles (2000) and Pyles et al. (2000). The ACASA model has been successfully applied to the Wind River Canopy Crane site, which is an AmeriFlux site near Skamania, Washington, with a full set of eddy-covariance measurements that includes CO₂ flux (see Paw U et al., 2004, for a site description). The ACASA model has

been also applied and tested in a spruce forest site in Germany (Staudt et al., 2010) and a Mediterranean maquis ecosystem in Italy (Marras et al., 2011). All of the three studies have shown the ACASA model agrees well with surface observation of energy, moisture, and carbon dioxide fluxes.

2.2. Carbon dioxide tracer

In addition to examining the atmosphere-biosphere carbon dioxide exchange, the WRF-ACASA model also investigates the interaction of the carbon dioxide between neighboring regions in California. Because physiological processes vary across different land cover types and growing seasons, the carbon uptake or emission of one land cover should impact other regions. However, these interactions are difficult to determine since traditional in-situ carbon studies are limited to small areas with homogeneous land cover type. A carbon dioxide tracer is introduced to the WRF model. The new CO₂ tracer transports carbon dioxide, simulated through the surface plant physiological process, in the atmosphere, and modifies the atmospheric CO₂ concentration. It, consequently, induces interactions between neighboring regions.

The carbon dioxide tracer uses the same transport physics as for moisture, but without the chemical reactions and phase changes, in the MRF boundary layer model (Hong and Pan, 1996). This moisture transport scheme has been well used and tested within the WRF model. The model is initialized with a background atmospheric carbon dioxide concentration of 385 ppm. It is then changed through biosphere-atmosphere exchange of carbon dioxide from plant physiological processes in time and space. Atmospheric CO₂ concentration is calculated using a terrain-following hydrostatic pressure vertical coordinate. These vertical

sigma coordinates are normalized hydrostatic pressure levels derived between surface pressure and a constant upper atmosphere pressure (Laprise, 1992; Klemp et al., 2003).

2.3. Data

The WRF-ACASA coupled model simulation was for carbon dioxide and exchange for all of California. This area covers geographic regions with various complex ecosystems and climate variations. Many characteristic ecosystems in California (chaparral, agricultural crops, Central Valley grassland, woodland, conifer forest, and steppe) are included. The extensive topographic and vegetation variability in this region provides a great opportunity to study the interactions of neighboring land cover types and their effects on carbon flux. The climate in the region is mostly Mediterranean with warm and dry summer while the winter is cool and moist.

There are six Ameriflux Network Eddy Covariance stations in California that are available to evaluate the WRF-ACASA coupled model over the simulation period of 2005 and 2006. Due to the model horizontal resolution, the Vaira Ranch and the Tonzi Ranch stations share the same model grid cell; however, the surface characteristic differ considerably. In addition, the Vaira Ranch grass vegetation growing season falls between Octobers and May, which is not represented in the model simulation due to horizontal homogeneous assumption within each grid cell. The three Sky Oak sites are all located in a single grid cell over Southern California (Fig. IV.1). Consequently, carbon dioxide flux simulations from the WRF-ACASA model are compared to the carbon flux measurements from these sites over different vegetation covers.

An important challenge in comparing model simulations and surface observations is the

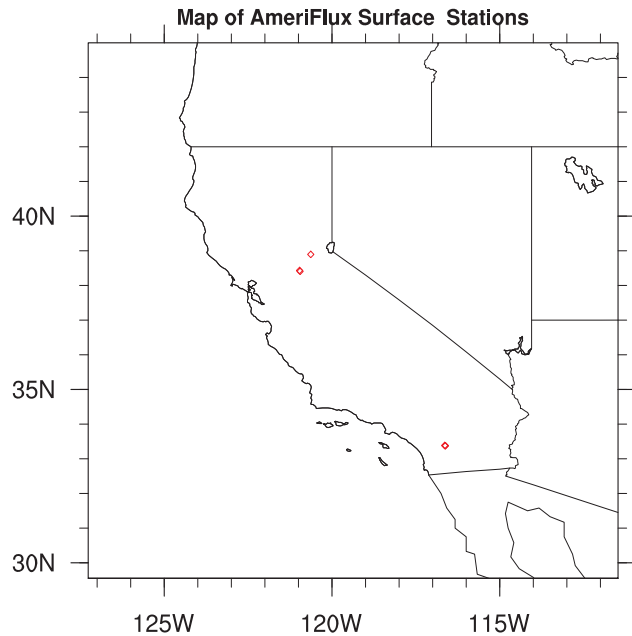


Figure IV.1: Locations of the six AmeriFlux sites used in this study. In Northern California, Blodgett Forest site is northeast of the Tonsi and Vaira sites (shown as one point). All three Southern California sites are at the same location.

difference between the heights and station landscape of the observational stations and the heights of the simulations grid points. The Plant Functional Types (PFT) used in the WRF-ACASA simulations match poorly with the observed PFT at the sites (Table IV.1). Previous chapters show that the land cover type is an important component of the surface representation in land surface models, especially high complexity land surface model such as ACASA. Therefore, the mismatch of PFT in the WRF-ACASA coupled model is an initial condition error that negatively impacts the plant physiological simulations. When the PFTs in the WRF-ACASA coupled model agree with the observed PFT, the simulated carbon dioxide exchange improved.

Table IV.1: AmeriFlux sites used and information.

Station	Latitude	Longitude	WRF Plant Functional Type (PFT)	WRF-ACASA Canopy height (m)	Site observed PFT
USBLO	38.8953	-120.633	Evergreen Needleleaf Forest	17	Evergreen Needleleaf Forest
USVAR	38.4067	-120.951	Savanna	10	Grasslands
USTON	38.4316	-120.966	Savanna	10	Woody savannas
USSO2	33.3739	-116.623	Evergreen Needleleaf Forest	17	Woody Savannas
USSO3	33.3772	-116.623	Evergreen Needleleaf Forest	17	Closed Shrublands
USSO4	33.3844	-116.64	Evergreen Needleleaf Forest	17	Closed Shrublands

2.4. Model setup

Two WRF-ACASA simulations are compared: (1) WRF-ACASA with constant atmosphere carbon dioxide concentration at 385 ppm, and (2) WRF-ACASA with CO₂ transport in the atmosphere using the new CO₂ tracer. Simulations are forced by the MODIS LAI dataset and the Northern America Regional Reanalysis (NARR) dataset for surface and meteorological conditions to drive the initialization and boundary conditions of the WRF models (Mesinger et al., 2006). Year 2005 and 2006 are simulated over California at an 8 km x 8 km horizontal resolution. Each run contains 13 months of simulations with the first month being discarded as spin-up. For example, year 2006 is simulated from December 2005 to December 2006. Atmospheric physics schemes used in this study are the Purdue Lin et al. scheme for microphysics (Chen and Sun, 2002), the Rapid Radiative Transfer Model for long wave radiation (Mlawer et al., 1997), the Dudhia scheme for shortwave radiation (Dudhia, 1989), the Monin-Obukhov Similarity scheme for surface layer physics of non-vegetated surfaces and the ocean (Monin and Obukhov, 1954), and the MRF scheme for the planetary boundary layer (Hong and Pan, 1996). Results presented here are mostly from year 2006 because of the large amount of missing observational data in 2005.

3. Results and discussion

The diurnal patterns of carbon dioxide flux simulated by WRF-ACASA model with or without varying atmospheric CO₂ concentration are shown in Fig. IV.2 and IV.3. Both WRF-ACASA simulations have good agreements with the surface observations when plant functional types (PFT) match between the surface observation and model. Observed diurnal patterns are created only from days with complete 24-hour data. As pointed out in previous

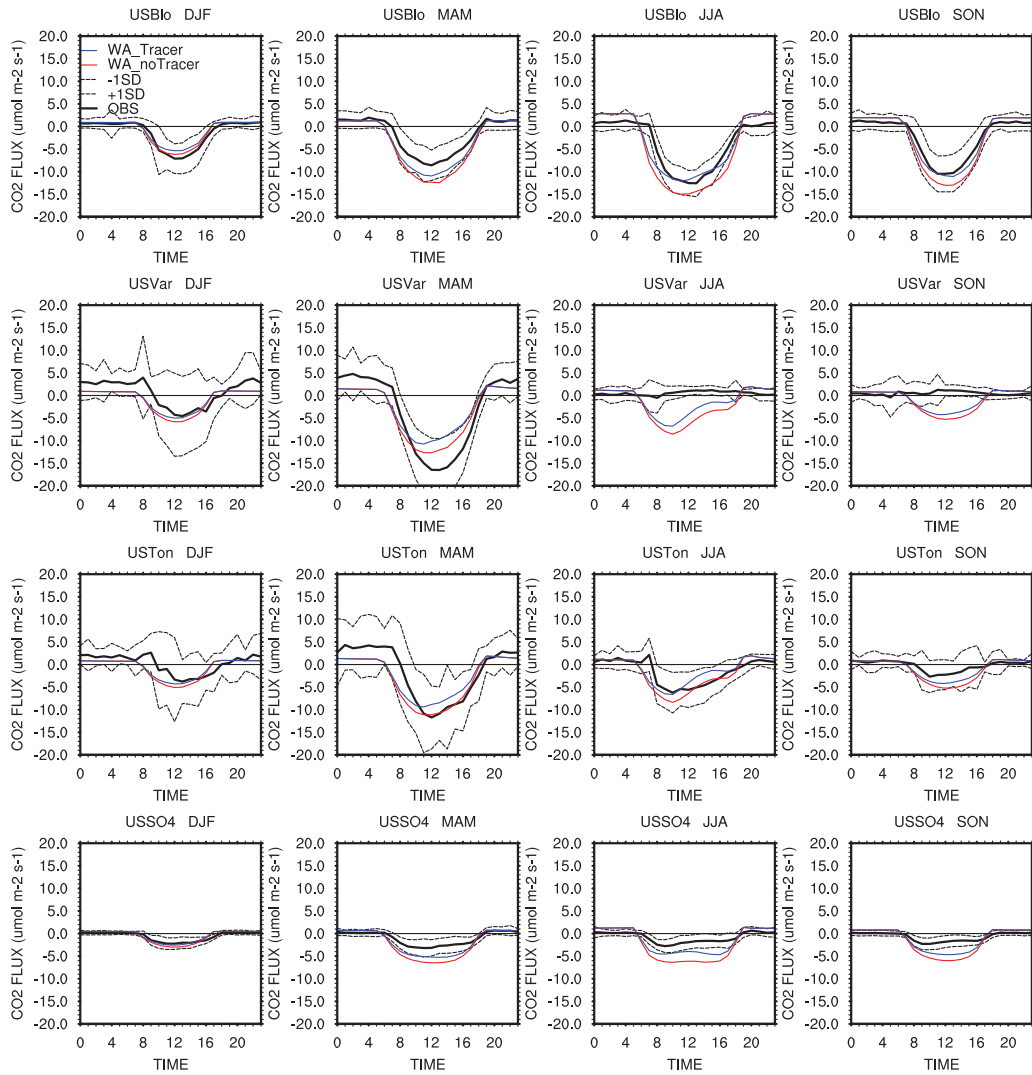


Figure IV.2: Diurnal patterns of carbon dioxide flux for the AmeriFlux sites for year 2005.

chapters, accurate surface representation is important for a land surface model; especially with the high complexity models such as WRF-ACASA. Both simulations perform well over the Blodgett forest and the Tonzi Ranch, where PFTs match between observation and model. The simulated diurnal patterns of CO₂ flux over the Blodgett forest and Tonzi Ranch sites are well within the one standard deviation of the surface measurements. This shows that the complex plant physiological processes in the WRF-ACASA model are robust and able to simulate the CO₂ fluxes correctly across the region. Although the WRF-ACASA model overestimates the CO₂ exchange at the three Sky Oak sites and Vaira Ranch, these flux problems are due to the input biases of PFT mismatch and lack of heterogeneous surface representation. Improvement of these surface representations will improve the WRF-ACASA simulations.

The scatter plots of hourly CO₂ flux (FCO₂) are shown in Fig. IV.4 for the WRF-ACASA simulations without and with CO₂ tracer over the AmeriFlux sites for 2006. Both WRF-ACASA simulations compared well with the surface observations except for the Vaira Ranch during warm months of summer and autumn, when the site vegetation is dormant due to summer drought. There are no significant differences between the two simulations from the scatter plots. The statistical analysis, however, shows that the WRF-ACASA simulation with CO₂ tracer reduces the Root Mean Square Error (RMSE) values for almost all stations and all seasons (Table IV.2).

Figures IV.2, IV.3 and IV.4, along with Table IV.2, illustrate a positive impact of varying atmospheric CO₂ concentration on plant physiological processes. This positive impact mainly occurs during the daytime when plants are most active. Photosynthesis by plants reduces the ambient CO₂ concentrations, and new CO₂ is transported to the site through the atmosphere.

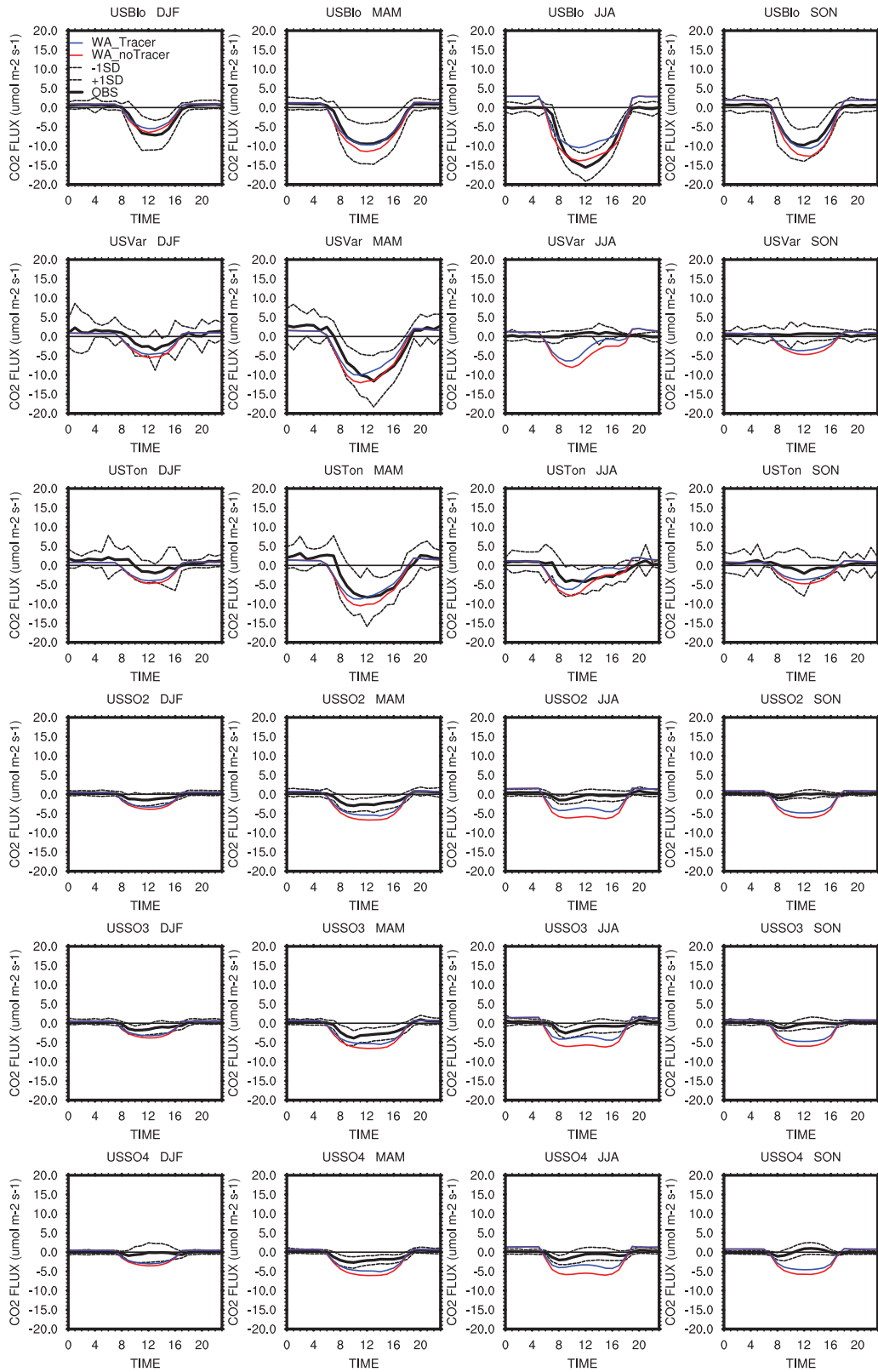


Figure IV.3: Same as Fig. IV.2 but for year 2006.

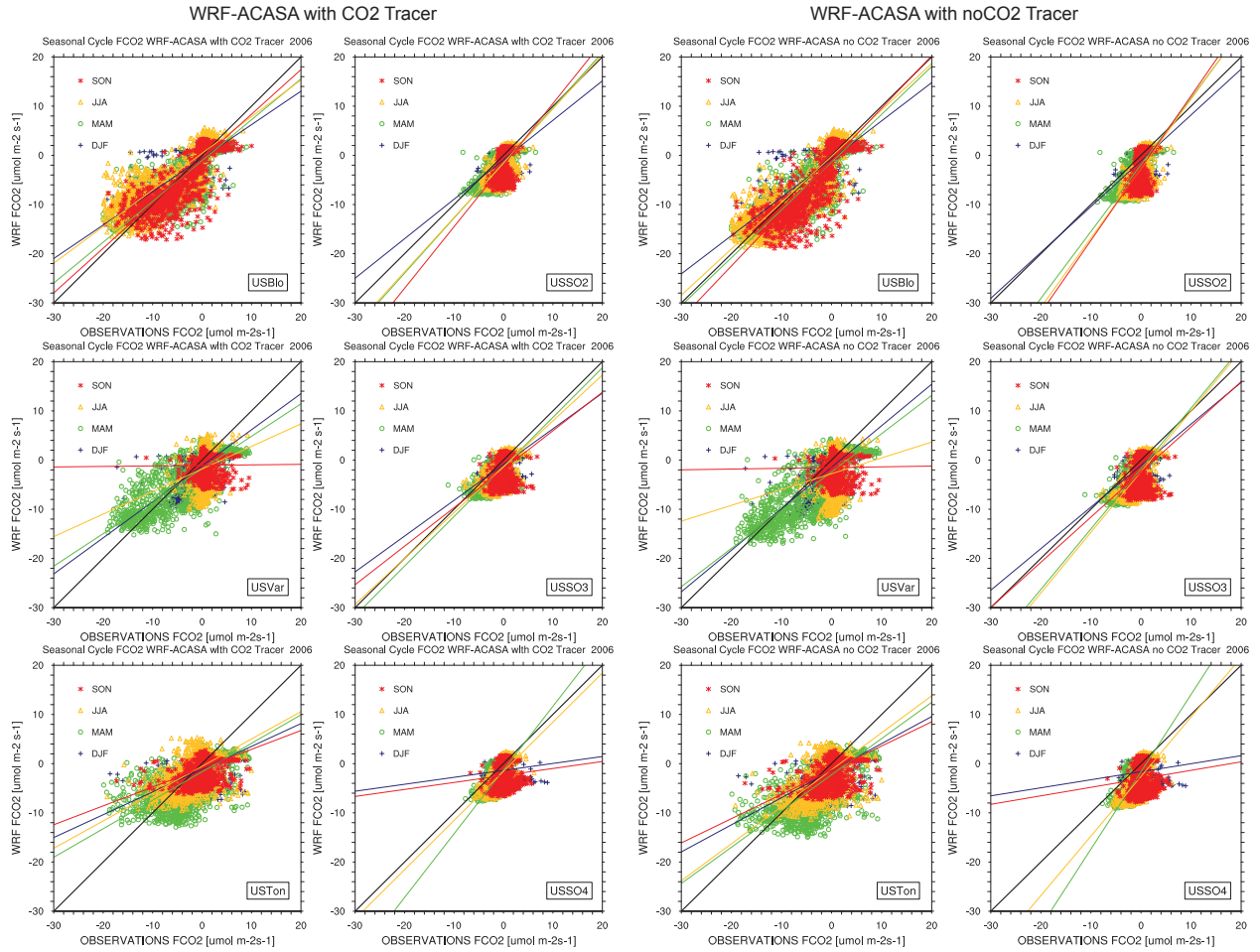


Figure IV.4: Scatter plots of CO_2 flux (FCO2) by season.

When less CO_2 is available in the atmosphere, photosynthetic uptake of carbon by plants is reduced. As a result, it reduces the overestimation of photosynthesis and the RMSE values when no tracer is used and the ambient CO_2 concentration is held constant at 385 ppm (Table IV.2). For example, the diurnal CO_2 flux for the Blodgett forest improves during the spring, summer, autumn of 2005 and spring and autumn of 2006 with a CO_2 tracer (Fig. IV.2 and Fig. IV.3).

The time series of net ecosystem CO_2 exchange (NEE) for each of the AmeriFlux sites during the year 2005 and 2006 display the overall ecosystem physiological activities (Fig. IV.5

Table IV.2: AmeriFlux sites used and information.

Row Labels	DJF			MAM			JJA			SON		
	RMSE	R2	RC									
WRF-ACASA no CO₂ Tracer												
USBlo	2.79	0.89	0.77	3.44	0.95	0.96	3.58	0.99	0.89	3.66	0.96	1.04
USVar	3.00	0.76	0.74	4.51	0.82	0.74	5.14	0.16	0.19	3.84	0.06	0.02
USTon	3.61	0.37	0.40	4.98	0.69	0.63	3.67	0.62	0.57	3.35	0.30	0.36
USSO2	1.93	0.79	0.93	3.25	0.77	1.36	4.04	0.72	1.41	4.11	0.71	1.47
USSO3	1.89	0.76	0.84	3.01	0.80	1.23	3.71	0.76	1.23	3.89	0.71	0.92
USSO4	2.78	0.26	0.16	3.21	0.75	1.57	3.84	0.73	1.21	4.52	0.28	0.17
WRF-ACASA with CO₂ Tracer												
USBlo	2.67	0.80	0.68	3.08	0.94	0.82	4.32	0.82	0.71	3.16	0.97	0.89
USVar	2.71	0.68	0.64	4.28	0.71	0.63	3.99	0.23	0.29	3.30	0.05	0.01
USTon	3.26	0.31	0.36	4.83	0.48	0.49	3.45	0.35	0.42	3.02	0.19	0.28
USSO2	1.65	0.77	0.80	2.54	0.82	1.12	2.75	0.81	1.10	3.29	0.74	1.25
USSO3	1.63	0.72	0.73	2.35	0.84	1.01	2.51	0.83	0.93	3.14	0.69	0.78
USSO4	2.49	0.24	0.14	2.42	0.80	1.30	2.54	0.79	1.00	3.70	0.25	0.14

and Fig. IV.6). NEE is the cumulative net primary production of carbon minus respiration, and it is calculated as the cumulative sum of carbon flux throughout the year. When NEE at the site is positive at the end of the year, the site is a carbon source; having more CO₂ respired to the atmosphere than carbon uptake through photosynthesis. On the other hand, a negative annual NEE indicates an annual carbon sink.

As expected for the Blodgett forest in 2006, the usage of CO₂ tracer generally reduces the overestimation and improves the simulation of annual NEE. For example, the WRF-ACASA model with CO₂ tracer simulation of NEE (-930 gC m⁻² yr⁻¹) closely followed the observed NEE (-908 gC m⁻² yr⁻¹) for the Blodgett forest throughout year 2005 (Fig. IV.5, Fig. IV.6 and Table IV.3). And the CO₂ tracer simulated NEE for Tonzi Ranch site was -529gC m⁻² yr⁻¹, comparing well with the observed annual NEE of -505 gC m⁻² yr⁻¹.

There is, however, a large interannual variability between year 2005 and 2006 where carbon sinks were larger for most sites in 2005 except the Blodgett forest. The WRF-ACASA with CO₂ tracer underestimated the annual NEE magnitude in 2006 for the Blodgett forest

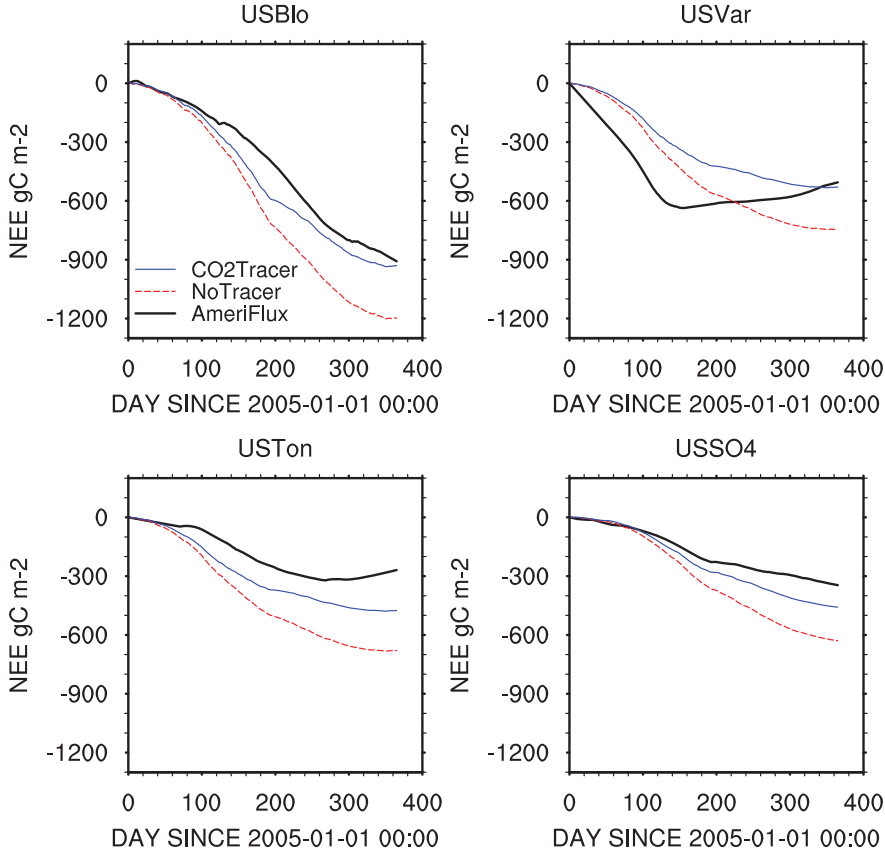


Figure IV.5: Time series of annual NEE for model simulations and surface observations for year 2005.

mainly due to the underestimate of photosynthesis during the summer months as indicated in Fig. IV.2 and Fig. IV.3. Meanwhile, the model overestimated the carbon uptake for the Tonzi Ranch during the autumn season for 2006. The carbon sinks for Vaira Ranch, Tonzi Ranch and the three Sky Oaks sites are also smaller in year 2006 than 2005. Although the WRF-ACASA model overestimated the NEE for the Sky Oak sites due to the initial mismatch of PFT, improvement in PFT will improve the WRF-ACASA model by using more appropriate parameters such as maximum carboxylation velocity for physiological processes.

The spatial distributions of NEE for the four seasons using WRF-ACASA model with and without CO₂ tracer are shown in Fig. IV.7. The inclusion of CO₂ tracer in the model

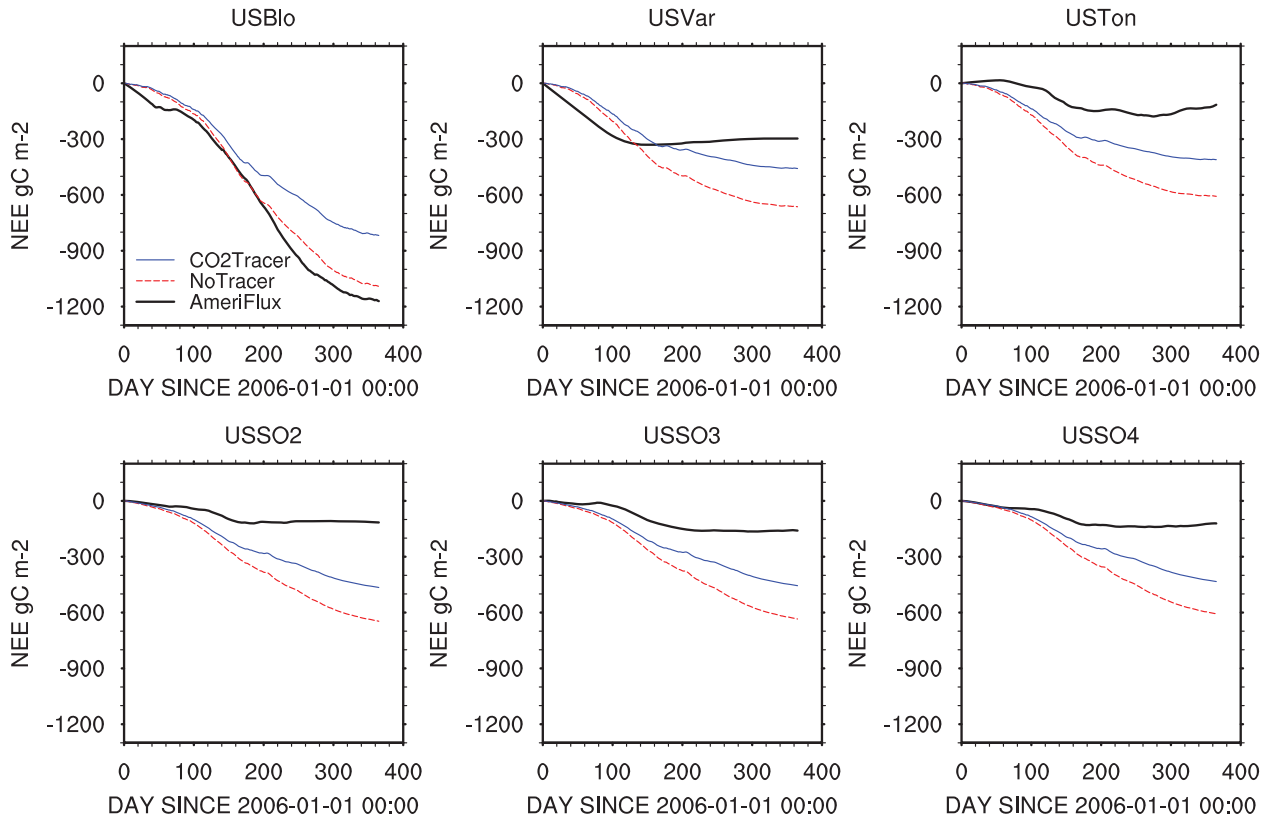


Figure IV.6: Same as Fig. IV.5 for year 2006.

reduced the seasonal NEE in several regions in California. The differences between the two simulations are small during the winter and autumn seasons, which are similar to the results shown in Figure 2; not surprisingly since the NEE magnitudes are smaller, and therefore the effects of advected CO_2 are reduced. During spring and summer, when plants are more active, however, the seasonal carbon sink or negative NEE values over the Sierra Nevada mountain regions is smaller when CO_2 tracer is used. Furthermore, the Central Valley changed from a carbon sink when no CO_2 tracer is used to a carbon source with CO_2 tracer during the summer months. This is due to the reduction in photosynthesis in response to the lower ambient CO_2 concentration when carbon (or in this case, depleted carbon concentrations) is transported in the atmosphere. This switch of carbon sink to carbon

source demonstrates the importance of a fully coupled biosphere-atmosphere interaction. Feedbacks between the two systems through exchange and transport of carbon reflect a more realistic representation of the natural processes of interaction between ecosystems and the atmosphere, and with advection of carbon dioxide concentrations, between the atmosphere and ecosystems downwind.

Overall, the annual NEE for 2006 show that plants in the Northern California regions actively uptake more carbon dioxide from the atmosphere than carbon emissions through respiration and create net carbon sinks (Fig. IV.8). The Southern California regions, which include the Mojave Desert and mostly low vegetation regions, are carbon sources where more carbon is released into the atmosphere than is absorbed. The coupled CO₂ tracer reduced the annual NEE over the northern California and the Sierra Nevada mountain regions. The regions with large carbon sources as indicated in red are generally urban areas where more

Table IV.3: Time series of annual NEE of the six AmeriFlux sites for year 2005 and 2006. No time series of NEE is displayed for Sky Oak sites, USSO2 and USSO3, due to large amount of missing data in 2005.

Annual NEE [gC m⁻² yr⁻¹]	AmeriFlux Sites	Observation	WRF-ACASA no CO₂ Tracer	WRF-ACASA CO₂ Tracer
2005	USBlo	-908	-1197	-930
	USVar	-506	-744	-529
	USTon	-269	-679	-475
	USSO2	No Data	-670	-491
	USSO3	No Data	-658	-481
	USSO4	-346	-629	-458
2006	USBlo	-1171	-1091	-818
	USVar	-297	-664	-458
	USTon	-116	-608	-411
	USSO2	-116	-647	-465
	USSO3	-160	-635	-456
	USSO4	-121	-607	-433

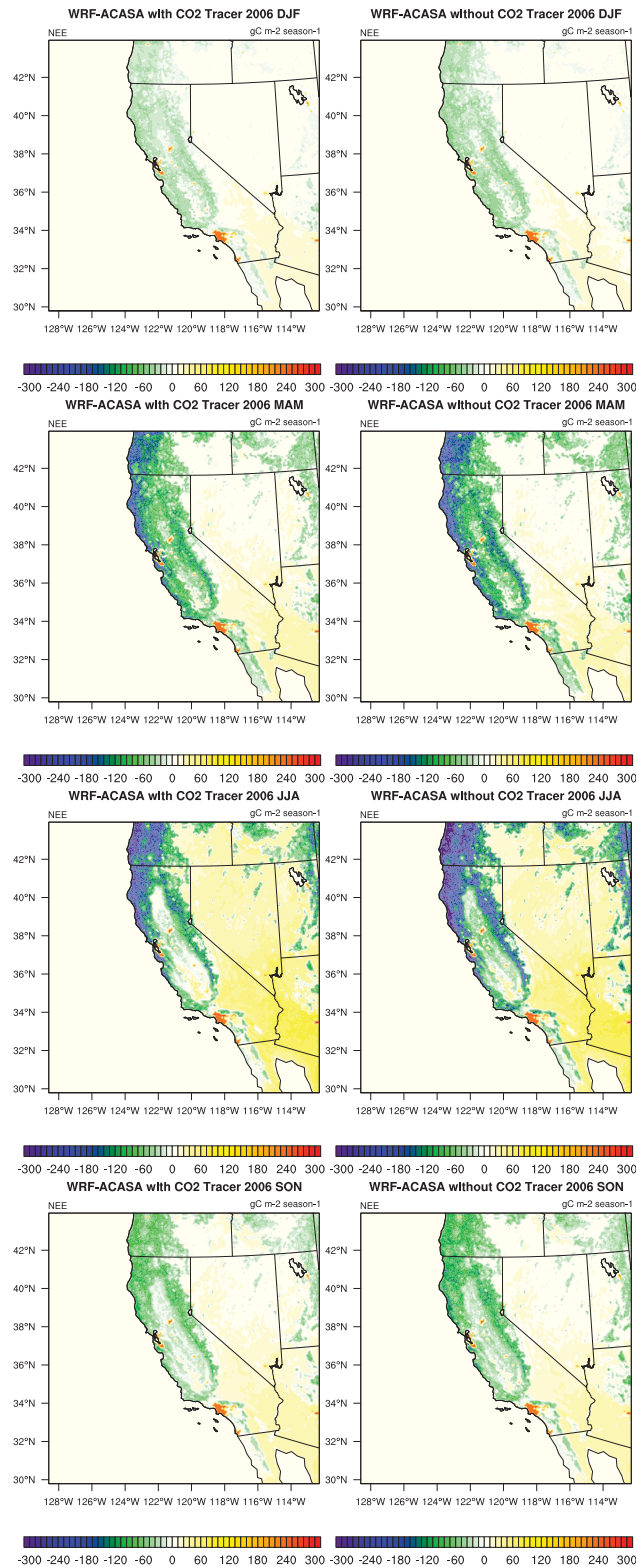


Figure IV.7: WRF-ACASA simulations of seasonal NEE with and without CO₂ Tracer for 2006. Results for 2005 is similar to 2006.

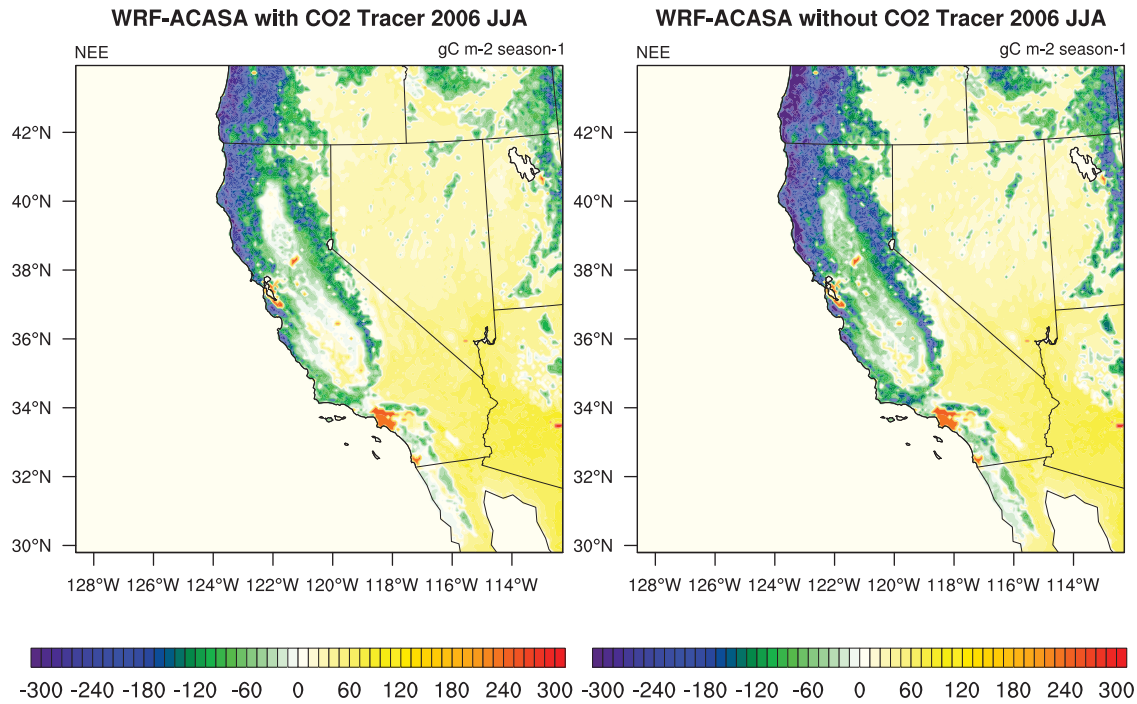


Figure IV.8: Annual NEE of carbon dioxide for year 2006 for WRF-ACASA simulations with and without CO₂ tracer.

carbon dioxide is released into the atmosphere than carbon uptake by vegetation. Default urban carbon emission from traffic is based on urban land use area. Future improvement on urban emission will link the model to observed urban population and traffic data. Even though, the WRF-ACASA model overestimated carbon uptakes for the AmeriFlux sites due to various reasons mentioned previously, the CO₂ concentration and transport in the atmosphere have an important role in modeling plant physiological processes.

Diurnal patterns of ambient CO₂ concentration are compared for each of the AmeriFlux site between observed values and the simulated values by the WRF-ACASA model, in which CO₂ tracer is used to transport carbon dioxide in the atmosphere (Fig. IV.9 and Fig. IV.10). They show that the CO₂ tracer in the WRF-ACASA model is able to mimic the natural evolution of atmospheric CO₂ concentration (ACO₂) due to changes in surface plant phys-

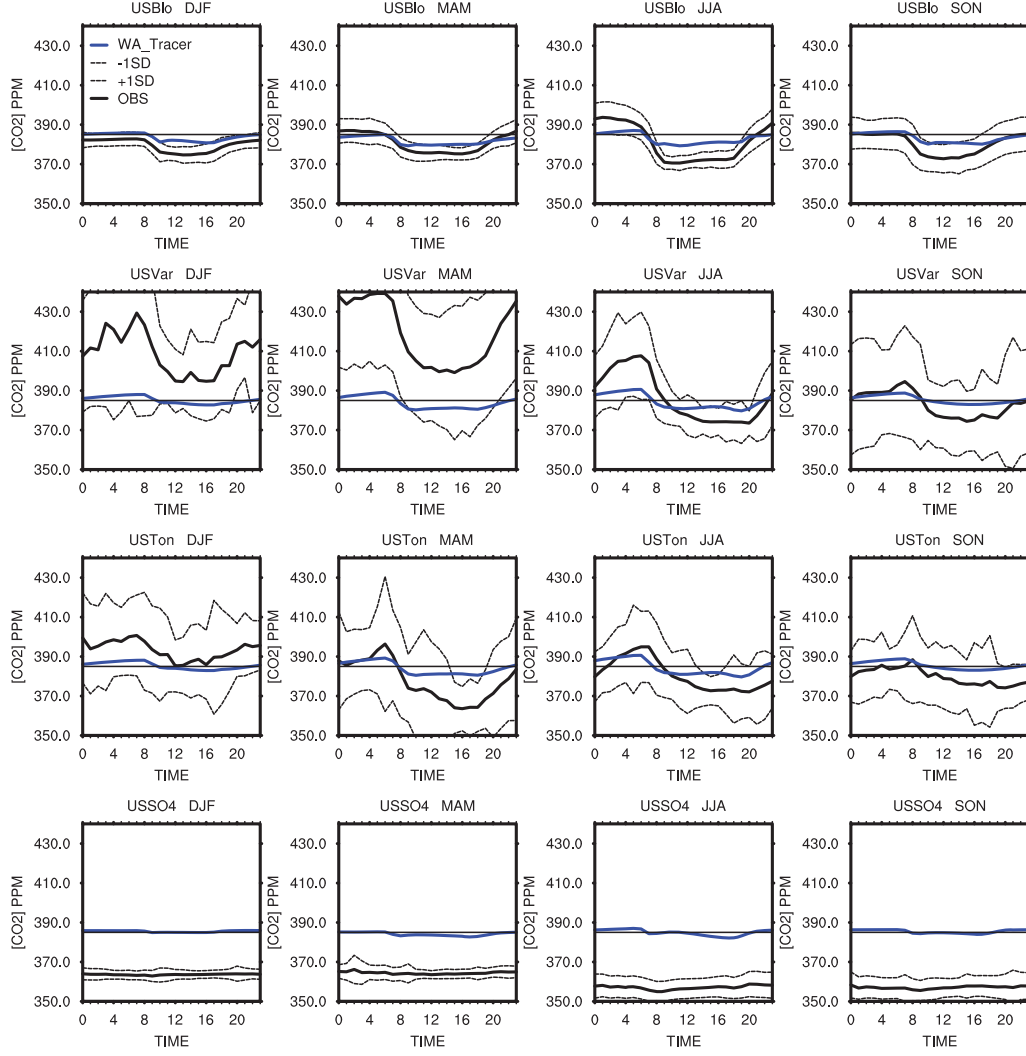


Figure IV.9: Diurnal patterns of atmosphere carbon dioxide concentration for the six AmeriFlux sites for year 2005. Black solid lines represent observation from AmeriFlux sites, and black dash lines represent one standard deviation below and above the diurnal means. Blue lines are WRF-ACASA simulations with CO_2 tracer.

iological processes and atmospheric transport. Photosynthesis from the vegetation actively removes carbon dioxide from the atmosphere and thus lowers the ambient CO_2 concentration during the daytime, whereas respiration increases the ambient CO_2 concentration.

When PFTs match between site observations and model assumptions, the simulated CO_2 concentrations over the Blodgett forest and the Tonzi Ranch have good agreements with the surface observation. The reduction of ambient CO_2 concentration is more pronounced over

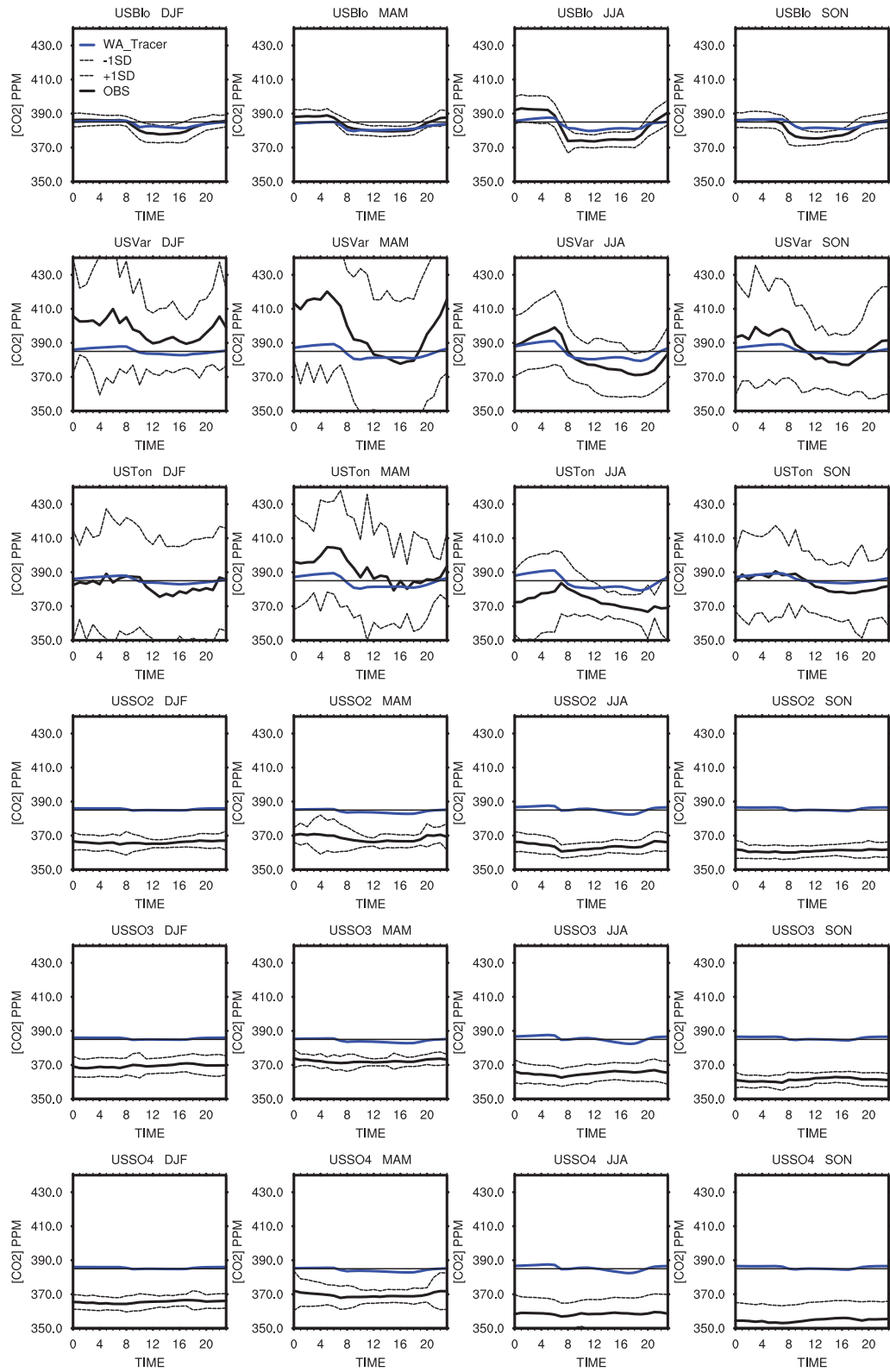


Figure IV.10: Same as Fig. IV.9 for year 2006.

sites with higher plant physiological activities such as the Blodgett forest, the Vaira and Tonzi ranches. For both years, the Blodgett forest reduced the ambient CO₂ concentration by an average of 6 to 7 ppm during the daytime. The lower ambient CO₂ concentration persisted into the evening when respiration slowly increased the CO₂ concentration toward and exceeded the initial 385 ppm. The time lags in the diurnal patterns of atmospheric CO₂ concentration compares to the diurnal patterns of CO₂ flux reflect the cumulative effect of daytime and nighttime carbon dioxide exchanges between the biosphere and atmosphere. Meanwhile, the atmospheric CO₂ concentration over the Sky Oaks sites exceeded the initial concentration during the winter season when plants released more CO₂ into the atmosphere than uptake by photosynthesis.

Over the Sky Oak sites where mismatch of PFT occurs, there are large differences between the simulated and observed diurnal pattern of ACO₂. The poor performance over the Sky Oak sites could be the result of initial conditions where a constant field of 385 ppm applied over the domain is much higher than the observed ACO₂ at around 365 to 370 ppm at these sites. Despite the bias from initial conditions, the changes in time and magnitude from the simulated ACO₂ match well with the observed ACO₂ seasonal and diurnal patterns for both year 2005 and 2006. While there are no data to evaluate the model performance in atmospheric carbon dioxide concentration over the entire region, the evaluations from the AmeriFlux sites shows that the CO₂ tracer in the WRF-ACASA model is robust and physically sound.

The WRF-ACASA model with CO₂ tracer simulates the seasonal averages of ACO₂ at different vertical levels. The spatial distribution of ACO₂ anomalies from the initial field of 385 ppm is shown in Fig. IV.11 for the year 2006, because the CO₂ is transported both

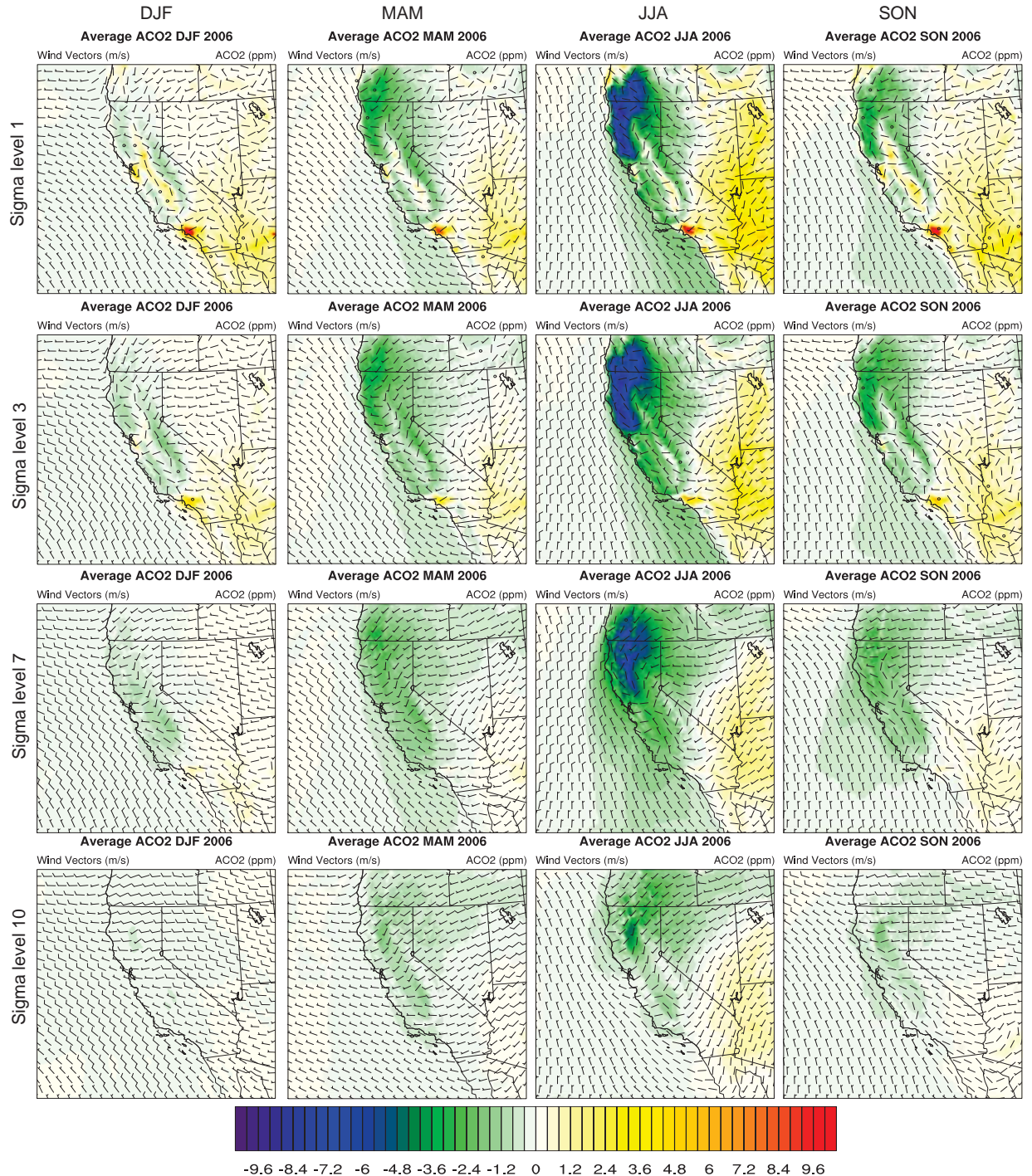


Figure IV.11: Map of atmospheric CO₂ concentrations and wind patterns using the CO₂ tracer by seasons and sigma levels for year 2006.

horizontally and vertically. Surface CO₂ concentration (sigma level 1) closely follows the plant physiological processes as shown in Fig. IV.7 and Fig. IV.8. The spatial distributions

of ACO₂ at higher vertical levels, however, show that the CO₂ concentration above the surface is also modified by transport of CO₂ through wind and diffusion. For example, during the summer of 2006 the large reduction of ACO₂ at the surface (sigma level 1) from photosynthesis propagated into the upper levels (sigma levels 3, 7 and 10) and spread to the surrounding areas. At sigma level 13, the surface effect on ACO₂ became negligible compared to the lower levels. As the vertical level increases, the effects on surface CO₂ flux decrease, and the CO₂ transport increases spatially to reach farther regions. Therefore, surface plant activities from one location would have an impact on the neighboring ecosystems as CO₂ concentration is transported in the atmosphere both spatially and temporally.

Furthermore, Fig. IV.12 shows the effect of plant physiological processes from one location on the neighboring ecosystems. The time series graphs of ACO₂ show that the CO₂ tracer transports the enhanced atmospheric CO₂ concentration from Los Angeles due to morning traffic eastward to the neighboring ecosystems. This CO₂ enrichment therefore influences the plant physiological processes in nearby regions. Active photosynthesis in the Northern California, on the other hand, creates lower ACO₂ air parcels that move southward to offset the urban carbon emission from San Francisco Bay and Sacramento regions.

The illustration of the vertical and horizontal transport of ACO₂ is also displayed in the vertical cross-section of a ACO₂ transect that stretches from the central coast across the Central Valley and to the Sierra Nevada Mountains (Fig. IV.13). The impact of surface plant physiological processes that change the atmospheric CO₂ concentration propagates high into the atmosphere and spreads throughout the region. During the night time, respiration increases the ACO₂ near the surface and increases ACO₂ over the Central Valley. The marine layer wind patterns carry these higher atmospheric CO₂ concentrations eastward

toward the foothills and up the Sierra Nevada Mountains. Photosynthesis during the daytime reduces the surface ACO₂. Stable atmospheric conditions allow the lower ACO₂ parcels to extend upward as shown during midday of Fig. IV.13. Land and sea breezes transport plumes of higher or lower CO₂ concentration air parcels across the region and influence the local ecosystems. Figure IV.13 demonstrates the interactions of neighboring ecosystems through atmospheric CO₂ transport at a regional scale. Plant physiological processes from one location would have an impact on the neighboring ecosystems.

The effect of varying CO₂ concentration in the atmosphere is not limited to plant physiological processes. It also modifies the meteorological conditions such as precipitation. The differences in precipitation over the six AmeriFlux sites are shown in Fig. IV.14. Although there are biases between the WRF-ACASA simulated precipitation and the surface observations, the differences between the two simulations with and without CO₂ tracer show the impact of surface physiological activities on meteorological conditions. They occur mostly during winter and spring seasons, i.e., the wet season of the region. The timing and mag-

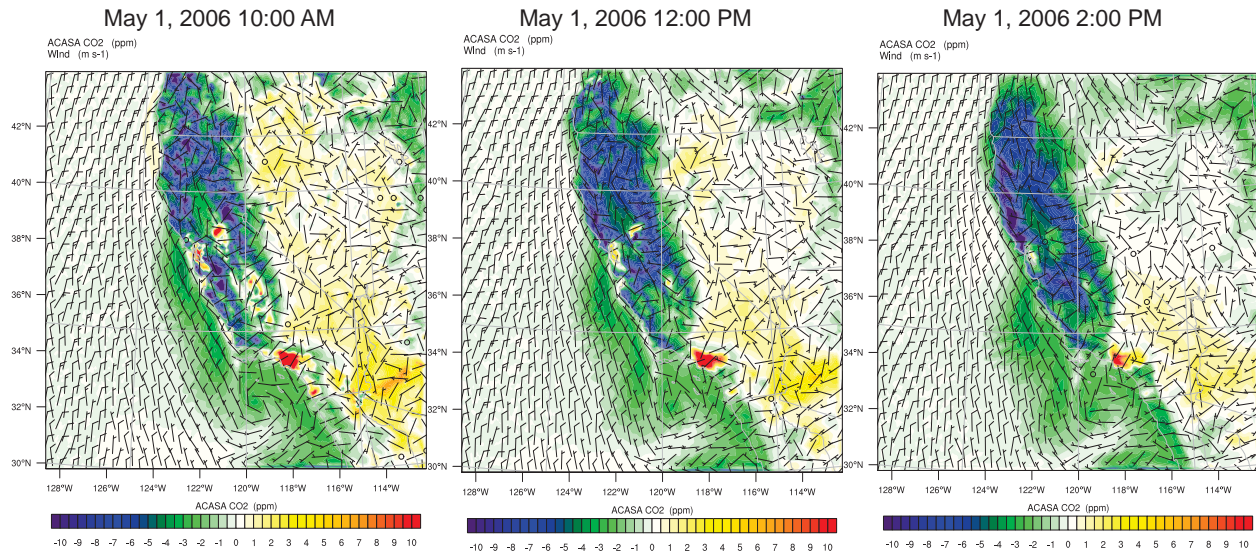


Figure IV.12: Atmospheric CO₂ concentration of May 1 2006 for 10 AM, 12 PM, and 2 PM.

nitude of differences in precipitation reaffirm the importance of CO₂ transport in regional study.

4. Summary and conclusion

In this study, a coupled WRF-ACASA model was used with a new CO₂ tracer routine to simulate CO₂ exchange between the atmosphere and the biosphere as well as the effect of CO₂ transport on surface plant physiology. Two simulations of CO₂ fluxes and ACO₂ using

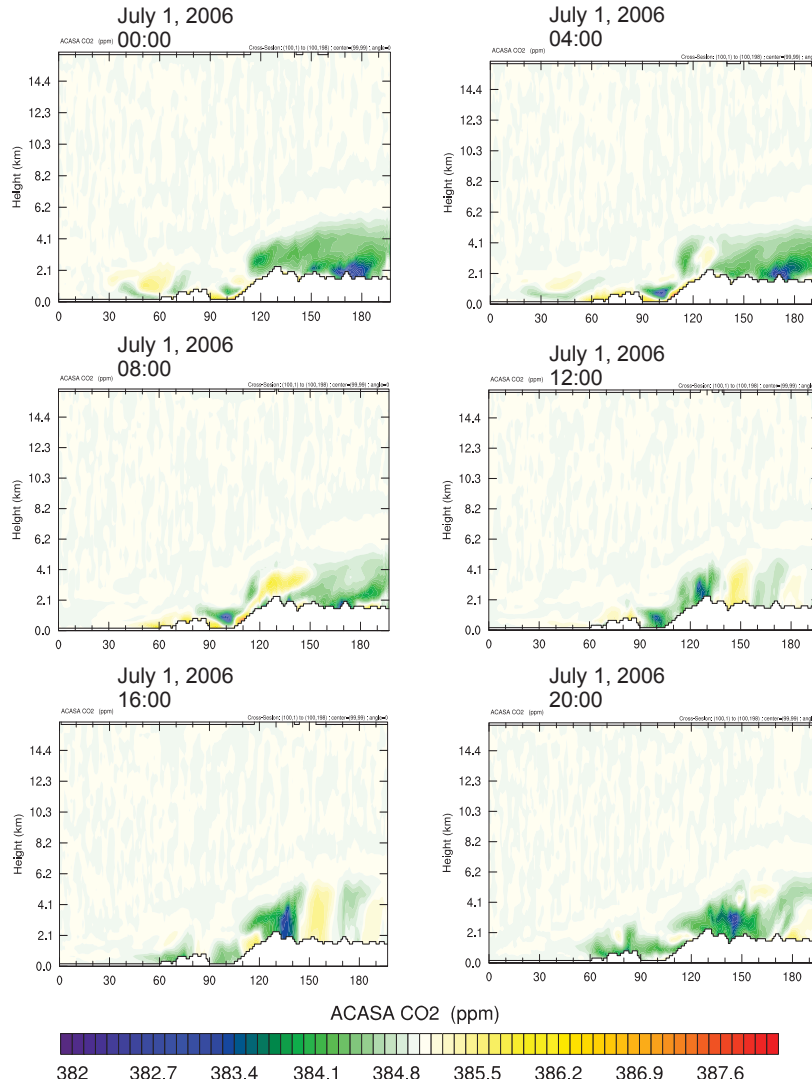


Figure IV.13: Vertical Cross-section of atmospheric CO₂ concentration

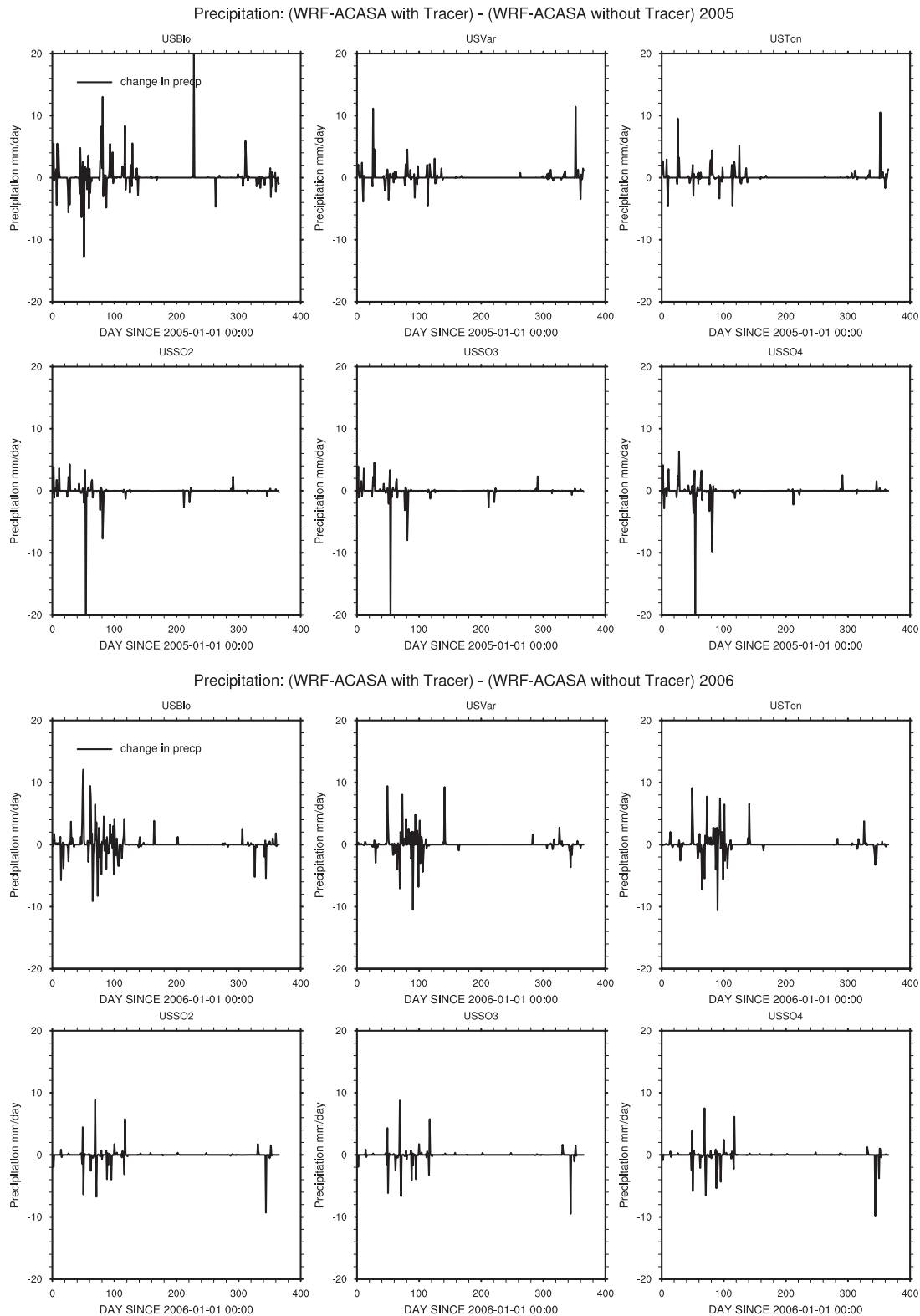


Figure IV.14: Differences in precipitation between the two WRF-ACASA models, i.e., with and without CO₂ tracer simulations for year 2005 and 2006.

the WRF-ACASA model with and without CO₂ tracers were performed over California for the years 2005 and 2006. The ACASA surface scheme calculated physiological processes of photosynthesis and respiration at the local surface level and carbon fluxes were fed back into the WRF atmosphere layers above. The CO₂ tracer modified the atmospheric CO₂ concentration according to the surface carbon fluxes and transported carbon dioxide both spatially and temporally through wind and diffusion. This two-way feedback between the biosphere and atmosphere reflected a more realistic representation of the natural system. Communications through carbon dioxide exchange between the various ecosystems allow us to examine the interactions across different geographical regions and identify the possible sources and sinks of carbon. Seasonal and annual distribution of carbon sinks and sources were determined.

When the model PFTs match the observed PFTs, carbon dioxide fluxes from the WRF-ACASA simulations agree well with the surface observations. For example, the simulated diurnal patterns of CO₂ flux for the Blodgett forest match well with the surface observations. Although the WRF-ACASA model overestimates the three Sky Oak sites and Vaira Ranch, the biases are due to initial PFT mismatch and lack of homogeneous land cover type in the grid cell rather than the model physics. As pointed out in the previous chapters, surface representation is crucial to the high complexity WRF-ACASA model. Improvement of PFT as well as inclusion of more than one vegetation type in each of the grid cell will improve the WRF-ACASA model performance for CO₂ flux.

There is a positive impact on simulating plant physiological processes from varying atmospheric CO₂ concentrations. The inclusion of the CO₂ tracer in the WRF-ACASA model reduces the overestimate of photosynthesis for most of the AmeriFlux sites. Active CO₂

uptake by plants reduces the ambient CO₂ concentration and thus lowers available CO₂ for plant physiological activities during the daytime. The CO₂ tracer therefore helps reduce the RMSE values for hourly CO₂ fluxes as well as improve the annual NEE. In addition, the effect of CO₂ transport in the atmosphere is not limited to the local areas as CO₂ is transported both horizontally and vertically throughout the region. Atmospheric transport of CO₂ concentration allows surface activities from one region to influence the neighboring ecosystems.

Overall, this study shows that the WRF-ACASA model is robust and able to simulate the CO₂ fluxes well across the region if given correct surface representations. The comparison between the two model simulations with and without CO₂ tracer shows that the impact of atmospheric CO₂ transport is important and it should not be neglected when simulating CO₂ flux at regional scale. The interactions between atmosphere and biosphere as well as between the neighboring ecosystems influence the plant physiological processes at both local and regional levels.

It must be noted that the atmospheric CO₂ concentration in this study is initialized with a constant field of 385 ppm, and it changes through time and space from surface processes. This initial condition, however, might not reflect the actual atmospheric concentrations since there are no available observations. Therefore, spatially distributed measurements of atmospheric CO₂ concentration could be a valuable input for the WRF-ACASA model in the future.

Chapter V

Summary and Future Direction

Land surface processes are important components of the earth system that influence carbon and hydrological cycles as well as physical processes such as wind and energy balance. Since the surface layer is the only physical boundary in an atmospheric model, there is a consensus that accurate simulations of atmosphere processes in an atmospheric model require good representations of the surface layer and its terrestrial ecosystems. This study introduced a high complexity bio-geophysical land surface model ACASA into the framework of the mesoscale model WRF to investigate the impact of surface representations, including leaf area index and plant function types, on model-simulated surface conditions. Also examined are the effects of model complexity including multi-layer turbulence and dynamically-varying varying atmospheric carbon dioxide concentration throughout the model atmosphere. Two different approaches and surface model complexities were used in this investigation. Specifically ACASA with and without a dynamic CO₂ Tracer, and NOAH land surface scheme were embedded in the state-of-art mesoscale model WRF were used to simulate certain surface conditions and plant physiological processes over California. With vast differences in land cover, ecological and climatological conditions, the complex terrain of California provides an ideal region to test and evaluate the two land surface models and the CO₂ Tracer effects. Analysis of model simulations for year 2005 and 2006 from the three models were compared with hundreds of surface observation stations from the California Air Resources Board network as well as the six AmeriFlux sites; to date one of the most extensive model evaluation efforts of its kind in this region.

The comparisons between model simulations and surface observations show that the WRF-ACASA model is able to soundly simulate surface and atmospheric conditions. Model estimates of temperature, dew point temperature, and relative humidity agree well with the surface observations overall. Compared to the WRF-NOAH model, the WRF-ACASA model possesses complex and detailed canopy and plant physiological process parameterizations that are either oversimplified (e.g., surface temperature calculations, turbulence) or remain entirely ignored (e.g., carbon dioxide concentration and flux) by most simpler models. This added model complexity is designed to more realistically represent the ecosystem-atmosphere interactions. Some have argued that the increase in model complexity does not translate into higher accuracy due to the increase in uncertainty introduced by the large number of input parameters needed by the more process-based models. However, that the WRF-ACASA model compares well with WRF-NOAH and surface observations does not suggest that increased model complexity increases model uncertainty. Therefore, the increase in model complexity in the WRF-ACASA model not only maintains model accuracy, it also properly accounts for the dominant biological and physical processes describing ecosystem-atmosphere interactions that are scientifically valuable.

The different complexities of physical and physiological processes in the WRF-ACASA and WRF-NOAH models highlight the impacts of different land surface and model components on atmospheric and surface conditions. This study involved examining model responses of detailed plant physiological processes to representations such as leaf area index and plant functional type (land use cover). Specifically reference evapotranspiration (ET₀) and actual evapotranspiration (ET_a) estimates were evaluated using both WRF-ACASA and WRF-NOAH models with two leaf area index datasets, MODIS LAI and USGS LAI. The

improvement of leaf area index and plant functional type generally improves simulations of ET_a for both models. How the overall representation affects surface processes, however, also depends on the model complexity. The surface processes of the WRF-ACASA model are more sensitive to the leaf area index than the simple, single layer WRF-NOAH model. The WRF-ACASA model is also sensitive to land use cover, whereas the WRF-NOAH model is not. There is little statistically-significant improvement in ETo or other meteorological variables with improved LAI in both models, due perhaps to the method of calculation and theoretical origins of this particular variable.

However significant improvement of WRF-ACASA simulations of ET_a using improved land surface representations (LAI and PFT) leads one to conclude that while the high complexity of the model increases the realism of the plant physiological processes, it must also be coupled with high accuracy in land surface representations. Consequently, there is a linear relationship between the model complexity and data quality in surface representations. The lower complexity land surface model is less restricted in its reliance on crucial measured morphological parameters, thus providing more flexibility when high accuracy land-surface data are not available. Higher complexity models, however, perform better over more diverse ecosystems such as forests. Depending on the target variables and study areas of interest, the model complexity and surface representation requirements vary.

Lastly, unlike the simple big-leaf WRF-NOAH model with no carbon dioxide simulation, the high complexity WRF-ACASA model is used to quantify the carbon dioxide exchange between the biosphere and atmosphere and to examine the importance of atmospheric carbon dioxide concentration on surface processes on a regional scale. A new CO₂ tracer is introduced into the WRF-ACASA coupled model to allow atmospheric carbon dioxide con-

centration to vary spatially and temporally according to surface plant physiological processes. Atmospheric CO₂ concentration is often assumed to be well-mixed in GCMs and other models, and so usually only one global mean value is used for the entire atmosphere. Terrestrial systems, however, actively uptake and emit CO₂ to and from the atmosphere, resulting in heterogeneous atmospheric CO₂ distributions. WRF-ACASA model simulations with and without a CO₂ tracer show that there is a beneficial impact on simulating plant physiological processes from varying atmospheric CO₂ concentrations. The inclusion of the CO₂ tracer in the WRF-ACASA model reduces the overestimation of photosynthesis for most of the AmeriFlux sites. Furthermore, changes in atmospheric CO₂ concentration also influence the surface and atmospheric conditions such as latent heat, sensible heat, moisture fluxes, and precipitation.

Overall, this study shows that the high complexity WRF-ACASA model is robust and able to simulate the surface conditions and CO₂ fluxes well across the region, particularly when given accurate surface representations. The comparison between the two model simulations with and without a CO₂ tracer shows that the impact of atmospheric CO₂ concentration and transportation are important, and therefore these should not be neglected when simulating CO₂ flux at regional scales. Interactions between atmosphere and biosphere, both vertically within and above the canopy and horizontally between neighboring ecosystems, influence the plant physiological processes at both local and regional levels. Hence, the WRF-ACASA model with a CO₂ tracer provides valuable insights into how varying carbon dioxide concentration in the atmosphere interacts with surface processes. This two-way feedback between the biosphere and atmosphere reflected a more realistic representation of the natural system. Communications through carbon dioxide exchange between the various

ecosystems allow us to examine the interactions across different geographical regions and identify the possible sources and sinks of carbon. Understanding these links will also become useful to society in many ways, including future land use planning and climate change mitigation efforts.

Future improvement in simulating surface processes, such as the evapotranspiration and carbon dioxide fluxes, can be achieved through improvement of the model grid cell representation and improvement of initial conditions. Both WRF-ACASA and WRF-NOAH models assume one dominant plant functional type in each grid cell. AmeriFlux data show that such homogeneous representation of PFT is inaccurate. Instead of using only one dominant PFT in each grid cell, future simulations of land surface processes can be improved by using a combination of PFTs in each grid cell. Although the impact of heterogeneous land use cover in each grid cell might not have a large impact on low or even moderate complexity models such as WRF-NOAH, this could benefit models such as the WRF-ACASA model. Moreover, it must be noted that the atmospheric CO₂ concentration in this study is initialized with a constant field of 385 ppm, while in reality it changes through time and space from surface processes. This initial condition, however, might not reflect the actual atmospheric concentrations since there are no available observations. Therefore, spatiotemporally distributed measurements of atmospheric CO₂ concentration could also be a valuable input for the WRF-ACASA model in the future.

References

- Abramowitz, G., R. Leuning, M. Clark, and A. Pitman, 2008: Evaluating the performance of land surface models. *J. Climate*, **21** (21), 5468–5481.
- Adegoke, J., R. Pielke, and A. Carleton, 2007: Observational and modeling studies of the impacts of agriculture-related land use change on planetary boundary layer processes in the central U.S. *Agric. For. Meteor.*, **142** (2), 203–215.
- Allen, R., I. Walter, R. Elliott, T. Howell, D. Itenfisu, M. Jensen, and R. Snyder, 2005: *The ASCE standardized reference evapotranspiration equation*. American Society of Civil Engineers.
- Anthes, R., 1984: Enhancement of convective precipitation by mesoscale variations in vegetative covering in semiarid regions. *J. Climate Appl. Meteor.*, **23** (4), 541–554.
- Baldocchi, D. and T. Meyers, 1998: On using eco-physiological, micrometeorological and biogeochemical theory to evaluate carbon dioxide, water vapor and trace gas fluxes over vegetation: a perspective. *Agric. For. Meteor.*, **90** (1-2), 1–25.
- Baldocchi, D., et al., 2001: FLUXNET: a new tool to study the temporal and spatial variability of ecosystem-scale carbon dioxide, water vapor, and energy flux densities. *Bull. Amer. Meteor. Soc.*, **82** (11), 2415–2434.
- Borge, R., V. Alexandrov, J. José del Vas, J. Lumbreiras, and E. Rodríguez, 2008: A comprehensive sensitivity analysis of the WRF model for air quality applications over the Iberian Peninsula. *Atmos. Environ.*, **42** (37), 8560–8574.

- Bougeault, P., 1991: Parameterization schemes of land-surface processes for mesoscale atmospheric models. *Land Surface Evaporation: Measurements and Parameterization*, 55–92.
- Bounoua, L., G. Collatz, S. Los, P. Sellers, D. Dazlich, C. Tucker, and D. Randall, 2000: Sensitivity of climate to changes in NDVI. *J. Climate*, **13** (13), 2277–2292.
- Chase, T., R. Pielke, T. Kittel, R. Nemani, and S. Running, 1996: Sensitivity of a general circulation model to global changes in leaf area index. *J. Geophys. Res.*, **101**, 7393–7408.
- Chen, F. and R. Avissar, 1994: The impact of land-surface wetness heterogeneity on mesoscale heat fluxes. *J. Appl. Meteor.*, **33** (11), 1323–1340.
- Chen, F. and J. Dudhia, 2001a: Coupling an advanced land surface-hydrology model with the Penn State-NCAR MM5 modeling system. Part I: Model implementation and sensitivity. *Mon. Wea. Rev.*, **129** (4), 569–585.
- Chen, F. and J. Dudhia, 2001b: Coupling an advanced land surface-hydrology model with the Penn State-NCAR MM5 modeling system. Part II: Preliminary model validation. *Mon. Wea. Rev.*, **129** (4), 587–604.
- Chen, F., Z. Janjic, and K. Mitchell, 1997: Impact of atmospheric surface-layer parameterizations in the new land-surface scheme of the NCEP mesoscale Eta model. *Bound. Lay. Meteorol.*, **85** (3), 391–421.
- Chen, S. and J. Dudhia, 2000: Annual report: WRF physics. *Air Force Weather Agency*.
- Chen, S. and W. Sun, 2002: A one-dimensional time dependent cloud model. *J. Meteor. Soc. Japan*, **80** (1), 99–118.

Collatz, G., J. Ball, C. Grivet, and J. Berry, 1991: Physiological and environmental regulation of stomatal conductance, photosynthesis and transpiration: a model that includes a laminar boundary layer. *Agric. For. Meteor.*, **54** (2), 107–136.

Collins, W., et al., 2006: Radiative forcing by well-mixed greenhouse gases: Estimates from climate models in the Intergovernmental Panel on Climate Change (IPCC) Fourth Assessment Report (AR4). *J. Geophys. Res.*, **111** (D14), D14 317.

de Arellano, J., B. Gioli, F. Miglietta, H. Jonker, H. Baltink, R. Hutjes, and A. Holtslag, 2004: Entrainment process of carbon dioxide in the atmospheric boundary layer. *J. Geophys. Res.*, **109** (D18), D18 110.

de Wit, M., 1999: Modelling nutrient fluxes from source to river load: a macroscopic analysis applied to the Rhine and Elbe basins. *Hydrobiologia*, **410**, 123–130.

Denmead, O. and E. Bradley, 1985: Flux-gradient relationships in a forest canopy. *The forest-atmosphere interaction: proceedings of the forest environmental measurements conference*, B. Hutchison and B. Hicks, Eds., D. Reidel Publishing Company, Oak Ridge, TN, 421–442.

Dickinson, R. and A. Henderson-Sellers, 2006: Modelling tropical deforestation: A study of GCM land-surface parametrizations. *Quart. J. Roy. Meteor. Soc.*, **114** (480), 439–462.

Dickinson, R., A. Henderson-Sellers, and P. Kennedy, 1993: Biosphere-Atmosphere Transfer Scheme (BATS) Version 1e as coupled to the NCAR community model. *NCAR Tech. Note NCAR/TN-387+ STR*, **72**.

Dirmeyer, P., D. Niyogi, N. de Noblet-Ducoudre, R. Dickinson, and P. Snyder, 2010: Impacts of land use change on climate. *Int. J. Climatol.*, **30** (13), 1905–1907.

- Duan, Q., S. Sorooshian, and V. Gupta, 1992: Effective and efficient global optimization for conceptual rainfall-runoff models. *Water Resour. Res.*, **28** (4), 1015–1031.
- Dudhia, J., 1989: Numerical study of convection observed during the winter monsoon experiment using a mesoscale two-dimensional model. *J. Atmos. Sci.*, **46** (20), 3077–3107.
- Etchevers, P., et al., 2004: Validation of the energy budget of an alpine snowpack simulated by several snow models (SnowMIP project). *Ann. Glaciol.*, **38** (1), 150–158.
- Falge, E., et al., 2002: Seasonality of ecosystem respiration and gross primary production as derived from FLUXNET measurements. *Agric. For. Meteor.*, **113** (1), 53–74.
- Farquhar, G., S. Von Caemmerer, et al., 1982: Modelling of photosynthetic response to environmental conditions. *Encyclopedia of plant physiology*, O. Lange, P. Nobel, C. Osmond, and H. Ziegler, Eds., Vol. 12, 549–587.
- Fesquet, C., P. Drobinski, C. Barthlott, and T. Dubos, 2009: Impact of terrain heterogeneity on near-surface turbulence structure. *Atmos. Res.*, **94** (2), 254–269.
- Gao, W., R. Shaw, and K. Paw U, 1989: Observation of organized structure in turbulent flow within and above a forest canopy. *Bound. Lay. Meteorol.*, **47** (1), 349–377.
- Gao, X., P. Dirmeyer, Z. Guo, and M. Zhao, 2008: Sensitivity of land surface simulations to the treatment of vegetation properties and the implications for seasonal climate prediction. *J. Hydrol.*, **9** (3), 348–366.
- Gutman, G. and A. Ignatov, 1998: The derivation of the green vegetation fraction from

NOAA/AVHRR data for use in numerical weather prediction models. *Int. J. Climatol.*, **19** (8), 1533–1543.

Hales, K., J. Neelin, and N. Zeng, 2004: Sensitivity of Tropical Land Climate to Leaf Area Index: Role of Surface Conductance versus Albedo. *J. Climate*, **17** (7), 1459–1473.

Henderson-Sellers, A., K. McGuffie, and A. Pitman, 1996: The project for intercomparison of land-surface parameterization schemes (PILPS): 1992 to 1995. *Clim. Dyn.*, **12** (12), 849–859.

Holtslag, A. and M. Ek, 1996: Simulation of surface flux and boundary layer development over the pine forest in HAPEX-MOBILHY. *J. Appl. Meteor.*, **35** (2).

Hong, S. and H. Pan, 1996: Nonlocal boundary layer vertical diffusion in a medium-range forecast model. *Mon. Wea. Rev.*, **124** (10), 2322–2339.

Houborg, R. and H. Soegaard, 2004: Regional simulation of ecosystem CO₂ and water vapor exchange for agricultural land using NOAA AVHRR and Terra MODIS satellite data. Application to Zealand, Denmark. *Remote Sens. Environ.*, **93** (1), 150–167.

Jacquemin, B. and J. Noilhan, 1990: Sensitivity study and validation of a land surface parameterization using the HAPEX-MOBILHY data set. *Bound.Lay. Meteorol.*, **52** (1), 93–134.

Jarvis, P., 1976: The interpretation of the variations in leaf water potential and stomatal conductance found in canopies in the field. *Philos. Trans. Roy. Soc. London A*, **273** (927), 593–610.

Jetten, V., A. de Roo, and D. Favis-Mortlock, 1999: Evaluation of field-scale and catchment-scale soil erosion models. *Catena*, **37** (3), 521–541.

Jones, H., 1992: *Plants and microclimate: a quantitative approach to environmental plant physiology*. Cambridge University Press.

Klemp, J., W. Skamarock, and O. Fuhrer, 2003: Numerical consistency of metric terms in terrain-following coordinates. *Mon. Wea. Rev.*, **131** (7), 1229–1239.

Knyazikhin, Y., et al., 1999: MODIS leaf area index (LAI) and fraction of photosynthetically active radiation absorbed by vegetation (FPAR) product (MOD15) algorithm theoretical basis document. Tech. rep., NASA Goddard Space Flight Center, Greenbelt, MD.

Laprise, R., 1992: The Euler equations of motion with hydrostatic pressure as an independent variable. *Mon. Wea. Rev.*, **120** (1), 197–207.

Law, B., 2007: AmeriFlux network aids global synthesis. *Eos*, **88** (28), 286.

Leuning, R., 1990: Modelling stomatal behaviour and photosynthesis of eucalyptus grandis. *Aust. J. Plant Physiol.*, **17** (2), 159–175.

Levitt, J. et al., 1980: *Responses of plants to environmental stresses. Volume II. Water, radiation, salt, and other stresses*. Ed. 2, Academic Press.

Mahrt, L. and M. Ek, 1984: The influence of atmospheric stability on potential evaporation. *Collections*.

Marras, S., R. Pyles, C. Sirca, K. Paw U, R. Snyder, P. Duce, and D. Spano, 2011: Evaluation

- of the Advanced Canopy–Atmosphere–Soil Algorithm (ACASA) model performance over Mediterranean maquis ecosystem. *Agric. For. Meteor.*, **151** (6), 730–745.
- Marras, S., D. Spano, C. Sirca, P. Duce, R. Snyder, R. Pyles, U. Paw, and K. Tha, 2008: Advanced-Canopy-Atmosphere-Soil Algorithm (ACASA model) for estimating mass and energy fluxes. *Ital. J. Agron.*, **3** (3 Suppl.), 793–794.
- Mesinger, F., et al., 2006: North American regional reanalysis. *Bull. Amer. Meteor. Soc.*, **87** (3), 343–360.
- Meyers, T., 1985: A simulation of the canopy microenvironment using higher order closure principles. Ph.D. thesis, Purdue University.
- Meyers, T. and K. Paw U, 1986: Testing of a Higher-Order Closure Model for Modeling Airflow within and above Plant Canopies. *Bound. Lay. Meteorol.*, **37**, 297–311.
- Meyers, T. and K. Paw U, 1987: Modelling the plant canopy micrometeorology with higher-order closure principles. *Agric. For. Meteor.*, **41** (1), 143–163.
- Miglietta, M. and R. Rotunno, 2005: Simulations of moist nearly neutral flow over a ridge. *J. Atmos. Sci.*, **62** (5), 1410–1427.
- Mihailovic, D., R. Pielke, B. Rajkovic, T. Lee, and M. Jeftic, 1993: A resistance representation of schemes for evaporation from bare and partly plant-covered surfaces for use in atmospheric models. *J. Appl. Meteor.*, **32**, 1038–1054.
- Mintz, Y., 1981: A brief review of the present status of global precipitation estimates. *Report*

of the Workshop on Precipitation Measurements from Space, D. Atlas and T. O.W., Eds.,

NASA Goddard Space Flight Center, Greenbelt, MD.

Mlawer, E., S. Taubman, P. Brown, M. Iacono, and S. Clough, 1997: Radiative transfer for inhomogeneous atmospheres: RRTM, a validated correlated-k model for the longwave. *J. Geophys. Res.*, **102 (D14)**, 16 663–16.

Monin, A. and A. Obukhov, 1954: Basic laws of turbulent mixing in the atmosphere near the ground. *Tr. Akad. Nauk SSSR Geofiz. Inst.*, **24 (151)**, 163–87.

Noilhan, J. and S. Planton, 1989: A simple parameterization of land surface processes for meteorological models. *Mon. Wea. Rev.*, **117 (3)**, 536–549.

Paw U, K., 1997: The Modeling and Analysis of Crop Canopy Interactions with the Atmosphere under Global Climatic Change Conditions. *J. Agric. Meteorol.*, **52 (5)**, 419–428.

Paw U, K. and W. Gao, 1988: Applications of solutions to non-linear energy budget equations. *Agric. For. Meteor.*, **43 (2)**, 121–145.

Paw U, K., et al., 2004: Carbon dioxide exchange between an old-growth forest and the atmosphere. *Ecosystems*, **7 (5)**, 513–524.

Perrin, C., C. Michel, and V. Andréassian, 2001: Does a large number of parameters enhance model performance? Comparative assessment of common catchment model structures on 429 catchments. *J. Hydrol.*, **242 (3)**, 275–301.

Pielke, R. and R. Avissar, 1990: Influence of landscape structure on local and regional climate. *Landscape Ecol.*, **4 (2)**, 133–155.

- Pielke, R., G. Marland, R. Betts, T. Chase, J. Eastman, J. Niles, S. Running, et al., 2002: The influence of land-use change and landscape dynamics on the climate system: relevance to climate-change policy beyond the radiative effect of greenhouse gases. *Philos. Trans. Roy. Soc. London A*, **360** (1797), 1705–1719.
- Pielke, R. and D. Niyogi, 2010: The role of landscape processes within the climate system. *Landform-Structure, Evolution, Process Control*, 67–85.
- Pitman, A., M. Zhao, and C. Desborough, 1999: Investigating the sensitivity of a land surface schemes simulation of soil wetness and evaporation to spatial and temporal leaf area index variability within the Global Soil Wetness Project. *J. Meteor. Soc. Japan*, **77**, 281–290.
- Pleim, J. and A. Xiu, 1995: Development and testing of a surface flux and planetary boundary layer model for application in mesoscale models. *J. Appl. Meteor.*, **34** (1), 16–32.
- Potter, C., J. Randerson, C. Field, P. Matson, P. Vitousek, H. Mooney, and S. Klooster, 1993: Terrestrial ecosystem production: a process model based on global satellite and surface data. *Global Biogeochem. Cycles*, **7** (4), 811–841.
- Powers, J., 2007: Numerical prediction of an Antarctic severe wind event with the Weather Research and Forecasting (WRF) model. *Mon. Wea. Rev.*, **135** (9), 3134–3157.
- Pyles, R., 2000: The development and testing of the UCD Advanced Canopy–Atmosphere–Soil Algorithm (ACASA) for use in climate prediction and field studies. Ph.D. thesis, University of California, Davis.

Pyles, R., K. Paw U, and M. Falk, 2004: Directional wind shear within an old-growth temperate rainforest: observations and model results. *Agric. For. Meteor.*, **125** (1), 19–31.

Pyles, R., B. Weare, and K. Paw U, 2000: The UCD Advanced Canopy-Atmosphere-Soil Algorithm: comparisons with observations from different climate and vegetation regimes. *Quart. J. Roy. Meteor. Soc.*, **126**, 2951–2980.

Pyles, R., B. Weare, K. Paw U, and W. Gustafson, 2003: Coupling between the University of California, Davis, Advanced Canopy-Atmosphere-Soil Algorithm (ACASA) and MM5: Preliminary results for July 1998 for western North America. *J. Appl. Meteor.*, **42** (5), 557–569.

Raupach, M. and J. Finnigan, 1988: 'Single-layer models of evaporation from plant canopies are incorrect but useful, whereas multilayer models are correct but useless': Discuss. *Aust. J. Plant Physiol.*, **15** (6), 705–716.

Rowntree, P., 1991: Atmospheric parameterization schemes for evaporation over land: Basic concepts and climate modeling aspects. *Land Surface Evaporation: Measurement and Parameterization*, T. Schmugge and J.-C. André, Eds., Springer-Verlag, New York, 5–29.

Rutter, N., et al., 2009: Evaluation of forest snow processes models (SnowMIP2). *J. Geophys. Res.*, **114** (D6), D06111.

Sagan, C. and B. Khare, 1979: Tholins-organic chemistry of interstellar grains and gas. *Nature*, **277**, 102–107.

Sellers, P., C. Tucker, G. Collatz, S. Los, C. Justice, D. Dazlich, and D. Randall, 1996: A revised land surface parameterization (SiB2) for atmospheric GCMs. Part II: The generation of global fields of terrestrial biophysical parameters from satellite data. *J. Climate*, **9** (4), 706–737.

Shuttleworth, W., 1984: Observations of radiation exchange above and below Amazonian forest. *Quart. J. Roy. Meteor. Soc.*, **110** (466), 1163–1169.

Smirnova, T., J. Brown, and S. Benjamin, 1997: Performance of different soil model configurations in simulating ground surface temperature and surface fluxes. *Mon. Wea. Rev.*, **125** (8), 1870–1884.

Smirnova, T., J. Brown, S. Benjamin, and D. Kim, 2000: Parameterization of cold-season processes in the MAPS. *J. Geophys. Res.*, **105** (D3), 4077–4086.

Staudt, K., E. Falge, R. Pyles, and T. FOKEN, 2010: Sensitivity and predictive uncertainty of the ACASA model at a spruce forest site. *Biogeosciences*, **7** (11), 3685–3705.

Staudt, K., A. Serafimovich, L. Siebicke, R. Pyles, and E. Falge, 2011: Vertical structure of evapotranspiration at a forest site (a case study). *Agric. For. Meteor.*, **151** (6), 709–729.

Stauffer, D. and N. Seaman, 1990: Use of four-dimensional data assimilation in a limited-area mesoscale model. Part I: Experiments with synoptic-scale data. *Mon. Wea. Rev.*, **118** (6), 1250–1277.

Stauffer, D., N. Seaman, and F. Binkowski, 1991: Use of four-dimensional data assimilation in a limited-area mesoscale model. II- Effects of data assimilation within the planetary boundary layer. *Mon. Wea. Rev.*, **119**, 734–754.

Stull, R. B., 1988: *An introduction to boundary layer meteorology*. Kluwer Academic Publishers.

Su, H., K. Paw U, and R. Shaw, 1996: Development of a coupled leaf and canopy model for the simulation of plant-atmosphere interactions. *J. Appl. Meteor.*, **35**, 733–748.

Thompson, S., B. Govindasamy, A. Mirin, K. Caldeira, C. Delire, J. Milovich, M. Wickett, and D. Erickson, 2004: Quantifying the effects of CO₂-fertilized vegetation on future global climate and carbon dynamics. *Geophys. Res. Lett.*, **31** (23), L23211.

Trenberth, K. and D. Shea, 2006: Atlantic hurricanes and natural variability in 2005. *Geophys. Res. Lett.*, **33** (12), L12704.

Wieringa, J., 1986: Roughness-dependent geographical interpolation of surface wind speed averages. *Quart. J. Roy. Meteor. Soc.*, **112** (473), 867–889.

Wigley, T. and D. Schimel, 2005: *The carbon cycle*, Vol. 6. Cambridge University Press.

Wohlfahrt, G., M. Bahn, U. Tappeiner, and A. Cernusca, 2001: A multi-component, multi-species model of vegetation–atmosphere CO₂ and energy exchange for mountain grasslands. *Agric. For. Meteor.*, **106** (4), 261–287.

Xiu, A. and J. Pleim, 2001: Development of a land surface model. Part I: Application in a mesoscale meteorological model. *J. Appl. Meteor.*, **40** (2), 192–209.

Zhan, X. and W. Kustas, 2001: A coupled model of land surface CO₂ and energy fluxes using remote sensing data. *Agric. For. Meteor.*, **107** (2), 131–152.

Zhao, M., A. Pitman, and T. Chase, 2001: The impact of land cover change on the atmospheric circulation. *Clim. Dyn.*, **17** (5), 467–477.